

**Identification and characterization of the molecular  
complex formed by the P2X<sub>2</sub> receptor subunit and the  
adapter protein Fe65 in rat brain**

Dissertation

zur Erlangung des Doktorgrades

der Mathematisch-Naturwissenschaftlichen Fakultäten

der Georg-August-Universität zu Göttingen

vorgelegt von

Marianela Masin

aus Reconquista, Argentinien

Göttingen 2006

D7

Referent: Prof. Dr. H-J. Fritz

Korreferent: Prof. Dr. H. Jäckle

Tag der mündlichen Prüfung: 03.05.06

*For those who seek the nature of Divinity  
and not fail to see Divinity in Nature...*

## ZUSAMMENFASSUNG

Die Erregungsübertragung an chemischen Synapsen des Nervensystems beginnt mit der Freisetzung von Neurotransmittermolekülen aus präsynaptischen Nervenendigungen. Diese Transmittermoleküle aktivieren spezifische Rezeptoren in der postsynaptischen Membran. ATP ist ein Neurotransmitter, der zur synaptischen Übertragung im zentralen und peripheren Nervensystem verwendet wird. Dabei bindet ATP an ionotrope Rezeptoren in der postsynaptischen Membran. Diese Rezeptoren nennt man P2X Rezeptoren. In Säugetieren existieren sieben verschiedene P2X Rezeptoruntereinheiten (P2X<sub>1</sub>–P2X<sub>7</sub>). Von diesen sind hauptsächlich die P2X<sub>2</sub>, P2X<sub>4</sub> und P2X<sub>6</sub> Untereinheiten im Gehirn exprimiert. Mittels goldmarkierter Antikörper konnten die Lokalisation dieser Rezeptoren im äusseren Abschnitt der postsynaptischen Spezialisierung elektronenmikroskopisch dargestellt werden. Diese präzise Lokalisierung der P2X Rezeptoren legte die Vermutung nahe, dass P2X Rezeptoren, ähnlich anderen synaptischen Rezeptoren, mit intrazellulären regulatorischen Proteinen interagieren. Bislang jedoch wurden keine entsprechenden Proteine identifiziert.

In der vorliegenden Arbeit wurde daher mittels der Hefe-Zwei-Hybrid Methode eine Rattenhirn cDNA Bibliothek mit dem Carboxyterminus der P2X<sub>2</sub> Untereinheit nach potentiellen Interaktionspartnern durchsucht. So gelang es das Protein Fe65 als wichtigen neuronalen Interaktionspartner von P2X<sub>2</sub> Rezeptoren zu identifizieren. Die Interaktion von Fe65 und P2X<sub>2</sub> Untereinheiten wurde zunächst mit Hefe-Zwei-Hybrid Methoden und GST-pulldown Experimenten näher charakterisiert. Dabei zeigte sich, dass Fe65 spezifisch mit P2X<sub>2</sub> nicht aber mit anderen P2X Untereinheiten (z.B. P2X<sub>4</sub> und P2X<sub>7</sub>) oder mit einer natürlich vorkommenden Spleissvariant von P2X<sub>2</sub> (P2X<sub>2(b)</sub>) interagiert. Neben Fe65 konnte auch für das verwandte Protein Fe65-like1 nachgewiesen werden, dass es an den P2X<sub>2</sub> Carboxyterminus bindet.

Durch Generierung von Deletionen und Punktmutationen in den Sequenzen beider Interaktionspartner konnte weiter gezeigt werden, dass die Bindung dieser Proteine zwischen der WW Domäne von Fe65 und einer prolinreichen Sequenz (PPPP) im Carboxyterminus der P2X<sub>2</sub> Untereinheit stattfindet.

Zwei Antikörper gegen Fe65 wurden generiert, charakterisiert und zur elektronenmikroskopischen Darstellung der subzellulären Lokalisierung von Fe65 eingesetzt. Fe65 wurde dabei in der prä- und postsynaptischen Membran der Synapsen von Schaffer Kollateralen und hippocampalen Pyramidenzellen nachgewiesen. Doppelte Immunogoldmarkierung zeigte ferner, dass P2X<sub>2</sub> Untereinheiten und Fe65 im äusseren Abschnitt der postsynaptischen Spezialisierung kolokalisiert sind. Darüberhinaus gelang es beide Proteine gemeinsam aus Membranextrakten von Hirngewebe zu immunopräzipitieren. In der Zusammenschau lassen diese Ergebnisse den Schluss zu das Fe65 und P2X<sub>2</sub> Untereinheit *in vivo* in postsynaptischen Membranen des Zentralnervensystems interagieren.

Um zu untersuchen, ob die Bindung von Fe65 die Rezeptoreigenschaften von P2X<sub>2</sub> reguliert, wurden elektrophysiologische Untersuchungen an HEK Zellen und *Xenopus laevis* Oozyten, die diese Proteine einzeln oder zusammen exprimierten, durchgeführt. Während P2X<sub>2</sub> Rezeptoren mit Fe65 ähnliche pharmakologische Eigenschaften zeigten und Amplitude und Kinetik der Ströme vergleichbar den durch P2X<sub>2</sub> Rezeptoren ohne Fe65 vermittelten waren, zeigten sich drastische Unterschiede bei der Permeabilität von P2X<sub>2</sub> Rezeptoren mit und ohne Fe65. So wurde die zeit- und aktivierungsabhängige Änderung der Ionenselektivität von P2X<sub>2</sub> Rezeptoren durch Assoziation mit Fe65 nahezu komplett unterdrückt. Dies legt die Schlussfolgerung nahe, dass die Bindung von Fe65 die Motilität des P2X<sub>2</sub> Carboxyterminus einschränkt und damit die Permeabilität dieser Rezeptoren für grössere organische Kationen reduziert. Dies stellt einen neuartigen Regulationsmechanismus von ionotropen Rezeptoren und damit der ATP-vermittelten synaptischen Erregungsübertragung im Nervensystem dar.

## SUMMARY

Synaptic transmission in the nervous system is achieved through the release of neurotransmitters from presynaptic terminals, resulting in the activation of neurotransmitter receptors at postsynaptic membrane. ATP is a neurotransmitter that mediates fast synaptic transmission in the central and peripheral nervous system, by activating a family of ATP-gated ionotropic receptors called P2X receptors. Mammalian P2X receptors are formed by seven subunits (P2X<sub>1</sub>–P2X<sub>7</sub>) of which mainly P2X<sub>2</sub>, P2X<sub>4</sub> and P2X<sub>6</sub> subunits are expressed in the brain. By using postembedding immunogold labeling combined with electron microscopy, the three subunits have been localized at the peripheral portion of the excitatory postsynaptic membrane. This precise localization of P2X subunits at excitatory synapses suggests an interaction with intracellular regulatory or anchoring proteins, as described for other synaptic receptors. However, interaction partners of P2X receptor subunits in the synapse have not been identified so far.

In the present work, that question was answered by performing a yeast two-hybrid (Y2H) screening of a rat brain cDNA library employing the C-terminal domain of the P2X<sub>2</sub> subunit as a bait. This approach allowed us to isolate the protein Fe65 as the main interacting partner of neuronal P2X<sub>2</sub> receptor subunits. Characteristics of the interaction were confirmed *in vitro* by complementary Y2H assays and GST-pulldown experiments. Other members of the P2X family, as P2X<sub>4</sub> and P2X<sub>7</sub> were not able to interact with Fe65, revealing the specificity of the interaction. An interaction was found for P2X<sub>2</sub> and the Fe65-related protein Fe65-like1, but was not observed between Fe65 and the naturally occurring P2X<sub>2</sub> splice variant P2X<sub>2(b)</sub>, indicating that alternative splicing may regulate complex assembly. Deletions and point mutations on both interacting partners helped to identify that the interaction is driven by the WW domain of Fe65 which specifically recognizes the proline rich sequence PPPP at the C-terminus of the P2X<sub>2</sub> receptor.

Two antibodies against Fe65 were generated, characterized and employed to assay the subcellular localization of this protein by immunogold-labeling electron microscopy. Labeling for Fe65 was found at the pre- and postsynaptic specialization of CA1 hippocampal pyramidal cell/Schaffer collateral synapses. By double immunogold labeling, the co-localization of Fe65 with P2X<sub>2</sub> subunits at the postsynaptic specialization of excitatory synapses was observed, suggesting that the interaction occurs *in vivo*. As expected by the overlapping distribution of P2X<sub>2</sub> and Fe65, both proteins could be co-immunoprecipitated from brain membrane extracts. This experiment demonstrates that both proteins are present in the same molecular complex providing more evidence on the occurrence *in vivo* of such association.

The assembly with Fe65 was found to regulate certain functional properties of P2X<sub>2</sub> receptors as demonstrated by electrophysiology recordings on HEK cells and *Xenopus laevis* oocyte heterologously expressing both proteins. While Fe65-bound P2X<sub>2</sub> receptors showed comparable basic pharmacological properties, as current amplitudes, kinetics and ATP EC<sub>50</sub> values, permeability changes were affected. Thus, the time- and activation-dependent change in ionic selectivity of P2X<sub>2</sub> receptors was inhibited by coexpression with Fe65. We propose that Fe65 tethers the C-terminus of the receptor and impairs its ability permeate bulky organic cations, suggesting a novel mechanism for intracellular proteins in regulating receptor function and thus ATP-mediated synaptic transmission.

---

## TABLE OF CONTENTS

TABLE OF CONTENTS .....	i
I. ABBREVIATIONS .....	iv
1. INTRODUCTION .....	1
1.1 Cell communication in synaptic transmission. ....	1
1.2 Ionotropic receptors .....	3
1.2.1 The ionotropic glutamate receptor family .....	4
1.2.2 The nicotinic acetylcholine receptor superfamily .....	4
1.2.3 The P2X ATP-gated receptor family .....	5
1.3 Purinergic receptors .....	6
1.3.1 ATP as a neurotransmitter activating P2 receptors .....	6
1.3.2 P2X receptors .....	7
1.3.2.1 Membrane topology .....	7
1.3.2.2 Multimerization .....	11
1.3.2.3 Functional and pharmacological characteristics of heterologously expressed P2X receptors .....	11
1.4 Role of scaffolding and adapter proteins in synaptic transmission .....	14
1.4.1 Fe65 is a brain-specific adapter protein .....	15
2. AIMS OF THIS STUDY .....	18
3. MATERIAL AND METHODS .....	20
3.1. Materials .....	20
3.1.1. Equipment .....	20
3.1.2. Chemicals and reagents .....	20
3.1.3. Antibiotics .....	22
3.1.4. Enzymes, inhibitors, substrates .....	23
3.1.5. Molecular weight standards .....	24
3.1.6. Kits and ready-to-use reagents .....	24
3.1.7. Plasmids .....	24
3.1.8. Synthetic oligonucleotide primers .....	25
3.1.9. List of DNA constructs .....	25
3.1.10. Antibodies .....	28
3.1.11. Organisms and growth media .....	29
3.1.11.1. Bacterial strain genotype .....	29
3.1.11.2. Bacterial media .....	29
3.1.11.3. Yeast strain genotype .....	30
3.1.11.4. Yeast media .....	30
3.1.11.5. Cell lines .....	31
3.1.11.6. Cells media .....	31
3.1.12. Buffers .....	31
3.2. Methods .....	33
3.2.1. Molecular biology procedures .....	33
3.2.1.1. Designing and preparation of DNA constructs .....	33
3.2.1.2. Purification, cloning, and isolation of DNA constructs .....	35
3.2.2. Basic techniques of biochemistry .....	36
3.2.3. Yeast two-hybrid assays .....	42
3.2.3.1. Yeast glycerol stock for Y2H screening .....	43
3.2.3.2. Yeast transformation for Y2H Screening .....	44
3.2.3.3. Yeast transformation for direct Y2H assay .....	45
3.2.3.4. $\beta$ -Galactosidase assay .....	46



3.2.4.	Probing protein-protein interactions <i>in vitro</i> by pull-down assays .....	47
3.2.4.1.	Pull-down assays.....	47
3.2.5.	Characterization of protein-protein interaction <i>in vivo</i> .....	48
3.2.5.1.	Co-immunoprecipitation assays.....	48
3.2.6.	Immunocolocalization assays.....	49
3.2.7.	Electrophysiology .....	49
3.2.7.1.	Whole cell Patch-clamp technique.....	49
3.2.7.2.	Two-electrode voltage clamp .....	52
4.	RESULTS .....	57
4.1.	Isolation of proteins interacting with the C-terminus of the P2X <sub>2</sub> receptor....	57
4.2.	Studying the interaction between Fe65 and P2X <sub>2</sub> cytoplasmic domain by a direct Y2H assay.....	61
4.2.1.	Confirming the interaction between Fe65-like 1 and the cytoplasmic tail of P2X <sub>2</sub> subunit by a direct Y2H assay .....	62
4.2.2.	Probing the specificity of the interaction between Fe65 and P2X <sub>2</sub> CD by a direct Y2H assay .....	63
4.2.3.	Probing the interaction between Fe65 and the splice variant of P2X <sub>2</sub> subunit by a direct Y2H assay.....	64
4.2.4.	Delimiting residues of P2X <sub>2</sub> responsible for the interaction.....	65
4.2.4.1.	The first proline-rich domain of P2X <sub>2</sub> CD is necessary for the interaction with Fe65.....	66
4.2.4.2.	Structural integrity of the WW domain is required for Fe65 binding to the first proline-rich domain of P2X <sub>2</sub> CD.....	67
4.2.5.	Drawbacks of the yeast two hybrid assay.....	68
4.3.	Generation and Western blot characterization of Fe65 antibodies .....	69
4.4.	The complex between Fe65 and P2X <sub>2</sub> is formed by direct interaction of the proteins <i>in vitro</i> .....	71
4.5.	Occurrence <i>in vivo</i> of the complex between Fe65 and the P2X <sub>2</sub> receptor.....	74
4.6.	The Amyloid precursor protein may take part of the macromolecular complex between Fe65 and P2X <sub>2</sub> .....	78
4.7.	Fe65 and P2X <sub>2</sub> colocalize in excitatory postsynaptic specializations of the hippocampus.....	79
4.7.1.	Characterization of the Fe65 antibodies by peroxidase immunostaining.....	79
4.7.2.	Fe65 is present at excitatory synapses in the hippocampus.....	80
4.7.3.	Fe65 and P2X <sub>2</sub> co-localize in excitatory postsynaptic specializations of the hippocampus.....	81
4.8.	Fe65 inhibits the ATP-induced pore dilation of P2X <sub>2</sub> channels.....	82
4.8.1.	Electrophysiology whole cell recordings.....	82
4.8.2.	Two electrode voltage-clamp recordings in <i>Xenopus laevis</i> oocytes.....	87
5.	DISCUSSION .....	93
5.1.	Synaptic signaling through protein-protein interactions .....	93
5.2.	Dissecting the interaction between Fe65 and the P2X <sub>2</sub> receptor.....	96
5.3.	The role of genetic variability in the interaction between Fe65 and the P2X <sub>2</sub> receptor .....	100
5.4.	Fe65 is present in hippocampal excitatory synapses where colocalize with P2X <sub>2</sub> receptors .....	104
5.5.	Fe65 regulates the function of P2X <sub>2</sub> receptors by binding of its cytoplasmic domain .....	106
5.6.	Outlook.....	115
6.	CONCLUSIONS.....	117

---

<b>7. REFERENCES</b> .....	118
<b>II. APPENDIX</b> .....	viii
<b>II.I. Oligonucleotides</b> .....	viii
<b>II.II. Cloned constructs</b> .....	x
<b>II.III. Nucleotide and amino acid sequence of rat P2X<sub>2</sub> receptor</b> .....	xi
<b>II.IV. Nucleotide and amino acid sequence of rat Fe65 protein (APBB1)</b> .....	xiii
<b>II.V. Partial nucleotide and amino acid sequence of rat Fe65 Like 1 isolated in the Y2H screening (APBB2)</b> .....	xv
<b>II.VI. Predicted nucleotide and amino acid sequence of rat Fe65 Like 1 (APBB2)</b> ..	xvi
<b>ACKNOWLEDGMENTS</b> .....	xx
<b>LEBENS LAUF</b> .....	xxi
<b>VERÖFFENTLICHUNGEN</b> .....	xxii

---

## I. ABBREVIATIONS

Ab	Antibody
$\alpha,\beta$ -mATP	$\alpha,\beta$ -Methyleneadenosine-5'-triphosphate
A $\beta$	$\beta$ -amyloid peptide
AD	Activation domain
ADP	Adenosine- 5'-diphosphate
Ala (A)	Alanine
AMPA	$\alpha$ -Amino-3-hydroxy-5-methyl-4-isoxazole propionic acid
APP	Amyloid precursor protein
APBB1	Amyloid precursor protein-binding protein 1
Arg (R)	Arginine
Asp (D)	Aspartic acid
ATP	Adenosine -5'-triphosphate
BAPTA	1,2-Bis(2-aminophenoxy)ethane-N, N, N', N'-tetraacetic acid-tetrapotassium salt
BD	Binding domain
bp	Base pair
BSA	Bovine serum albumin
BzATP	2',3'-(4-benzoyl)-benzoyl ATP
°C	Celsius
CNS	Central nervous system
cDNA, cRNA	Complementary DNA, RNA
DEPC	Diethyl pyrocarbonate
DMSO	Dimethyl sulfoxide
DNA	Desoxyribonucleic acid
DNase	Deoxyribonuclease
dNTP	Deoxyribonucleoside triphosphate
DTT	Dithiothreitol
EC <sub>50</sub>	Concentration of agonist producing half maximal effect
ECL	Enhanced chemiluminescence
EDTA	Ethylenediamine tetraacetic acid
EGTA	EthyleneGlycol-bis ( $\beta$ -aminoethyl ether)- N, N, N', N'-tetraacetic acid

---

ER	Endoplasmic reticulum
EtBr	Ethidium bromide
EtOH	Ethanol
F, pF	Farad, picoFarad
FCS	Fetal calf serum
g	Acceleration
GABA	$\gamma$ -Aminobutyric acid
GABA <sub>A</sub> R	$\gamma$ -aminobutyric acid receptor
g, mg, $\mu$ g	Gram, milligram, microgram
Glu (E)	Glutamic acid
GluR	Glutamate receptor
GlyR	Glycine receptor
G protein	Guanine nucleotide-binding protein
G $\Omega$	GigaOhm
h	Hour
HEK cells	Human embryonic kidney cells
HEPES	(2-hydroxyethyl)-1-piperazine ethanesulphonic acid
5-HT <sub>3</sub>	5-hydroxytryptamine receptor
HS	Horse serum
I	Current
IP	Immunoprecipitation
IPTG	Isopropyl- $\beta$ -D-thiogalactopyranoside
KA	Kainate receptors
kb	kilobases
kDa	KiloDalton
l	Liter
LB	Luria broth (medium)
LGICs	Ligand-gated ion channels
Lys (K)	Lysine
2MeSATP	2-methylthio-ATP
$\mu$ A	MicroAmpere
ml, $\mu$ l	Milliliter, microliter
M, mM, $\mu$ M	Molar, millimolar, micromolar

---

MOPS	3-(N-Morpholino) propanesulfonic acid
MΩ	MegaOhm
mV	MilliVolt
ms	Milliseconds
MW	Molecular weight
nA	nanoAmpere
nAChR	Nicotinic acetylcholine receptors
ng	Nanogram
NMDA	N-Methyl-D-Aspartate
NMDG <sup>+</sup>	N-Methyl-D-Gluamine
Ni-NTA	Ni <sup>2+</sup> -Nitriloacetic acid
Ω	Ohm
OD	Optical density
O.N.	Overnight
pA	picoAmpere
PBS	Phosphate buffered saline
P <sub>Ca</sub> /P <sub>Na</sub>	Ratio of permeability to Ca <sup>2+</sup> respect permeability to Na <sup>+</sup>
PCR	Polymerase chain reaction
PDZ	PSD-95/disc-large/Zo-1 domain
PFA	Paraformaldehyde
PID	Phosphotyrosine interaction domain
PKA	Cyclic AMP (cAMP)-dependent protein kinase
PKC	Protein kinase C
PMSF	Phenylmethylsulfonyl fluoride
P <sub>NMDG</sub> /P <sub>Na</sub>	Ratio of permeability to NMDG <sup>+</sup> respect permeability to Na <sup>+</sup>
PPDAS	Pyridoxalphosphate-6-azophenyl-2', 4'-disulfonic acid
Pro (P)	Proline
PSD	Postsynaptic density
PTB	Phosphotyrosine binding domain
R	Resistance
RNA	Ribonucleic acid
RNase	Ribonuclease
rpm	Revolutions per minute
RT	Room temperature

---

Ser (S)	Serine
s	Second
SDS	Sodium dodecyl sulphate
SDS-PAGE	SDS-polyacrylamide gel electrophoresis
SV	Splice variant
TEMED	N'N'N'N Tetramethylethyldiamine
TEVC	Two-electrode voltage clamp
Thr (T)	Threonine
TM	Transmembrane domain
U	Unit
Val (V)	Valine
V	Volt
V <sub>m</sub>	Membrane voltage
v/v	Volume to volume
<i>wt</i>	Wild-type
w/v	Weight to volume
Trp (W)	Tryptophan
X-Gal	5-bromo-4-chloro-3-indolyl-beta-D-galactopyranoside
Tyr (Y)	Tyrosine
YAP	Yes-kinase associated protein
Y2H	Yeast-two-hybrid

---

## 1. INTRODUCTION

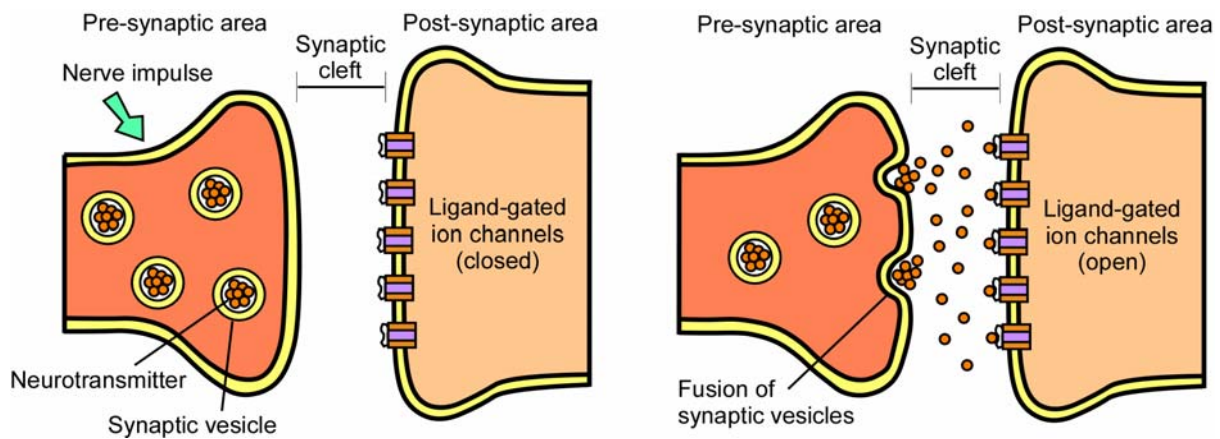
### 1.1 Cell communication in synaptic transmission.

Neurons communicate with each other through special structures called synapses (Shepherd, 1994). A synapse can be either electrical or chemical depending on how the synaptic areas are arranged. In electrical synapses the presynaptic and postsynaptic membranes are in direct contact with each other and small channels permit ions to easily flow through. Electrical synapses, therefore, transmit signals very rapidly. Chemical synapses, on the other hand, require the release of a chemical transmitter substance (neurotransmitter) by the presynaptic cell in order to stimulate the postsynaptic neuron. This is the predominant mode of neuronal communication in adult brain (Squire *et al.*, 2002).

Neurotransmitters are small hydrophilic molecules synthesized and released by neurons that act as chemical messengers from a stimulated neuron to a target cell at a synapse. Most neurotransmitters are stored in synaptic vesicles, including acetylcholine, glycine, glutamate, dopamine, norepinephrine, epinephrine, serotonin, histamine and  $\gamma$ -aminobutyric acid (GABA). Nucleotides such as ATP, ADP and UTP and the nucleoside adenosine, also function as neurotransmitters (Lodish *et al.*, 2000).

Because of its hydrophilic nature, neurotransmitters are unable to cross the plasma membrane at the postsynaptic specialization, thus they exclusively act by binding to cell surface receptors (Lodish *et al.*, 2000).

Neurotransmitters secreted by presynaptic vesicles diffuse through the synaptic cleft and arrive to the plasma membrane of the postsynaptic area, where the type of receptor activated determines the nature of the response (Figure 1.1). These neurotransmitter receptors can either mediate the direct opening of an ion channel (ionotropic receptor) promoting a fast transmission, or alter the concentration of intracellular metabolites (metabotropic receptor) resulting thus in a slow transmission (Squire *et al.*, 2002).



**Figure 1.1. Chemical synapse through neurotransmitter-gated ion channels.** The arrival of a nerve impulse at the terminus of the neuron triggers the fusion of synaptic vesicles with the plasma membrane, resulting in the release of neurotransmitters from the presynaptic cell into the synaptic cleft. The neurotransmitter binds to receptors and opens ligand-gated ion channels in the target cell plasma membrane. Adapted from Cooper, M. The cell, a molecular approach, 2<sup>nd</sup> ed.

Ionotropic receptors are involved in fast synaptic signaling since binding of the neurotransmitter is followed within milliseconds by a fast conformational change that results in the opening of the intrinsic ion channel at the postsynaptic membrane (Unwin, 1993). They assemble in multisubunit complexes typically composed of different individual receptors that combine to form a ligand binding site and an integral ion channel (Nicke *et al.*, 1999). In contrast, binding of the neurotransmitter to metabotropic receptors activates nearby G-proteins. This catalyzes a series of reactions that results in the release of second messengers which bind, between others, to proteins forming an ion channel (Hille, 1992). The binding event alters the configuration of the channel and triggers for instance the opening of the pore, allowing ions to flow through. This is an indirect mechanism requiring a series of biochemical reactions that builds a response of slower onset and longer duration, typically in a time range from 100 ms to many seconds.



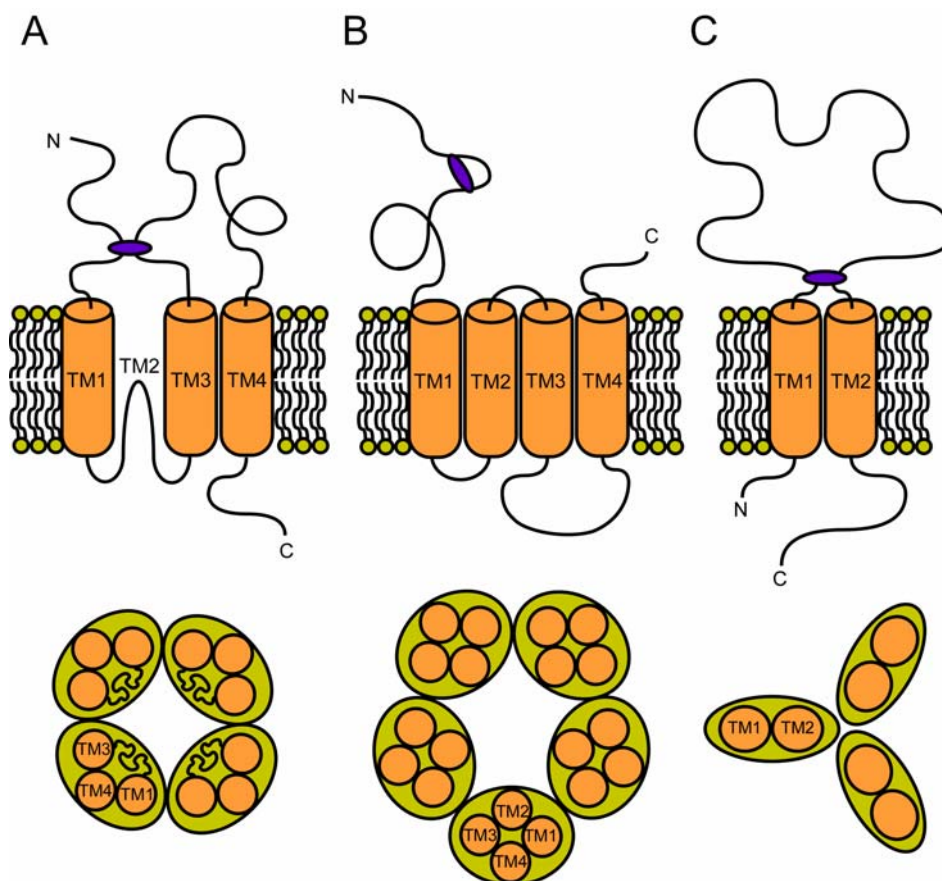
---

## 1.2 Ionotropic receptors

Ionotropic receptors, also known as ligand-gated ion channels (LGICs), are transmembrane, allosteric proteins which are regulated by binding of a ligand (neurotransmitter). The three major classes of ionotropic receptors are represented by:

- Ionotropic glutamate receptor family,
- Nicotinic acetylcholine receptor superfamily, and
- P2X ATP-gated receptor family.

The main differences between the three families are present at the level of the subunits structure and on how they arrange around the ion channel, as shown on figure 1.2 (Stromgaard, 2005). The principal characteristics of each family will be discussed below.



**Figure 1.2. Schematic representation of the structure of the three main families of ionotropic receptors.** (A) the ionotropic glutamate (iGlu) receptors, (B) the nicotinic acetylcholine (nACh) receptor family, and (C) the ATP-gated purinergic receptors (P2X). *Upper part.* Transmembrane topology, intra- and extracellular loops, and ligand-binding site of a single subunit. The binding region for the ligand is depicted in blue. *Lower part.* Assembly of the subunits around the channel pore. TM: transmembrane domain.

---

### 1.2.1 The ionotropic glutamate receptor family

Ionotropic Glutamate receptors (iGluRs) are expressed in the brain and spinal cord in pre- and postsynaptic cell membranes, playing an essential role in excitatory transmission and synaptic plasticity. The dysfunction of these receptors leads to several neuropathologies as epilepsy, ischemic brain damage and disruptive perception of pain (Madden, 2002). An iGluR consists of four subunits arranged as a dimer of dimers, whereas each subunit has three transmembrane domains (TM1, TM3, and TM4) and one re-entrant loop forming the pore (Figure 1.2A). The N-terminal domain lies at the extracellular side of the membrane whereas the C-terminal domain is located in the intracellular side of the membrane (Stromgaard, 2005). According to their selectivity to *N*-methyl-D-aspartate (NMDA) these ionotropic receptors are classified into NMDA and non-NMDA receptors. The latest are subsequent divided in two subfamilies depending on their response to selective glutamate analogues: the kainic acid and the  $\alpha$ -amino-3-hydroxy-5-methyl-4-isoxazolepropionic acid (AMPA). In mammals four AMPA receptors genes (GluR1-4), five kainate receptors genes (GluR5-7 and KA1-2), seven NMDA receptor genes (NR1, NR2A-D, NR3A and NR3B), and two delta subunits genes are known (Mayer, 2005). Ionotropic Glutamate receptors are permeable to both  $K^+$  and  $Na^+$ , and, depending on subunit composition, they can be permeable to divalent cations as well. NMDA receptors present a slow kinetic of activation that results in a large  $Ca^{2+}$  influx and require glycine as a co-transmitter (Furukawa and Gouaux, 2003).

### 1.2.2 The nicotinic acetylcholine receptor superfamily

The nicotinic acetylcholine receptors, also called Cys-loop receptors, constitute the largest and most studied neurotransmitter-gated channel family. It comprises both excitatory cation-conducting ionotropic receptor channels, like the nicotinic acetylcholine receptor (nAChR) and the 5-hydroxytryptamine receptor ( $5-HT_3$ ), and inhibitory  $Cl^-$ -conducting ionotropic receptors as the  $\gamma$ -aminobutyric acid receptor ( $GABA_A$ R) and the glycine receptor

---

(GlyR). All of them assemble as homo- or heteropentamers, sharing a common membrane topology and exposing extracellularly a large N-terminal domain with a Cys-loop (Figure 1.2B). Each subunit presents three membrane spanning regions (TM1 to TM3) with small intracellular linkers in between, a long cytoplasmic loop, and a fourth transmembrane region (TM4), which place the C-terminal domain at the extracellular side of the membrane (Jensen *et al.*, 2005).

The nAChRs and 5-HT<sub>3</sub>Rs conduct small monovalent cations with poor discrimination between them, being Na<sup>+</sup> and K<sup>+</sup> the main ions fluxing across the channel. However, a Ca<sup>2+</sup> conductance is also observed in many nAChRs especially in the neuronal nAChRs where the Ca<sup>2+</sup> permeability is the highest (Bertrand *et al.*, 1993).

### **1.2.3 The P2X ATP-gated receptor family**

ATP-gated P2X receptors are a large family of ionotropic receptors proposed to pre-synaptically facilitate and post-synaptically modulate fast synaptic transmission (Illes and Ribeiro, 2004), although their exact role in neuronal function has not been elucidated so far. P2X receptors belong to the growing family of purinergic receptors, since they are gated by a purine-based neurotransmitter (ATP). Their electrophysiological properties account for cation-selectivity with almost equal permeability to Na<sup>+</sup>, K<sup>+</sup>, and significant permeability to Ca<sup>2+</sup> (Soto *et al.*, 1997). Activation of these receptors is generally associated with an increase of the intracellular Ca<sup>2+</sup> level, which can be due to both direct Ca<sup>2+</sup> influx through the intrinsic pore and indirectly by depolarization of the plasma membrane and subsequent activation of voltage-gated Ca<sup>2+</sup> channels. Mammalian P2X receptor family comprises at least seven proteins (P2X<sub>1</sub>-P2X<sub>7</sub>) that are between 379 (P2X<sub>6</sub>) and 595 (P2X<sub>7</sub>) amino acids in length (Soto *et al.*, 1997; North, 2002) and present 40 to 50 % identity in their amino acidic sequence.

---

Orthologue P2X subunits have been cloned from other vertebrates including chicken (Ruppelt *et al.*, 1999; Ruppelt *et al.*, 2001) and zebrafish (Boue-Grabot *et al.*, 2000a; Egan *et al.*, 2000), and they also have been found in the parasite *Schistosoma mansoni* (Agboh *et al.*, 2004). However, no P2X receptor subunits have been identified so far in worms, insects or bacteria.

In rodents, most P2X receptor subunits are ubiquitously expressed, with mainly P2X<sub>2</sub>, P2X<sub>4</sub> and P2X<sub>6</sub> subunits found in the brain (Collo *et al.*, 1996; Seguela *et al.*, 1996; Kanjhan *et al.*, 1999; Rubio and Soto, 2001). Remarkably, the three subunits have been found to be localized at the outer portion of the postsynaptic membrane in excitatory synapses of hippocampus and cerebellum (Rubio and Soto, 2001). This precise subcellular placement of P2X receptors might be crucial for their role in synaptic transmission.

The P2X<sub>2</sub> receptor is the focus of this thesis, thus the P2X receptors subunit family will be described individually in further detail.

### **1.3 Purinergic receptors**

Purine-gated receptors were first proposed in 1976 and two years later two types of purinergic receptors, P1 for adenosine and P2 for ATP/ADP responsive receptors, were pharmacologically described (Burnstock, 1978). All P1 adenosine receptors are typical metabotropic receptors associated to G-proteins of which four subtypes have been cloned so far, namely A<sub>1</sub>, A<sub>2A</sub>, A<sub>2B</sub> and A<sub>3</sub> (Ralevic and Burnstock, 1998). P2 receptors are subdivided into P2X and P2Y subtypes (Burnstock and Kennedy, 1985), being P2Y a family of G protein-coupled receptors (metabotropic) and P2X a family of neurotransmitter-gated ion channel receptors (ionotropic) (North and Barnard, 1997).

#### **1.3.1 ATP as a neurotransmitter activating P2 receptors**

More than 20 years ago it was reported a selective and potent excitation of a subpopulation of rat dorsal horn neurons by ATP (Jahr and Jessell, 1983) showing thus the

---

first direct evidence of a response in neurons induced by extracellular ATP. There are several sources of extracellular ATP, the most obvious of which is cytosolic ATP (3-5mM). ATP can be released by sudden breakage of intact cells or via intrinsic plasma membrane channels and pores in the absence of irreversible cytolysis (Dubyak, 1993). In addition, ATP is specifically concentrated within secretory granules or vesicles of many neuronal and non-neuronal cells, thus important amounts of extracellular ATP come from exocytic release. No longer ago it was found that also glial cells were a source of extracellular ATP during propagation of  $Ca^{2+}$ -waves, in the presence of glutamate or by mechanical stimulation (Haydon, 2001). It was recently shown that ATP released from glial cells can influence neuronal synaptic transmission (Newman, 2003), revealing a new role for this group of cells.

### **1.3.2 P2X receptors**

#### **1.3.2.1 Membrane topology**

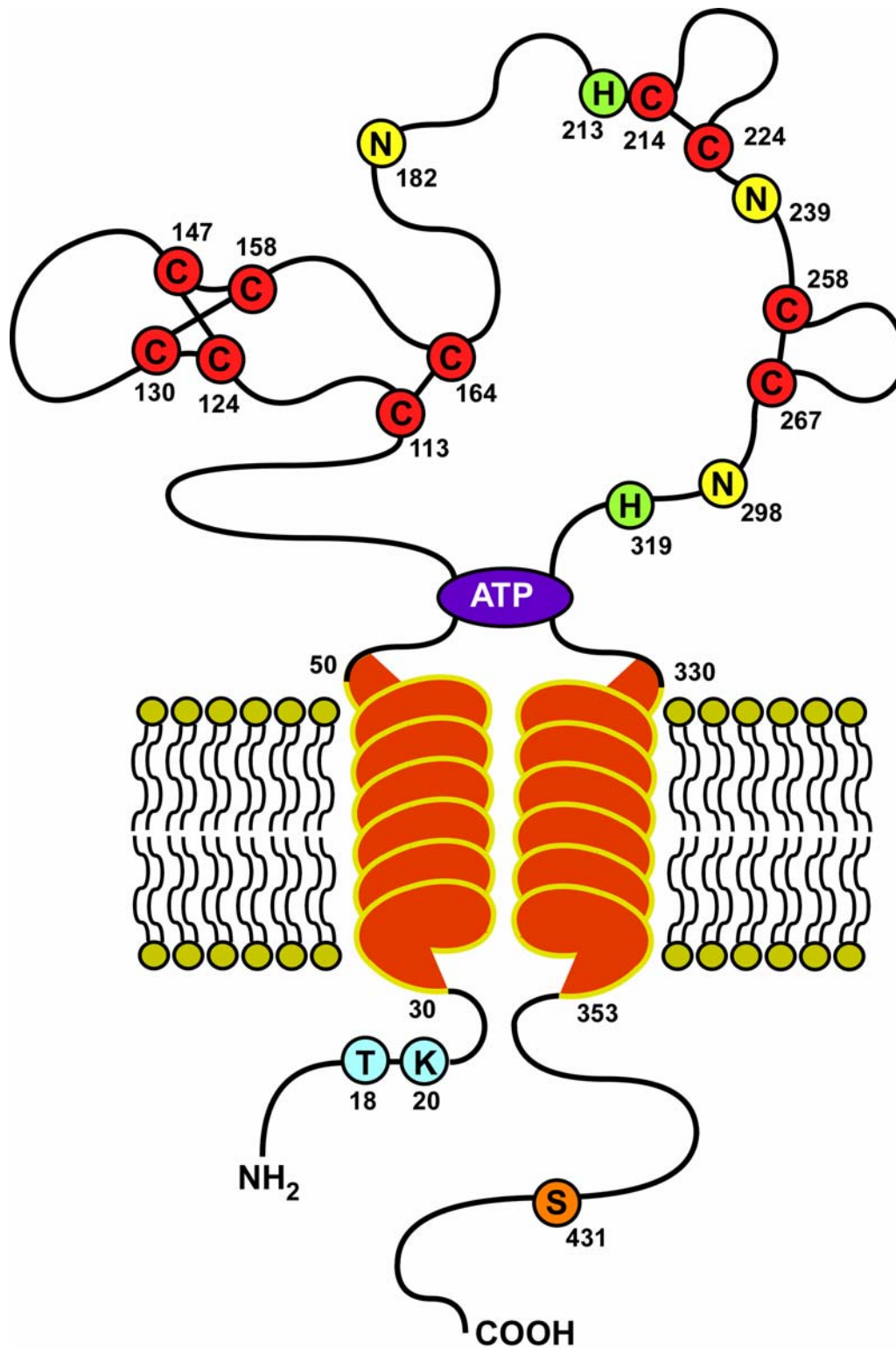
The proposed membrane topology of P2X receptors (Figure 1.2C) differs from that of the other two ionotropic receptors family mentioned above, but closely resembles that of several other families of ion channels with two membrane domains, as the epithelial sodium channel and related proteins (DEG/ENaC superfamily). Each P2X subunit has both the N- and C-terminus located intracellularly, with two transmembrane domains (TM1 and TM2) crossing the plasma membrane and placing the bulk of the protein extracellularly (North, 2002). This topology was predicted by hydrophobicity plots and was confirmed by the use of antibodies to putative intracellular or extracellular domains of P2X<sub>2</sub> (Torres *et al.*, 1998a), as well as N-glycosylation site tagging experiments (Newbolt *et al.*, 1998).

***The amino-terminal tail.*** The N-terminal domains of P2X subunits are short relative to the C-terminal domains. All P2X subunits contain a protein kinase C (PKC) putative phosphorylation site (Thr-X-Lys/Arg, PKC; Figure 1.3) in the amino-terminal tail (Khakh, 2001). Point mutations that remove the consensus PKC site increase the rate of channel

---

inactivation under prolonged exposure to the agonist (Boue-Grabot *et al.*, 2000b). In addition, cysteine-scanning mutagenesis of the P2X<sub>2</sub> receptor in residues Asp15, Pro19, Val23 and Val24 (Figure 1.3) indicated that methanethiosulfonates (which bind to free cysteine residues) can inhibit ATP-elicited currents by 60% (Jiang *et al.*, 2001). These results suggest that the intracellular N-terminus of P2X receptors could participate in the regulation of ionic conduction and that it may be part of the ion conducting pore.

***The extracellular loop.*** This domain spans for approximately 280 amino acids presenting a high degree of identity between all seven mammalian P2X subunits. It contains 10 conserved cysteines and 6 conserved lysines and, depending on the P2X subunits, it shows two to six putative N-linked glycosylation sites (North, 1996) (Figure 1.3). It is also believed that the extracellular domain contains the ATP binding site and regions for binding of antagonists and modulators. Thus, lysine residues of the extracellular domain have shown to be critical in the response to the antagonists PPADS and suramin, both in human and rat P2X<sub>4</sub> subunits (Buell *et al.*, 1996; Garcia-Guzman *et al.*, 1997). On the other hand, Jiang and colleagues, by alanine-scanning mutagenesis on the P2X<sub>2</sub> subunit, identified two lysine residues (Lys69 and Lys71) located proximal to the first transmembrane domain that are critical for the action of ATP (Jiang *et al.*, 2000).



**Figure 1.3. Representation of the P2X<sub>2</sub> subunit membrane topology.** The extracellular loop contains 10 conserved cysteines residues (red), three N-linked glycosylation sites (yellow) and two histidines implicated in metal binding and pH regulation (green). Both transmembrane domains adopt an  $\alpha$ -helical conformation positioning the carboxyl and amino terminus towards the intracellular side of the membrane. The N-terminal domain presents a PKC conserved site (light blue) and the C-terminal tail possess a PKA site (orange).

---

**Transmembrane domains.** The transmembrane domains (TM1 and TM2) in P2X receptors are long enough to span the plasma membrane in  $\alpha$ -helical conformation (Figure 1.3). It was shown by substituted cysteine accessibility, where residues are mutated individually to cysteine and the accessibility of the side-chain in the expressed channels is probed with a water soluble sulfhydryl reagent, that residues located near the border of the TM2 line the pore of P2X receptors (Rassendren *et al.*, 1997a ; Egan *et al.*, 1998). Later, Jiang and colleagues suggested that the Val48 located in the outer end of the TM1 takes part in the gating movement of P2X<sub>2</sub>, together with residues located in the outer portion of the TM2 (Jiang *et al.*, 2001). In the same work, the authors suggested that in both transmembrane segments all of the accessible residues mapped by cysteine scanning can be aligned along one face of an  $\alpha$ -helix. However, an alanine scan of both TMs in P2X<sub>2</sub> subunits revealed a model consistent with helical structure for TM1, but is inconclusive for TM2 (Li *et al.*, 2004). In addition, a recent tryptophan scan procedure provided evidence that TM1 and the outer region of TM2 adopt  $\alpha$ -helical secondary structures in P2X receptor channels (Silberberg *et al.*, 2005). In the P2X<sub>2</sub> subunit the second transmembrane domain seems to be  $\alpha$ -helical in the closed state, but not when the channel is open (Khakh, 2001).

**The carboxy-terminal tail.** The C-terminal tails are highly divergent both in length (from 28 to 242 residues) and amino acidic composition among the different P2X subunits. However, between orthologues the C-terminal domain is quite conserved both in length and sequence which may indicate some important role in function specialization.

The carboxyl terminus of P2X<sub>2</sub> receptor contains a consensus phosphorylation sites for cyclic AMP (cAMP)-dependent protein kinase (PKA; Figure 1.3), suggesting that the function of the P2X<sub>2</sub> receptor could be regulated by protein phosphorylation (Chow and Wang, 1998). Modification of this domain by mutations, deletion or splicing modulates the kinetics and pharmacological properties of the channel (Surprenant *et al.*, 1996; Eickhorst *et*



---

*al.*, 2002; Smart *et al.*, 2003). In addition, interaction of the C-terminal domain of P2X receptors with intracellular proteins is suggested to be important for the localization and function regulation of these channels (Wilson *et al.*, 2002; Gendreau *et al.*, 2003).

### **1.3.2.2 Multimerization**

The stoichiometry of P2X receptors is thought to involve three subunits, thus the channel could be a homo- or heterotrimer. Homomultimer association of P2X leads, in most of the receptors, to a functional ion channel and thus this is the preferred state to study the pharmacological properties of such receptors. Heteromultimers were evidenced for P2X<sub>2/3</sub> receptors in nodose ganglia (Lewis *et al.*, 1995), P2X<sub>4/6</sub> receptors in central nervous system (CNS) neurons (Le *et al.*, 1998), P2X<sub>1/5</sub> receptors (Torres *et al.*, 1998b; Haines *et al.*, 1999), P2X<sub>2/6</sub> receptors (Torres *et al.*, 1999; King *et al.*, 2000), and more recently P2X<sub>1/2</sub> receptors (Brown *et al.*, 2002) and P2X<sub>1/4</sub> (Nicke *et al.*, 2005). P2X<sub>6</sub> receptors do not assemble functional homomultimers (Soto *et al.*, 1996) though only form functional receptors in combination with other P2X subunits (Le *et al.*, 1998), while P2X<sub>7</sub> receptors form functional homomultimers but do not assemble with any other P2X subunit (Torres *et al.*, 1999). Heteromultimerization studies are of broad interest since P2X receptor subunits show overlapping distribution in many tissues, hence native P2X receptors might well mostly be of heteromultimeric composition. *In vitro*, P2X<sub>1</sub>, P2X<sub>2</sub>, P2X<sub>3</sub>, P2X<sub>5</sub> and P2X<sub>6</sub> subunits can associate with each other to form stable complexes (Torres *et al.*, 1999).

### **1.3.2.3 Functional and pharmacological characteristics of heterologously expressed P2X receptors**

Individual P2X subunits form functional ATP-gated cationic channels when expressed in heterologous systems. However, the efficiency in forming a functional P2X receptor differs from one subunit to another (Soto *et al.*, 1997). For example, functional expression of P2X<sub>6</sub> receptors has only been reported in HEK-cells (Collo *et al.*, 1996), but it is believed

---

that these cells express endogenous P2X<sub>4</sub> receptor. In fact, it was not possible to express functional P2X<sub>6</sub> receptor in *Xenopus* oocytes (Soto *et al.*, 1996). Also, small currents of rat P2X<sub>5</sub> were found in transient transfected cells when they were compared with any other P2X subunit (Collo *et al.*, 1996; Garcia-Guzman *et al.*, 1996). However, heterologous expression of chicken P2X<sub>5</sub> in HEK-293 cells leads to the formation of functional homomeric receptors (Ruppelt *et al.*, 2001).

P2X receptors activate in milliseconds upon binding of ATP and the current rise-time varies between 2 and 25 ms depending on the specific receptors. Another property that can be measured is how fast receptors tend to lose their ability to conduct ions in the continuous presence of the agonist (desensitization). Heterologously expressed P2X<sub>1</sub> and P2X<sub>3</sub> receptors desensitize in the presence of ATP with time constants in the 100-300 ms range, whereas P2X<sub>2</sub> and P2X<sub>4</sub> show sustained currents with a very slow desensitization (time constant of second to tens of seconds), and P2X<sub>7</sub> receptor shows no desensitization during application lasting for many seconds (North, 2002).

Like native P2X receptors, heterologously expressed P2X receptors discriminate poorly between monovalent cations (Edwards and Gibb, 1993). Homomeric P2X<sub>1</sub>, P2X<sub>3</sub>, and P2X<sub>4</sub> receptors present a high Ca<sup>2+</sup> permeability ( $P_{Ca}/P_{Na} \sim 4$ ) (Valera *et al.*, 1994; Evans *et al.*, 1995; Lewis *et al.*, 1995; Soto *et al.*, 1996; Garcia-Guzman *et al.*, 1997). Whereas, Ca<sup>2+</sup> permeability of P2X<sub>2</sub> receptors is lower ( $P_{Ca}/P_{Na} 2.2$ ) (Evans *et al.*, 1996) and moreover, Ca<sup>2+</sup> inhibits the currents evoked by ATP at rat P2X<sub>2</sub> receptor possibly by allosteric modulation of the ATP binding affinity (Soto *et al.*, 1997). Influx of Ca<sup>2+</sup> is of particular interest because it activates second messenger pathways. Thus, through Ca<sup>2+</sup>-permeable receptor channels, ATP may play a role in neuronal toxicity similar to glutamate through NMDA receptors, but without the necessity of membrane depolarization to produce the influx of Ca<sup>2+</sup> (Soto *et al.*, 1997).

---

Two kinds of deviations from these pore properties have been described. First, chicken and human P2X<sub>5</sub> receptors, in addition to cations, allow Cl<sup>-</sup> ions to pass (Ruppelt *et al.*, 2001; Bo *et al.*, 2003), and second, P2X<sub>2</sub>, P2X<sub>4</sub> and P2X<sub>7</sub> receptors become increasingly permeable to organic cations (e.g. N-methyl-D-Glucamine) and fluorescent dyes during prolonged or repeated exposure to extracellular ATP (Surprenant *et al.*, 1996; Khakh *et al.*, 1999; Virginio *et al.*, 1999). Changes on the selectivity of these channels from small cations towards anions or larger organic cations are influenced by many factors. For example, the kinetics and extend of these selectivity changes can be perturbed by point mutations in the transmembrane segments (Virginio *et al.*, 1999; Khakh and Egan, 2005), and by deletions, chimeras and point mutations in their intracellular C-terminal domain (Surprenant *et al.*, 1996; Rassendren *et al.*, 1997b; Eickhorst *et al.*, 2002; Fisher *et al.*, 2004).

***Agonist and antagonist pharmacology of P2X receptors.*** All cloned P2X receptors activate upon ATP application with a half maximal response (EC<sub>50</sub>) that oscillates between submicromolar concentrations for P2X<sub>1</sub> and P2X<sub>3</sub> and low micromolar concentrations for P2X<sub>2</sub>, P2X<sub>4</sub>, P2X<sub>5</sub> and P2X<sub>6</sub> subunits. For P2X<sub>7</sub> the EC<sub>50</sub> rise to concentrations of 100 mM and 1 mM for the rat P2X<sub>7</sub> and human P2X<sub>7</sub>, respectively (Soto *et al.*, 1997). All other P2X agonist known so far are ATP analogs as for example,  $\alpha,\beta$ -methylene-ATP ( $\alpha,\beta$ -meATP), 2-methylthio-ATP (2MeSATP), and 2',3'-(4-benzoyl)-benzoyl ATP (BzATP). P2X<sub>1</sub> and P2X<sub>3</sub> subunits are as sensitive to  $\alpha,\beta$ -meATP as to ATP, but not the remaining subunits, and BzATP is one order of magnitude more potent than ATP for P2X<sub>7</sub> receptors (Rassendren *et al.*, 1997b).

Several P2X antagonist have been studied, and they account for dyes such as reactive blue 2, reactive red, trypan blue, evans blue and brilliant blue, as well as for several compounds as the antitrypanocidal drug suramin, the ATP affinity label oxidized ATP, and the pyridoxalphosphate analogue PPDAS (Lambrecht, 1996). Different sensitivity to a given

---

antagonist among P2X subunits has been shown. Thus, P2X<sub>1</sub> and P2X<sub>2</sub> receptors are blocked by PPADS in an almost irreversible way, due to several minutes of wash are necessary before the blocking action is completely reversed. In contrast, block by PPADS of rP2X<sub>3</sub> and rP2X<sub>5</sub> is rapidly washed out. On the other hand, the block by suramin is rapidly reversible for all the P2X subunits (Soto *et al.*, 1997). However, both suramin and PPADS weakly affected currents evoked by ATP in cells expressing the rP2X<sub>4</sub> and rP2X<sub>6</sub> receptors (Collo *et al.*, 1996; Soto *et al.*, 1996).

#### **1.4 Role of scaffolding and adapter proteins in synaptic transmission**

The cytoplasmic surface of the postsynaptic membrane of excitatory synapses is known as the postsynaptic density (PSD). Besides ionotropic and G-protein-coupled receptors, many other molecules have been identified in the PSD, such as adapters and scaffolding proteins, enzymes involved in phosphorylation-dephosphorylation mechanisms, and cytoskeletal proteins. The current scenario is that the cross-talk between each of these proteins may have essential functions for the development of synaptic plasticity (Bockers *et al.*, 2001).

Adapter and scaffolding proteins are large multidomain proteins generally composed of many modules necessary for the assembly of signaling complexes. These modules are highly conserved protein-protein interaction domains such as phosphotyrosine binding domains (PTB), PSD-95/disc-large/Zo-1 domains (PDZ), *src* homology domains (SH2 and SH3), WW domains, and 14-3-3 domains (Pawson and Scott, 1997). Scaffolding and adapter proteins are widely recognized as major players in the organization of the postsynaptic signal transduction machinery, where they regulate receptor trafficking and clustering, modulate axon path finding, and drive the correct targeting of neuronal proteins to their appropriate cytoplasmic compartment (Bockers *et al.*, 2001).

---

#### 1.4.1 Fe65 is a brain-specific adapter protein

Fe65 is an adapter protein that was first identified as a product of a brain-specific transcript from differential screening of a rat brain library (Ermekova, 1998). Mammalian Fe65 genes encode three homologous proteins sharing a similar modular structure. These proteins are called Fe65, Fe65 like 1 (Fe65L1), and Fe65 like 2 (Fe65L2). Fe65 like 1 and Fe65 like 2 are ubiquitously expressed, whereas the Fe65 gene presents a high and widespread expression in brain regions as demonstrated by Northern analysis and *in situ* hybridization on mouse brain. These studies revealed that Fe65 is expressed in areas of the brain with the highest neural density, including the cerebellum, cortex, hippocampus, medial habenular nucleus, and olfactory bulb (Bressler *et al.*, 1996). During mouse embryo development, expression of this gene is restricted to neural structures, especially to nerve ganglia (Simeone *et al.*, 1994). However, low levels of Fe65 mRNA are also found in multiple non-neural tissues and cell types (Bressler *et al.*, 1996). There is a high level of conservation between the mouse, rat, and human Fe65 protein sequences. Human Fe65 mRNA is 88% similar to the rat Fe65 mRNA and the predicted human protein sequence is 95% similar to the predicted rat Fe65 protein (Duilio *et al.*, 1991; Bressler *et al.*, 1996). Furthermore, the human and rat protein sequences are essentially identical within their conserved protein-interacting domains.

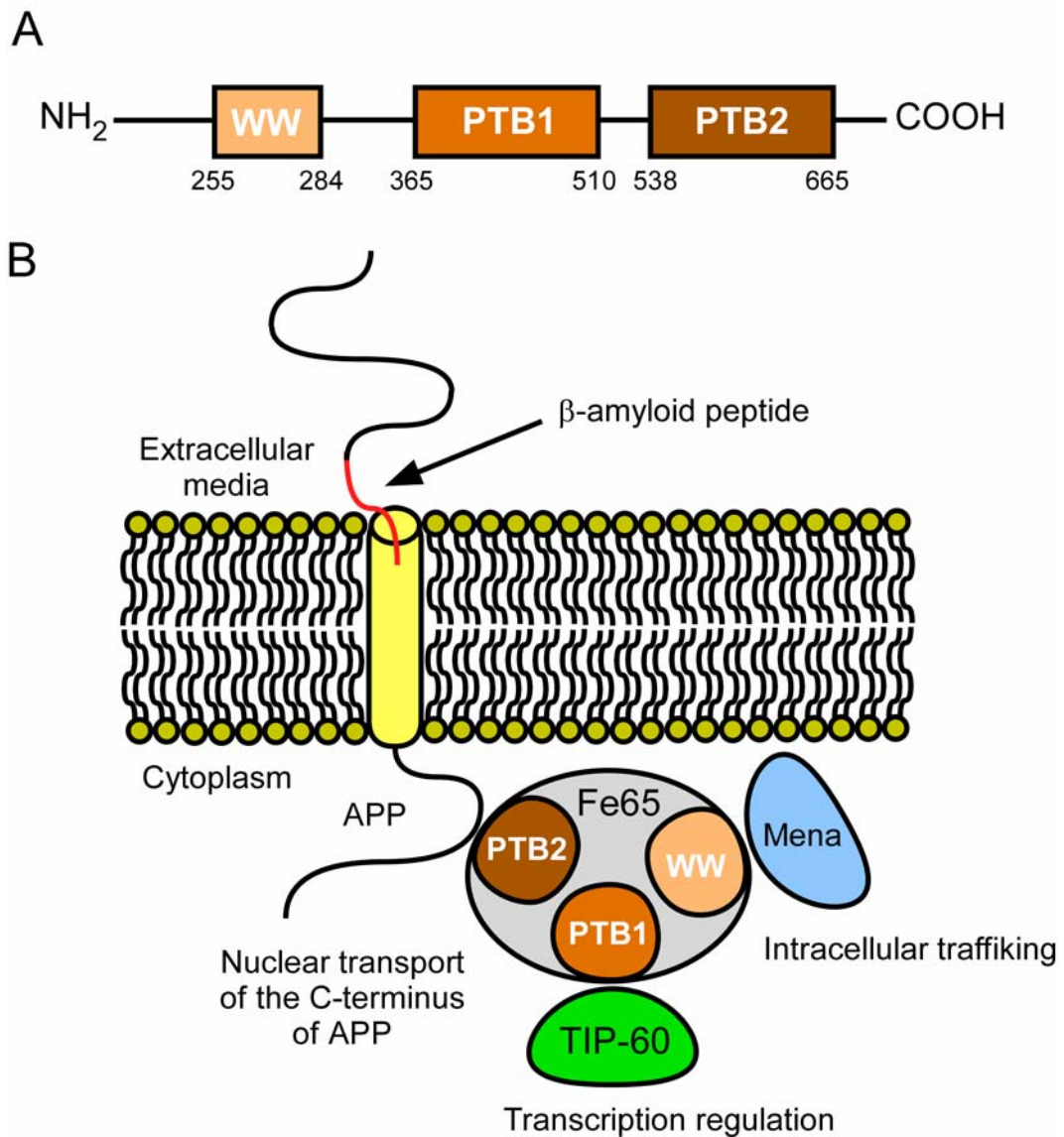
It has been suggested that Fe65 functions both as a transcription factor and as an adapter protein. Fe65 moves from the cytoplasm to the nucleus, and presents a short segment that functions as a strong transcription activator, suggesting that Fe65 could indeed activate transcription (Duilio *et al.*, 1991). Following the discovery in the Fe65 sequence of two novel protein-protein interaction domains, the PTB and the WW domain, it was suggested that Fe65 has also the characteristics of an adapter protein (Russo *et al.*, 1998) (Figure 1.4A).

---

**WW domains.** WW domains are small protein modules composed of approximately 40 amino acids that mediate protein-protein interactions by specific recognition of proline-rich ligands. The name refers to two signature tryptophan (W) residues that are spaced 20-22 amino acids apart and are present in most WW domains known to date (Bork and Sudol, 1994; Macias *et al.*, 2002). These domains are of special interest because they participate in a variety of cellular processes, including ubiquitin-mediated protein degradation, viral budding, RNA splicing, transcriptional co-activation, and mitotic regulation (Bedford *et al.*, 2000).

**PTB domains.** The phosphotyrosine binding domain, also known as the phosphotyrosine interaction domain (PID), is a modular interface of 100-170 amino acids important for protein-protein interaction. PTB domains share low sequence homology among themselves and exhibit extremely high ligand binding selectivity (Yan *et al.*, 2002). These domains preferentially bind to phosphorylated proteins containing an NPXpY motif (where pY is a phosphotyrosine and X is any amino acid) (Zhou, 1995; Yan *et al.*, 2002).

Through these domains Fe65 interacts with several proteins, participating thus in complex protein networks (Figure 1.4B). The most important role of Fe65 described up to date is the involvement in the trafficking of the cytoplasmic tail from the amyloid precursor protein (APP), relevant to the pathogenesis of Alzheimer disease, and thus Fe65 is also known as the amyloid precursor protein-binding protein 1 (APBB1). Via its C-terminal PTB domain, Fe65 interacts with APP, increases the proteolytic processing of APP to the  $\beta$ -amyloid peptide (Sabo *et al.*, 1999) and, together with a C-terminal fragment of APP, translocates to the nucleus, where both associate with the histone acetyltransferase Tip60 to regulate transcription (Cao and Sudhof, 2001). In addition, through its interaction with the mammalian homologue of *Drosophila* enabled (Ermekova *et al.*, 1997), Fe65 regulates axonal growth cone motility (Sabo *et al.*, 2001).



**Figure 1.4. Schematic representation of Fe65 structure and its interacting proteins.** (A) The three putative domains of Fe65 and their boundary residues. (B) Recognized protein-protein interaction partners of Fe65, and the proposed functional outcome of the complex.

---

## 2. AIMS OF THIS STUDY

The precise localization of P2X subunits at excitatory synapses suggests an interaction with intracellular proteins regulating function and/or anchoring of P2X receptors in the postsynaptic membrane. Thus, the hypothesis of this thesis work was that the intracellular C-terminus of P2X receptor subunits could associate with synaptic intracellular proteins. This interaction, either by determining localization or altering function, could mediate some aspects of the downstream signaling following synaptic P2X receptors activation.

The starting point to test this hypothesis was to perform a yeast two hybrid screening of a rat brain cDNA library employing the intracellular C-terminal domain of the rat P2X<sub>2</sub> subunit as bait. Among several proteins isolated, the brain-enriched adapter protein Fe65 was identified as an interacting partner of P2X<sub>2</sub> subunits.

To elucidate the nature of the interaction between the C-terminus domain of the rat P2X<sub>2</sub> receptor and the adapter protein Fe65 has been the major aim of this project. For this purpose we tackled different aspects of the complex formation employing a combination of molecular biological, biochemical, and electrophysiological techniques, as follows:

- Characterization of the complex formation *in vitro*. The molecular and structural basis of the interaction between Fe65 and P2X<sub>2</sub> subunits was analyzed by performing deletions and point mutations of the bait and prey proteins and testing the interaction by complementary yeast two-hybrid and GSTpull-down assays.
- Determination of the cellular and subcellular localization of Fe65 and its possible colocalization with P2X<sub>2</sub> subunits. Two different antibodies directed to Fe65 protein sequences were generated and characterized to determine the yet unknown distribution of Fe65 in rat brain. The same antibodies were used to study the colocalization of Fe65 and P2X<sub>2</sub> subunits in rat brain hippocampal synapses.



- 
- Determination of the direct interaction of Fe65 and P2X<sub>2</sub> *in vivo* by means of co-immunoprecipitation assays using specific antibodies for both proteins on crude rat brain membrane preparations. Using the same approach, investigation of whether APP, a major interaction partner of Fe65, takes also part of the same protein complex with P2X<sub>2</sub>.
  - Elucidation of the functional consequences of complex formation. The effect of this interaction on the functional properties of the receptor was investigated by electrophysiological approaches using as expression systems both mammalian cell lines and *Xenopus oocytes*.

---

### 3. MATERIAL AND METHODS

#### 3.1. Materials

##### 3.1.1. Equipment

Centrifuges	XL-90, Beckman
	J2-MI, Beckman
	5415 C, Eppendorf
	5402, Eppendorf
	Megafuge 2.0R, Heraeus
Developing machine	Curix 60, AGFA
Mini-PROTEAN II gel system	BIO-RAD
Patch-clamp amplifier (EPC-9)	HEKA Electronic
Photometer	Eppendorf
Pipette puller (HEKA PIP5)	HEKA Electronic
Refrigerated incubator innova 4330	New Brunswick Scientific
Speed Vac SC110	Savant
TRIO-Thermoblock™ (PCR)	Biometra
Transfer blot SD	BIO-RAD
Turbo TEC-10CD amplifier	NPI-Elektronik

##### 3.1.2. Chemicals and reagents

Acrylamide/Bisacrylamide Solution	BIO-RAD Laboratories
Agar	Gibco/BRL
Agarose	Gibco/BRL
AminoLink Plus Immobilization Kit	Pierce
Ammonium peroxydisulphate	Fluka

---

Adenosine 5'-Triphosphate Disodium salt (ATP)	Sigma
1,2-Bis(2-aminophenoxy)ethane- N, N, N', N'-tetraacetic acid- tetra potassium salt (BAPTA)	Sigma
Bromophenol Blue	Sigma
Chloroform	Sigma
Coomassie Brilliant Blue R250™	Biomol
Dextran sulfate	Amersham
Deoxycholic acid, sodium salt	Sigma
Diethyl pyrocarbonate (DEPC)	Sigma
Dimethylsulfoxide (DMSO)	Sigma
Dithiothreitol (DTT)	Sigma/Promega
dNTPs (100 mM)	Boehringer
Ethylenediamine tetraacetic acid (EDTA)	Sigma
EthyleneGlycol-bis (β-aminoethyl ether)- N, N, N', N'-tetraacetic acid (EGTA)	Sigma
Ethidium bromide	Fluka
Ficoll	Sigma
Films (X-Omat™ Blue Films)	Kodak
Filter 0,22 μm	Milipore
Formaldehyde	Fluka
Formamide	Fluka
FuGENE 6 (Transfection reagent)	Roche
Glass capillaries	Hilgenberg/Word Precision Instruments
Glutathione-agarose	Sigma
(2-hydroxyethyl)-1-piperazine ethanesulphonic acid (HEPES)	Biomol

---

Hybond ECL™ Nitrocellulose Membrane	Amersham Biosciences
Imidazole	Fluka
Isopropyl β-D-thiogalactopyranoside (IPTG)	Sigma
β-Mercaptoethanol	Sigma
m7G(5')ppp(5')G (CAP)	Boehringer Mannheim
N-Methyl-D-Glucamine (NMDG)	Sigma
Ni-NTA resin	QIAGEN
Paraformaldehyde	Fluka
Phenol	Gibco/BRL
Photographic fixer	Agfa
Photographic developer	Agfa
Protein G/A-agarose	Santa Cruz Biotechnology
Sodium dodecyl sulfate (SDS)	Fluka
Tetraaminethylenediamine (TEMED)	Sigma
Tris-base	Sigma
Tween 20 (Polyoxyethylenesorbitan monolaurate)	Sigma
Triton X-100	Sigma
Whatman™ filter paper	Schleicher & Schüll
5-bromo-4-chloro-3-indolyl-beta-D-galactopyranoside (X-Gal)	Biomol

All other chemicals, not listed above, were purchased from Merck.

### **3.1.3. Antibiotics**

Ampicillin	Roche
Geneticin™ (G418 sulphate)	Calbiochem

---

Kanamycin	Roche
Penicillin/Streptomycin	Gibco
Gentamicin (G1264)	Sigma
<b>3.1.4. Enzymes, inhibitors, substrates</b>	
A-, B-, L-, M-, H- Buffer	Roche
Bovine serum albumine (BSA)	Sigma
Collagen (rat)	Roche
Collagenase type 2	Worthington Biochemical Corporation
Complete Protease Inhibitor Cocktail Tablets (EDTA free)	Roche
DNase (RQ1) RNase free	Promega
Fetal calf serum (FCS)	Gibco
Horse serum (HS)	Gibco
Leupeptin	Sigma
NEBuffer	New England Biolabs
One-Phor-All Buffer (OPA)	Pharmacia
Pepstatin A	Sigma
<i>Pfu</i> DNA polymerase	Promega
<i>Pfu</i> 10X Rxn.buffer	Promega
Phenylmethylsulfonyl fluoride (PMSF)	Serva
Proteinase K	Roche
Phosphatase, alkaline	Promega
Poly-L-Lysin	Sigma
RNasin™ (RNase inhibitor)	Promega
T4-DNA-ligase	Promega

---

T7-RNA-polymerase	Promega
-------------------	---------

Transcription optimized 5 X buffer	Promega
------------------------------------	---------

### 3.1.5. Molecular weight standards

0.24-9.5 Kb RNA ladder	Invitrogen
------------------------	------------

1 kb DNA ladder	Invitrogen
-----------------	------------

100 bp DNA ladder	Invitrogen
-------------------	------------

Page Ruler™ Protein ladder	Fermentas
----------------------------	-----------

### 3.1.6. Kits and ready-to-use reagents

Bio-Rad Protein-Assay	BIO-RAD
-----------------------	---------

ECL™	Amersham Biosciences
------	----------------------

Midipreps DNA purification system	Wizard <sup>R</sup> Plus, Promega
-----------------------------------	-----------------------------------

NucleoBond PC 500	Macherey-Nagel
-------------------	----------------

NucleoSpin™ Plasmid	Macherey-Nagel
---------------------	----------------

ProLong Antifade Kit	Molecular Probes
----------------------	------------------

QIAEX II™ DNA purification kit	Qiagen
--------------------------------	--------

### 3.1.7. Plasmids

- *pcDNA3.1/myc-His B*. Invitrogen

- *pcDNA1*. Invitrogen

- *pEGFP-C3*. Clontech

- *pET32a* (+). Novagen

- *pGEX-4T-1*. Amersham Pharmacia Biotech

- *pGEM-T Easy*. Promega

---

- ***pLexN***. (Hollenberg *et al.*, 1995). Expresses the gene of interest as a fusion protein to the LexA-binding domain. It contains Ampicillin resistance and *Trp1* nutritional genes for selection in bacteria and yeast, respectively. For Y2H use.

- ***pSGEM***. Prof. Michael Hollmann, Bochum University. A vector based on pGEM-3Z vector containing 3' and 5' UTR from a *Xenopus laevis*  $\beta$ -globin gene flanking a polylinker derived from the MCS of pBluescript vector. Includes a cassette of four restriction sites upstream of the SP6 promoter for sense template linearization (Villmann *et al.*, 1997).

- ***pVP16-4***. (Hollenberg *et al.*, 1995). Generates fusion of the gene of interest to the GAL4-activation domain. It has ampicillin resistance and *Leu2* nutritional genes for selection in bacteria and yeast, respectively. For Y2H use.

### 3.1.8. Synthetic oligonucleotide primers

Synthetic oligonucleotide primers were used for PCR reactions, sequencing of DNA constructs or introduction of mutations into DNA. Primers were synthesized by Metabion (Planegg-Martinsried) in a HPLC purity grade. See list of primers on Appendix.

### 3.1.9. List of DNA constructs

- ***Fe65 constructs***. Different Fe65 plasmids were constructed by PCR-based strategies based on the corresponding full length rat sequence, a kind gift from Dr. Thomas Sudhof, University of Texas Southwestern, TX, USA.

- a) *Fe65 full length* in pcDNA3.1/myc-His B, for eukaryotic cell transfection.
- b) *Fe65 full length* in pSGEM, for cRNA production.
- c) *Fe65*<sub>(218-479)</sub> in pVP16-4. This is the consensus sequence derived from Y2H studies observed to interact with P2X<sub>2</sub>CD, named Fe65-202, cloned as a fusion of the VP16-activation domain, for direct Y2H assays. The numbers in brackets for this and next Fe65 constructs correspond to the amino acid as in the sequence gi:13377731 of GENBANK.

- 
- d) Fe65<sub>(218-309)</sub> in pVP16-4. Deletion mutant based on c), harboring the WW domain plus 5' and 3' flanking sequences, for direct Y2H assays.
- e) Fe65<sub>(218-284)</sub> in pVP16-4. Deletion mutant based on c), harboring the WW domain plus the 5' flanking sequence, for direct Y2H assays.
- f) Fe65<sub>(255-284)</sub> in pVP16-4. Deletion mutant based on c), harboring only the WW domain of Fe65, for direct Y2H assays.
- g) Fe65<sub>(285-479)</sub> in pVP16-4. Deletion mutant based on c), harboring the PTB1 domain of Fe65, for direct Y2H assays.
- h) Fe65L1<sub>(1-321)</sub> in pVP16-4. This is the consensus sequence derived from Y2H studies observed to interact with P2X<sub>2</sub>CD, cloned as a fusion of the VP16-activation domain. The numbers in brackets for this constructs correspond to the amino acid as in the sequence found in the screening (See Appendix).
- i) Fe65<sub>(218-479)</sub>M1 in pVP16-4\*. Triple mutant on the WW domain that disrupts its binding activity, constructed on the plasmid described in c). The following mutations were introduced: Y<sub>260</sub>A, Y<sub>261</sub>A and W<sub>262</sub>A, and the construct was employed for direct Y2H assays.
- j) Fe65<sub>(218-479)</sub> in pET32a(+). The consensus construct Fe65-202 derived from Y2H studies was cloned as a thioredoxin (Trx) fusion (Trx-Fe65-202), which allowed recombinant protein expression in *E. coli*, for pulldown assays.
- k) Fe65<sub>(218-479)</sub> in pGEX-4T-1. Consensus construct as in j) cloned as a glutathione-S-transferase (GST) fusion (GST-Fe65-202), allowing recombinant expression of the protein in *E. coli* for pulldown assays.
- l) Fe65<sub>(197-255)</sub> in pGEX-4T-1. GST fusion construct for recombinant expression in bacteria, employed for antibody generation (antibody anti-Fe65-32).



---

m) Fe65<sub>(40-100)</sub> in pGEX-4T-1, GST fusion construct for recombinant expression in bacteria, employed for antibody generation (antibody anti-Fe65-35).

- **P2X<sub>2</sub> constructs.** P2X<sub>2</sub> constructs were obtained via PCR-based strategies on the corresponding rat sequence. The original plasmid for P2X<sub>2</sub> and P2X<sub>2</sub> splice variant were a generous gift of Prof. David Julius and Dr. Elizabeth Glowatzki, respectively.

- a) P2X<sub>2</sub> *full length* in pcDNA1, for eukaryotic cell transfection and production of cRNA.
- b) P2X<sub>2</sub>(355-472) in pLexN. C-terminal domain of P2X<sub>2</sub> (P2X<sub>2</sub>CD) fused to the LexA-binding domain, employed as bait in Y2H assays.
- c) P2X<sub>2</sub>(355-416) in pLexN. Deletion of the last two Pro-rich domains of P2X<sub>2</sub>CD, constructed on the plasmid described on b), for direct Y2H assays.
- d) P2X<sub>2</sub>(417-472) in pLexN. Deletion of the first two Pro-rich domains of P2X<sub>2</sub>CD, constructed on the plasmid described on b), for direct Y2H assays.
- e) P2X<sub>2</sub>(355-400) in pLexN\*. Deletion of the P2X<sub>2</sub>CD containing only the first Pro-rich domain, constructed on the plasmid described on b), for direct Y2H assays.
- f) P2X<sub>2</sub>(401-472) in pLexN\*. Deletion of the P2X<sub>2</sub>CD containing the last three Pro-rich domains, constructed on the plasmid described on b), for direct Y2H assays.
- g) P2X<sub>2</sub>(355-403) SV in pLexN. C-terminal domain of the splice variant of the P2X<sub>2</sub> receptor ( $\Delta_{370-437}$ ) (P2X<sub>2(b)</sub>CD) fused to the LexA-binding domain, employed as bait in Y2H assays.

- 
- h) P2X<sub>2</sub>(<sub>355-472</sub>) in pET32a(+). Construct harboring the C-terminus of the P2X<sub>2</sub> receptor fused to Trx (Trx-P2X<sub>2</sub>CD), which allowed recombinant protein expression in *E. coli*, for pulldown assays.
  - i) P2X<sub>2</sub>(<sub>355-472</sub>) in pGEX-4T-1. Construct as in h) cloned as a GST fusion (GST-P2X<sub>2</sub>CD), allowing recombinant expression of the protein in *E. coli* for pulldown assays.
  - j) P2X<sub>2</sub>(<sub>355-403</sub>) SV in pET32a(+). C-terminal domain construct of the splice variant of the P2X<sub>2</sub> receptor ( $\Delta_{370-437}$ ) (P2X<sub>2(b)</sub>CD) as a fusion to Trx (Trx-P2X<sub>2(b)</sub>CD), which allowed recombinant protein expression in *E. coli*, for pulldown assays.

- **P2X<sub>7</sub> constructs.** The full length rat P2X<sub>7</sub> was employed as a negative control on various cellular studies.

- a) P2X<sub>7</sub> *full length* in pSGEM, for eukaryotic cell transfection and production of cRNA.

\* These plasmids were constructed by Anja Bremm.

See list of constructs, respective primers, and the nucleotide and amino acid sequences of P2X<sub>2</sub>, Fe65 and Fe65-like 1 in Appendix.

### 3.1.10. Antibodies

- **Anti-P2X<sub>2</sub> receptor** - rabbit polyclonal antibody raised against residues 457-472 of rat P2X<sub>2</sub> (Alomone labs).

- **Anti-P2X<sub>2</sub> receptor** - rabbit polyclonal antibody raised against residues 457-472 of rat P2X<sub>2</sub> (USBiological).

- **Anti-P2X<sub>4</sub> receptor** - rabbit polyclonal antibody raised against residues 370-388 of rat P2X<sub>4</sub> (Alomone labs).

---

- ***Anti-P2X<sub>7</sub> receptor*** - rabbit polyclonal antibody raised against residues 576-595 of rat P2X<sub>7</sub> (Calbiochem).

- ***Anti-APP*** - rabbit polyclonal antibody raised against the C-terminal domain of the human Amyloid precursor protein (amino acids 676-695) (Sigma).

- ***Anti-GST (B-14)*** - mouse monoclonal IgG antibody directed to the GST protein encoded by a pGEX.3X vector (Santa Cruz Biotechnology).

***Anti-Fe65-32*** - polyclonal antibody raised in rabbit against amino acids 197-255 of Fe65 (custom generated by Eurogentec using a fusion protein produced in our laboratory).

- ***Anti-Fe65-35*** - polyclonal antibody raised in rabbit against amino acids 40-100 of Fe65 (custom generated by Eurogentec using a fusion protein produced in our laboratory).

- ***Anti-c-myc*** - mouse monoclonal antibody (clone 9E10), recognizes the 9E10 epitope (Roche).

- ***IgG rabbit*** - IgG rabbit serum (Sigma-Aldrich logistik).

- ***Goat-anti-rabbit*** - Horseradish peroxidase-labeled (HRP) secondary antibody raised against rabbit IgG (BIO-RAD).

- ***Goat-anti-mouse*** - Horseradish peroxidase-labeled (HRP) secondary antibody raised against mouse IgG (BIO-RAD).

### **3.1.11. Organisms and growth media**

#### **3.1.11.1. Bacterial strain genotype**

- ***Escherichia coli DH5 $\alpha$*** . F<sup>-</sup>, *endA1*, *hsdR17* (r<sub>k</sub><sup>-</sup>m<sub>k</sub><sup>-</sup>), *supE44*, *thi1*, *recA1*, *gyrA*(Nal<sup>r</sup>), *relA1*,  $\Delta$ (*lacZYA-argF*)U169,  $\phi$ 80-d *lacZ* $\Delta$ M15.

- ***Escherichia coli BL21 (DE 3)***. F<sup>-</sup>, *ompT*, *hsdS* $\beta$ (r $\beta$ -m $\beta$ -), *dcm*, *gal*, (DE3) *tonA*.

#### **3.1.11.2. Bacterial media**

- ***Bacterial LB (Luria Broth) Medium***. The ready to use powder mix (Gibco, BRL) was dissolved in the appropriate amount of H<sub>2</sub>O<sub>dd</sub>. Solid media was obtained adding agar at a

---

final concentration of 1.5% (w/v). Agar plates were poured, dried overnight at room temperature and stored at 4°C.

After autoclavation LB or LB-agar media were supplemented with the following antibiotics: Ampicilin 100 µg/ml or Kanamycin 50 µg/ml.

### 3.1.11.3. Yeast strain genotype

- *Saccharomyces cerevisiae* **L40**. *MATa*, *his3Δ200*, *trp1-901*, *leu2-3112*, *ade2*, *LYS2::(4lexAop-HIS3)*, *URA3::(8lexAop-lacZ)*, *GAL4 gal80*.

### 3.1.11.4. Yeast media

- **UT medium**. 1.2 g/l Yeast nitrogene base, 5g/l Ammoniumsulfate, 10 g/l Succinic acid, 6 g/l NaOH, 0.65 g/l Drop-out mix\*, 0.01% Lysine, 0.005% Histidine, and 0.1% leucine. After autoclavation sterile 20% Glucose, 0.05% Aspartic, and 0.1% Threonine were added.

- **UTL medium**. 1.2 g/l Yeast nitrogene base, 5g/l Ammoniumsulfate, 10 g/l Succinic acid, 6 g/l NaOH, 0.65 g/l Drop-out mix\*, 0.01% Lysine, and 0.005% Histidine. After autoclavation sterile 20% Glucose, 0.005% Aspartic, and 0.01% Threonine were added.

\*Drop-out mix: 2 g Adenine, 2 g Arginine, 2 g Cysteine, 1 g Isoleucine, 1 g Methionine, 1 g Phenylalanine, 1 g Proline, 1 g Serine, 1 g Tyrosine, 1 g Valine.

- **YAPD medium**. 10 g/l Yeast extract, 20 g/l Bactopepton, 0.1 g/l Adenine. After autoclavation 20% sterile Glucose was added.

- **THULL plates**. 1.2 g Yeast nitrogene base, 5 g Ammoniumsulfate, 10 g succinic acid, 6 g NaOH, 0.65 g Drop-out mix, 2.5 (or 7.5) mM Amino-Triazol, and 16 g/l agar. After autoclavation sterile solutions of 20% Glucose, 0.005% Aspartic, and 0.01% Threonine were added.

- **UT plates**. 1.2 g/l Yeast nitrogene base, 5g/l Ammoniumsulfate, 10 g/l Succinic acid, 6 g/l NaOH, 0.65 g/l Drop-out mix\*, 0.01% Lysine, 0.005% Histidine, 0.1% Leucine,

---

and 16 g/l agar. After autoclavation sterile solutions of 20% Glucose, 0.05% Aspartic, and 0.1% Threonine were added.

- **UTL plates.** 1.2 g/l Yeast nitrogen base, 5g/l Ammoniumsulfate, 10 g/l Succinic acid, 6 g/l NaOH, 0.65 g/l Drop-out mix, 0.01% Lysine, 0.005% Histidine, and 16 g/l agar. After autoclavation sterile solutions of 20% Glucose, 0.005% Aspartic, and 0.01% Threonine were added.

- **X-Gal.** Stock solution 50 mg/ml in dimethyl sulfoxide.

#### **3.1.11.5. Cell lines**

- **P2X<sub>2</sub>-HEK-293 cells.** Human embryonic cells permanently transfected with full length P2X<sub>2</sub> (generous gift of Prof. Anmarie Surprenant and Prof. Alan North, Institute of Molecular Physiology, University of Sheffield).

#### **3.1.11.6. Cells media**

- **OptiMEM.** Serum-free medium (Gibco, BRL).

- **D-MEM: F12.** (Gibco, BRL) Supplemented with 10% FCS and 1% Penicillin/Streptomycin.

#### **3.1.12. Buffers**

- **Anode 1 buffer:** 0.3 M Tris-HCl (pH 10.4), 10% Methanol.

- **Anode 2 buffer:** 25 M Tris-HCl (pH 10.4), 10% Methanol.

- **Cathode buffer:** 25 M Tris-HCl (pH 9.4), 40 mM ε- Amino-n-hexaacid, 20% Methanol.

- **Coomassie staining solution :** 0,25% Coomassie Brilliant Blue R250 (w/v), 45% Methanol (v/v), 9% Acetic acid (v/v).

- **Destaining solution 1 :** 45% Methanol (v/v), 7,5% Acetic acid (v/v).

- **Destaining solution 2 :** 10% Methanol (v/v), 7,5% Acetic acid (v/v).

---

- **DNA loading buffer:** 15% Ficoll 400, 0.2% Bromophenol Blue, 0.2% Xylene cyanol, 0.2 M EDTA.

- **Elution-buffer :** 50 mM NaH<sub>2</sub>PO<sub>4</sub>, 300 mM NaCl, 250 mM Imidazole (pH 8.0).

- **Ethidium bromide solution :** 10 mg/ml Ethidium bromide in H<sub>2</sub>O<sub>dd</sub>.

- **Ligation buffer (5X):** 100 mM Tris-HCl (pH 7,5), 50 mM MgCl<sub>2</sub>, 50 mM DTT, 5 mM ATP.

- **Lysis-buffer :** 50 mM NaH<sub>2</sub>PO<sub>4</sub>, 300 mM NaCl, 10 mM Imidazole (pH 8.0).

- **LP buffer:** 200 mM NaCl, 100 mM HEPES pH 7.4, 10 mM EDTA, 100 mM NaF, 20 mM NaVO<sub>3</sub>, 2 mM PMSF, and 1.4% Triton X-100.

- **Lower-Tris buffer (4X):** 1.5 M Tris-HCl (pH 8.8), 0.4% SDS.

- **MOPS buffer (20X):** 0.8 M 3-morpholinopropanesulfonic acid (pH 7.0), 200 mM NaAc, 20 mM EDTA.

- **PBS:** 140 mM NaCl, 2.7 mM KCl, 1.8 mM KH<sub>2</sub>PO<sub>4</sub>, 10 mM Na<sub>2</sub>HPO<sub>4</sub>, pH 7.3.

- **PD buffer:** 2.7 mM KCl, 140mM NaCl, 10 mM Na<sub>2</sub>HPO<sub>4</sub>, 1.8 mM K<sub>2</sub>HPO<sub>4</sub> pH 7.3, 1 mM EDTA, 2 mM DTT, 0.1% Triton X-100, and proteinase inhibitors (complete mini-protease inhibitor mixture tablets, Roche Applied Science).

- **Protein loading buffer:** 125 mM Tris/HCl, 15% Glycerol, 3% SDS, 5% β-mercaptoethanol, and 0,05% bromphenolblue.

- **PonceauS solution (10X):** 2% Ponceau, 30% Sulfosalicyl acid, 30% Trichloro acetic acid.

- **RNA loading buffer:** For 10 samples: 22.15 µl 20 X MOPS buffer, 125 µl Formamide, 44 µl Formaldahide 37%, 41,5 µl 6 X Dye-buffer, 7 µl EtBr 10mg/ml.

Dye-buffer (6X): 15 % Ficoll 400, 0.25 % Bromophenol Blue, 0.25% Xylene cyanol FF.

- **Running buffer:** 14.4 g/l Glycine, 3 g/l Tris-base, 0.1% SDS.

---

- **Sol-buffer:** 50 mM TrisHCl (pH 7.5), proteinase inhibitors (complete mini-protease inhibitor mixture tablets, Roche Applied Science).

- **TBE:** 90 mM Tris, 90 mM Boric acid, 20 mM EDTA, pH 8.0.

- **TBS (10 X):** 1,4 M NaCl, 0,2 M Tris-HCl (pH 7,5).

- **Upper-Tris buffer (4X):** 0.5 M Tris-HCl (pH 6.8), 0.4% SDS.

- **Wash-buffer :** 50 mM NaH<sub>2</sub>PO<sub>4</sub>, 300 mM NaCl, 20 mM (40 mM) Imidazole (pH 8).

- **Western buffer A:** 5% dry milk, 5% Goat serum, 1 X TBS, 0.1% Tween 20.

- **Western buffer B:** 1 X TBS, 0.1% Tween 20.

## 3.2. Methods

### 3.2.1. Molecular biology procedures

#### 3.2.1.1. Designing and preparation of DNA constructs

- **P2X<sub>2</sub> constructs.** For yeast two hybrid (Y2H) assays the cDNA sequence corresponding to the full cytoplasmic domain of P2X<sub>2</sub> comprising amino acids 355-472 (P2X<sub>2</sub>CD) was amplified by PCR using full length P2X<sub>2</sub> cDNA as template. In addition, the sequence coding for P2X<sub>2</sub> splice variant cytoplasmic domain comprising amino acids 355-403 (P2X<sub>2(b)</sub>CD) was also amplified by PCR using the P2X<sub>2(b)</sub> cDNA as template. For both constructs the oligonucleotides utilized were N° 2178 and N° 2181 which carried *EcoRI* and *BamHI* sites, respectively. The obtained PCR products were cloned in the pLexN vector using the *EcoRI/BamHI* sites. Employing the P2X<sub>2</sub>CD in pLexN construct as template, several additional constructs were performed. The sequence coding for amino acid 355-416, 417-472, 355-400, and 401-472 of P2X<sub>2</sub>CD were amplified by PCR with its corresponding primers, listed on Appendix, and cloned in pLexN vector through *EcoRI/BamHI* sites.

For recombinant protein expression the sequences coding for P2X<sub>2</sub>CD and P2X<sub>2(b)</sub>CD were amplified by PCR with oligonucleotides N° 2184 and N° 2185 containing *BamHI* and *NotI* sites respectively, and the digested PCR products were cloned in frame in pGEX-4T-1

---

vector (Amersham Biosciences) and pET-32a(+) vector (Novagen) which generate the protein fused to Glutathione-S-transferase (GST) and Thioredoxine (Trx), respectively.

- **Fe65 constructs.** The sequences coding for Fe65 fragments comprising amino acids 218-479 (Fe65-202) was amplified by PCR using primers N° 2196 and N° 2197 on the full length Fe65 cDNA as template. The PCR product was digested with *EcoRI* /*BamHI* and cloned in pVP16-4 vector. From the resultant construct Fe65-202 in pVP16-4 vector, a number of deletions were carried out, thus the sequences coding for amino acids 218-309, 218-284, 255-284 and 285-479 of Fe65 were amplified by PCR with the corresponding primers, listed on Appendix, and cloned in pVP16-4 vector using the same strategy as before.

For recombinant protein expression the sequence coding for amino acids 218-479, 197-255 and 40-100 were amplified by PCR employing the corresponding oligonucleotides, listed on Appendix, and cloned in frame both into the pGEX-4T-1 and pET-32a(+) vectors employing the same strategy as with the P2X<sub>2</sub>CD.

- **PCR reactions.** The PCR reactions were performed typically in 50 µl of final volume. The standard PCR mixture contents were as follows: 1X *pfu* polimerase buffer (Promega), 1 µM of both sense and antisense primers, 0.8 mM dNTP mixture, 10 ng of the template DNA and 1 unit of the DNA *pfu* polymerase (Promega). The amplification was started with incubation for 5 minutes at 95°C followed by 25 amplification cycles of denaturing, annealing, and polymerization with parameters depending on the nature of the primer and on the size of the cDNA to amplify. The amplified fragments were subjected to electrophoresis in agarose gels and the band of interest was purified using the QIAEX II DNA purification kit (Qiagen).



---

### 3.2.1.2. Purification, cloning, and isolation of DNA constructs

- **Agarose Gel Electrophoresis.** The DNA fragments were separated by agarose gel electrophoresis. The 1-2% agarose gels were prepared with 1 X TBE buffer. The gels were stained with ethidium bromide (EtBr; 0,5 µg/ml) and the DNA bands were visualized under ultraviolet light ( $\lambda$  340nm). The EtBr stained DNA bands were excised from the gel and purified by the QIAEX II kit.

- **Preparation of PCR products and vectors for cloning.** The purified PCR products and vectors were treated with the corresponding restriction endonuclease to prepare the fragments with cohesive ends, for efficient cloning. Digestion were performed typically in 50 µl final volume containing 1,5-3 µg plasmid DNA or purified PCR product, 1X corresponding buffer (OPA or A-, B-, L-, M-, H- Buffer), and 0.5 U/µl of DNA restriction enzyme. The reactions were performed at 37°C for 2h. After digestion, inactivation of the enzyme was performed by incubation at 65 or 85°C for 15 min, depending on the enzyme employed. The sticky ends of the digested vectors were dephosphorylated by alkaline phosphatase (Promega) during 1h at 37°C, to prevent self-ligation of the vector.

The DNA fragments were separated by agarose gel electrophoresis and purified by the QIAEX II DNA purification kit prior to the ligation.

- **Transformation of *E.coli* Competent Cells.** Ligations were performed with a rate of 3:1 (digested PCR product : digested vector), 1X ligation buffer and 1U of T4-DNA ligase (Promega) at 10 µl final volume for 1 h at RT or O.N. at 4°C. The ligation mixture was used directly for transformation of *E. coli* DH5 $\alpha$  or BL21(DE 3) chemically competent cells. 50 µl of competent cells were defrost on ice and mixed with 2 µl of the ligation reaction. After incubation for 30 minutes on ice, the cells were heat-shocked for 1min at 42°C and chilled for 3 min on ice. Following, 500 µl of LB-medium were added and bacteria were incubated for 1 h at 37°C with gentle agitation. Finally, cells were plated onto LB-agar plates containing

---

appropriate antibiotics (100 µg/ml ampicillin or 50 µg/ml kanamycin) and grown overnight at 37°C.

**- DNA isolation.**

*Small-scale preparation of plasmid DNA (Miniprep).* MACHEREY-NAGEL NucleoSpin™ Plasmid Kit was used to purify small amounts of plasmid DNA. For this, 5 ml of LB medium containing the appropriate antibiotics were inoculated with a single *E. Coli* colony and incubated for 10-16 h at 37°C, 220 rpm. Bacterial cultures were centrifuged (1500 x g, 10 min at 4°C), and the pellet was treated according to the manufacturer's protocol.

*Large-scale preparation of plasmid DNA (Midiprep).* For the preparation of large-scale bacterial cultures, 5 ml of LB medium containing appropriate antibiotics were inoculated with a single colony and incubated for 6-8 h at 37°C, 220 rpm. Thereafter, 100 ml of LB-medium with the appropriate antibiotic were inoculated with 0.2 ml of this culture and incubated overnight at 37°C, 220 rpm. The plasmid DNA was isolated with Midipreps DNA purification system Wizard<sup>R</sup> Plus (Promega) according to the user's manual.

**3.2.2. Basic techniques of biochemistry**

**-Recombinant protein expression in bacteria.** The constructs Fe65(218-479), Fe65(197-255), Fe65(40-100) and P2X<sub>2</sub>(355-472) were cloned in frame in pGEX-4T-1 vector (GST-fusion proteins) and Fe65(218-479), P2X<sub>2</sub>(355-472), Fe65(197-255), Fe65(40-100) and P2X<sub>2</sub>(355-403)SV were cloned in frame in pET32a(+) vector (Trx-fusion proteins) as described above (3.2.1.1). After clonation in *E. coli* BL21(DE3) competent cells, one colony was inoculated in 20 ml LB-medium plus 100 µg/ml ampicillin and the resultant culture was incubated at 37°C O.N. A dilution 1:50 of the O.N. culture in 500 ml of LB-amp medium was then performed, and the new culture was further incubated until it reached an OD<sub>600nm</sub> 0.5-0.7. Protein expression was induced by adding IPTG (0.5 mM and 0.1 mM IPTG for pGEX-4T-1 and pET32a(+) vector, respectively), and for soluble expression of the

---

protein product inducted cultures were grown at 25° for 4h. The bacteria were then collected by centrifugation at 4000 x g at 4°C for 10 min. The resultant pellet was resuspended in 50 ml STE-Buffer or Lysis-Buffer for pGEX-4T-1 and pET32a(+) vector respectively, and divided in 5 tubes of 10 ml each. The 10 ml tubes were centrifuge at 6200 x g at 4°C during 10 min, the supernatant was discarded and the pellet was frozen in liquid nitrogen and stored at -70°C for posterior purification.

**-Purification of recombinant proteins.** The resultant recombinant proteins GST, GST-P2X<sub>2</sub>CD, GST-P2X<sub>2(b)</sub>CD, GST-Fe65-202, GST-Fe65<sub>(197-255)</sub>, GST-Fe65<sub>(40-100)</sub>, Trx-P2X<sub>2</sub>CD, Trx-P2X<sub>2(b)</sub>CD, Trx-Fe65<sub>(197-255)</sub>, Trx-Fe65<sub>(40-100)</sub> and Trx-Fe65-202 were purified by affinity chromatography. Proteins expressed in pGEX-4T-1 vector were purified using glutathione-agarose beads (Sigma), and proteins expressed in pET32a(+) vector with Ni-NTA resin (Qiagen). After purification, the proteins were dialyzed against 1X PBS O.N. at 4°C, and the protein concentration was determined by the Bio-Rad protein assay (BIO-RAD) reagent according to the manufacturer's protocol.

*Purification of Trx-fusion proteins by Ni<sup>-2+</sup> resin.* The pET32a(+) vector allows the expression of the recombinant protein both as a Trx-fusion protein and as His-tagged protein, allowing the purification of the protein of interest by Ni<sup>2+</sup> resin affinity. For this approach, one pellet, corresponding to 100 ml bacterial culture, was thaw for 10 min on ice and resuspended in 5 ml lysis-buffer plus 0.1 mg/ml lysozyme. The mixture was then incubated on ice for 15 min and 0.1 mM PMSF was added. Sonication during 1 min with continuous pulse (25% intensity, TT13 sonotrode) was performed on ice, for proper lysis of the cells. The lysate was cleared at 6200 x g for 10 min at 4°C. The supernatant (containing all soluble proteins including the recombinant His-tagged protein) was transferred to a new Falcon tube to proceed with the purification. In the meantime, 500 µl of Ni<sup>2+</sup> resin (Ni-NTA, Qiagen) was equilibrated as follow: 500 µl agarose slurry was centrifuged at 500 x g for 5 min, the

---

supernatant was discarded, 1 ml of lysis-buffer was added for washing of the beads by centrifugation at 500 x g for 5 min, and the supernatant was eliminated. The washing step was repeated up to 5 times. Then, the equilibrated Ni<sup>+2</sup> resin and the cleared supernatant (1ml resin per 5 ml of supernatant) were mixed and incubated with rotation for 1 h at 4°C. Thereafter the resin was spin down (500 x g, 1 min, 4°C) and the supernatant was discarded. The washes steps were performed 1 x with 4 ml of wash-buffer (20 mM Imidazole) and 2 x with 4 ml of wash-buffer (40 mM Imidazole). Finally the proteins were eluted with 4 x 1 ml of elution-buffer and each eluate was collected in a different tube for subsequent concentration determination and dialysis. Aliquots of each wash and elution steps were collected for gel analysis.

*Purification of GST-fusion proteins by Glutathione agarose beads.* One pellet, corresponding to 100 ml bacterial culture, was thaw for 10 min on ice and resuspended in 5 ml STE-buffer plus 0.1 mg/ml lysozyme. The mixture was then incubated on ice for 15 min and 0.1 mM PMSF was added. Sonication during 1 min with continuous pulse (25% intensity, TT13 sonotrode) was performed on ice. The lysate was cleared at 6200 x g for 10 min at 4°C, and the supernatant was transferred to a new Falcon tube to proceed with the purification. 500 µl of glutathione-agarose beads were centrifuged 5 min at 500 x g, the supernatant was discarded and the beads were equilibrated by addition of 5 ml of 1 X PBS and centrifugation (500 x g, 5min, 4°C), the supernatant was removed, and the washing step repeated. Glutathione-agarose equilibrated beads were added to the cleared supernatant and incubated with rotation for 1 h at 4°C. Afterward, spin down of the beads (500 x g, 5 min, 4°C) was performed and the supernatant discarded. Washes steps were performed 4 x 10 ml by 1 X PBS and the elution of the protein 4 x 1 ml of reduced glutathione 10 mM in 50 mM Tris-HCl (pH 8). The eluates were collected in a different tube for subsequent concentration

---

determination and dialysis. In each wash or elution step an aliquot was collected for gel analysis.

- ***SDS-Polyacrylamide gel electrophoresis (SDS-PAGE)***. For protein analyses one dimensional polyacrylamide gel electrophoresis under denaturing conditions (SDS-PAGE) were performed. 10% polyacrilamide gel was used for the separation of proteins with the size between 60-120 kDa, while 12% gel was used for the separation of proteins with molecular masses below 60 kDa. The gel was divided in a 'stacking gel' with a low level of cross-linkage and low pH, allowing proteins to enter the gel and be resolved without smearing, and a 'resolving gel' with a higher pH, in which the proteins are separated according to molecular weights (charge/size ratio is constant due to SDS addition). For two (8 x 10 x 0.1 cm) gels the following preparation were used:

- Stacking gel (3%): 1.25 ml Upper-Tris buffer, 3.21 ml H<sub>2</sub>O<sub>dd</sub>, 0.5 ml Acrylamide solution, 30 µl 10% APS, 10 µl TEMED.

- Resolving gel (10%): 2.5 ml Lower-Tris buffer, 4.09 ml H<sub>2</sub>O<sub>dd</sub>, 3.33 ml Acrylamide solution, 70 µl 10% APS, 10 µl TEMED.

- Resolving gel (12%): 2.5 ml Lower-Tris buffer, 3.42 ml H<sub>2</sub>O<sub>dd</sub>, 4 ml Acrylamide solution, 70 µl 10% APS, 10 µl TEMED.

The resolving gel solution was carefully poured between glass plates, overlaid with H<sub>2</sub>O<sub>dd</sub> and allowed to polymerize at room temperature for 30 min. After pouring off the overlaying H<sub>2</sub>O<sub>dd</sub>, the stacking gel solution was poured and a comb was inserted. The gel was allowed to polymerize for further 30 min. Probes were supplemented with protein-loading buffer, boiled at 95°C for 5 min and loaded on the gel and migrated under the influence of the applied electrical field (75 V for stacking gel and 150 V for resolving gel) in the running buffer. To define the protein size, the molecular weight marker (Fermentas) was loaded in parallel with the probes.

---

After running, the gel was staining with coomassie blue solution for protein visualization or subjected to transfer to nitrocellulose membrane for Western blot.

- **Coomassie brilliant blue staining of proteins in polyacrylamide gels.** The visualization of protein was performed by stained of the gel with Coomassie staining solution for 15 min. The background was subsequently reduced by soaking the gel in destaining solution 1 for 15 min and destaining solution 2 for 15 min up to several hours. Finally, gels were placed in a plastic frame between two cellophane sheets and dried overnight at room temperature.

- **Western blot.** After completion of the electrophoresis, the proteins were transfer from the gel to a nitrocellulose membrane (0.2  $\mu\text{m}$  pore diameter) by a standard semy-dry procedure (Trans-Blot SD). For that propose the following transfer 'sandwich' was prepared:

- 1 sheet of Whatmann paper pre-soaked in Anode buffer 1
- 2 sheets of Whatmann paper pre-soaked in Anode buffer 2
- Pre-soaked nitrocellulose membrane in Anode buffer 2
- polyacrilamide gel
- 3 sheets of Whatmann paper pre-soaked in Catode buffer

The transference was performed by application of a current of 2.5 mA / 1cm<sup>2</sup> for 30 min. Following protein transfer, the membrane was stained with PonceauS solution for 1-2 min at RT for molecular weight marker visualization. For destaining, the membrane was placed in H<sub>2</sub>O<sub>dd</sub> until the background appeared white (2-5 min). Thereafter, the membrane was blocked by incubation O.N. in Western buffer A at 4°C, and then with the corresponding primary antibody (1.5  $\mu\text{g}/\text{ml}$  of anti-P2X<sub>2</sub> or anti-P2X<sub>7</sub>, 5  $\mu\text{g}/\text{ml}$  of anti-Fe65-32, 6.5  $\mu\text{g}/\text{ml}$  of anti-APP or 0.2  $\mu\text{g}/\text{ml}$  of anti-GST) dissolved in the same solution for 2 h at RT. The membranes were washed 4 x 5 min with 10 ml of Western buffer A, incubated with the secondary horseradish-peroxidase conjugated antibody (BIO-RAD) at 1:5000 dilution for 1 h

---

at RT, washed again 4 x 5 min with 10 ml of Western buffer A, 1 x 5 min with 10 ml of Western buffer B and 1 x 5 min with 10 ml of 1 X TBS and finally subjected to detection.

For peroxidase activity detection, the chemiluminescent ECL Western Blotting Detection system (Amersham Bioscience) was used and the protein bands were visualised by chemiluminescence exposure to the X-Omat™ Blue films (Kodak). The exposure of autoradiographic films was performed in a dark room using a film cassette to insure a tight fit between membrane and film. Usually, exposures ranging from 5 s up to 30 min were performed.

- **Generation of antibodies.** Polyclonal antibodies were raised in rabbits using the GST-Fe65<sub>(197-255)</sub> and GST-Fe65<sub>(40-100)</sub> fusion proteins (Antibody Fe65-32 or Fe65-35, respectively) as antigens. Immunization of the rabbits (2 per antigen) was performed by Eurogentec (Seraing, Belgium) and the antibodies were purified using Trx-Fe65<sub>(197-255)</sub> and Trx-Fe65<sub>(40-100)</sub> proteins. The sera 32, 33, 34 and 35 obtained from the final bleeding of the immunized rabbits were tested by Western blot using the corresponding Trx-fusion proteins. Two of the rabbits sera, 32 and 35 showing satisfactory performance were affinity purified using the AminoLink Plus Immobilization kit (Pierce). For purification of one antibody 2 mg of the corresponding Trx-fusion protein was resuspended in 2 ml of *coupling-buffer* (pH 10) and the OD<sub>280nm</sub> was measured. The column was equilibrated with 5 ml of *coupling-buffer* and then incubated with the protein sample O.N. at RT. The day after, the column was washed with 15 ml of *wash-solution* and, in order to determine the efficiency of coupling, the OD<sub>280nm</sub> of the flow-through was measured and compared with that of the protein before coupling. Afterwards, the remaining active sites were blocked by addition of 4 ml of *Quenccching buffer*, washed again and finally the column was equilibrated with 5 ml of *binding-buffer* for posterior addition of 1.5 ml of the corresponding rabbit serum. After a wash step with 12 ml of *wash-solution*, the elution was performed with 8 ml of *Glycine-*

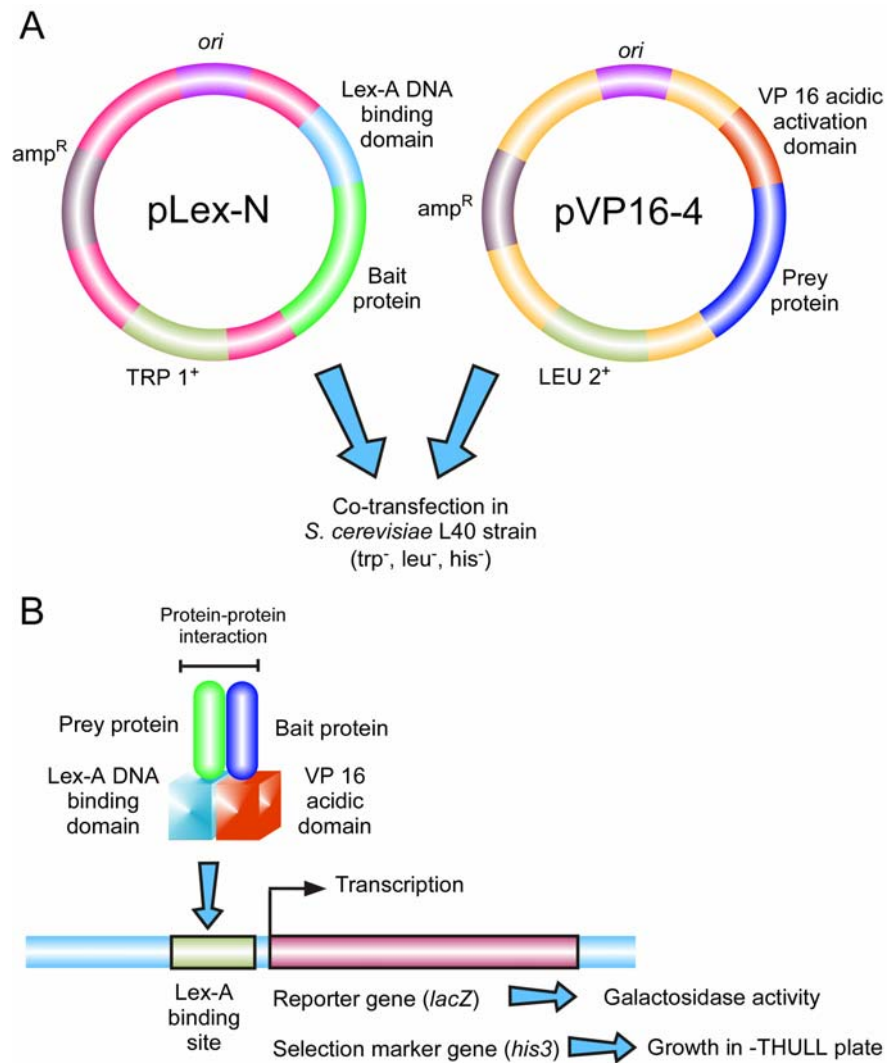
---

*buffer* (pH 2.5). Fractions of 1 ml were collected and 100  $\mu$ l of 1M Tris (pH 8) were added to each fraction for neutralization. The OD<sub>280nm</sub> of the eluates was determined and those with the highest absorbance were pooled together with 1 mg/ml of BSA. A subsequent dialysis was performed in 0.1 X PBS O.N. at 4°C, and the resultant product was aliquoted, lyophilized and stored at -20°C.

### **3.2.3. Yeast two-hybrid assays**

The two-hybrid assay (Y2H) is a useful method that allows the detection of interacting partners for the protein of interest and/or the study of a known protein-protein interaction. The method is based on two fusion proteins, the protein of interest (bait), which is engineered to have a DNA binding domain (DB) attached to its N-terminus, and its potential binding partner (prey), which is fused to an activation domain (AD; Figure 3.1A). Co-transformation of both constructs in an engineered yeast strain is then required. The strain used for transformation is deficient in producing nutrients required for its growth, thus by supplying the gene which protein product overcomes such deficiency in the bait or prey plasmid allows cells containing both plasmids to survive on the minimal media. In addition, interaction of the prey protein with the bait protein will form an intact and functional transcriptional activator. This newly formed transcriptional activator will then transcribe two types of reporter genes, prototrophics and enzymatics, which will allow the detection of the positive interactions (Figure 3.1B). In this way, the amount of the reporter produced can be used as a measure of the interaction between the protein of interest and its potential partner. Thus identification of positive clones occurs in two rounds: primarily cells successfully transformed with both plasmids are selected on a first minimal media, and afterwards a second minimal media selects cells where prey and bait are interacting. Enzymatic assays are commonly carried out on the first media (Fields and Sternglanz, 1994).





**Figure 3.1 A schematic diagram of the Y2H system.** (A) The bait and prey fusion proteins are constructed in the same manner. The bait DNA is isolated and inserted into a plasmid adjacent to the Lex-A binding domain (BD), and the prey fusion protein contains the PV16 activating domain (AD). (B) The yeast two-hybrid technique evidences protein-protein interactions by measuring transcription of a reporter gene. If bait and prey proteins interact, their DB and AD will then combine to form a functional transcriptional activator which will transcribe the reporter gene that is paired with its promoter.

### 3.2.3.1. Yeast glycerol stock for Y2H screening

The L40 yeast strain was used by all Y2H assays in this work. At the time to perform a Y2H screening, a stock of yeast already transformed with the desired vector is necessary. For preparation of a glycerol stock containing L40-yeast transformed with pLexN vector yeast transformation was performed (section 3.2.2.3). In this case, the cells were plated in -UT plates to allow only the growth of that yeast that contain pLexN vector which carry a *Trp*

---

gene for selection. One colony of the -UT plates was then inoculated on -UT medium and incubated at 30°C and 320 rpm until a OD<sub>600nm</sub> of 0.5 - 0.8 was reached. Thereafter, 1 ml of this yeast suspension was mixed with 1 ml sterile 30% Glycerol, in liquid nitrogen shock-froze and stored at -70°C.

### **3.2.3.2. Yeast transformation for Y2H Screening**

The plasmid P2X<sub>2</sub>CD-pLexN was used as bait to isolate putative interacting proteins from a rat brain cDNA library. The library, derived from postnatal day 8 animals (P8), was cloned into the pVP16-3 vector (Okamoto and Südhof, 1997). The P2X<sub>2</sub>CD-pLexN and the cDNA library were cotransformed into the *S. cerevisiae* reporter strain L40 using the lithium-acetate/single-stranded carrier DNA/polyethylene glycol method (LiAc/SS carrier DNA/PEG method; (Gietz *et al.*, 1992)). One -UT plate was spread with L40-pLexN glycerol stock (section 3.2.2.1) and incubated for 72 h at 30°C. Then, one colony was inoculated in 3 x 5 ml -UT medium. After incubation O.N. at 30°C and 320 rpm the saturated cultures were re-inoculated in 100 ml of -UT medium and again incubated for 24 h (30°C, 320 rpm). On the next morning all three cultures (OD<sub>600nm</sub> 1.0) were transferred in 1 l of pre-heated YAPD medium and incubated approximately 3 h with 30°C and 320 rpm, until an OD<sub>600nm</sub> of 0.8 was reached. The yeast cells were then centrifuged (2000 x g, 5 min) and the pellet was washed with 500 ml TE (pH 7.5). The washed pellet was resuspended in 20 ml of 100 mM LiAc/TE plus 8.8 mg denatured salmon sperm carrier-DNA and 750 µg of the DNA library. After addition of 140 ml LiAc/PEG/TE the mixture was incubated 30 min at 30°C. Then, 17.6 ml DMSO were added and a heat shock was performed by 6 min at 42°C in a water-bath following by an addition of 400 ml of ice cooled YAP medium. The cells were then centrifuged (2000 x g, 5 min, RT), washed with 500 ml of YAP medium and resuspended in 1 l of pre-heated YAPD medium. The treated cells were incubated 1 h at 30°C with gently shaker (70 rpm).

---

In order to determine the efficiency of the primary transformation, cells corresponding to 1 ml aliquot were resuspended in 1 ml -UTL medium and different quantities (10  $\mu$ l and 1  $\mu$ l) were plated on -UTL plates. The remaining yeast culture was centrifuged (2000 x g, 5 min, RT) and washed with 500 ml -UTL medium. After wash and centrifugation the pellet was resuspended in 1 l of pre-heated -UTL medium and incubated 4 h at 30°C and 270 rpm. The yeast were centrifuged again (2000 x g, 5 min, RT) and washed 2 x 500 ml of -THULL medium. The final pellet was resuspended in 10 ml -THULL medium and 100  $\mu$ l of the preparation were plated on -THULL plates (60 plates).

For the determination of the transformation efficiency after 4 h of regeneration, different dilutions of the yeast final suspension were plated on -UTL plates, again.

The L40 strain harbors the reporter genes *lacZ* and *his3*, therefore cotransformants were plated on -THULL plates (lacking tryptophan, leucine, uracil, lysine and histidine) to assay for activation of the *HIS3* reporter gene, and thus, the growth of the yeast on -THULL plates indicated that the tested proteins interact in the yeast system. The -UTL plates (lacking tryptophan, leucine and uracil) represent control for the successful transformation of both plasmids. In addition, to confirm the positive interaction, the cotransformants plated on -UTL plates were tested for  $\beta$ -Galactosidase activity. Positive colonies were selected, amplified by PCR employing the pGEM-T easy vector strategy (Promega) and sequenced. Identity of the interacting proteins was obtained via BLAST on the NCBI-ENTREZ database (<http://www.ncbi.nlm.nih.gov/entrez/>).

### **3.2.3.3. Yeast transformation for direct Y2H assay**

Direct Y2H assays were performed to study the interaction between P2X<sub>2</sub> and Fe65 (or Fe65L1). Small scale transformation of yeast was also accomplished according to the LiAc/SS carrier DNA/PEG method. For ten transformations 11 ml of YAPD medium were inoculated with a L40-colony coming from a YAPD plate, and incubated O.N. at 30°C and

---

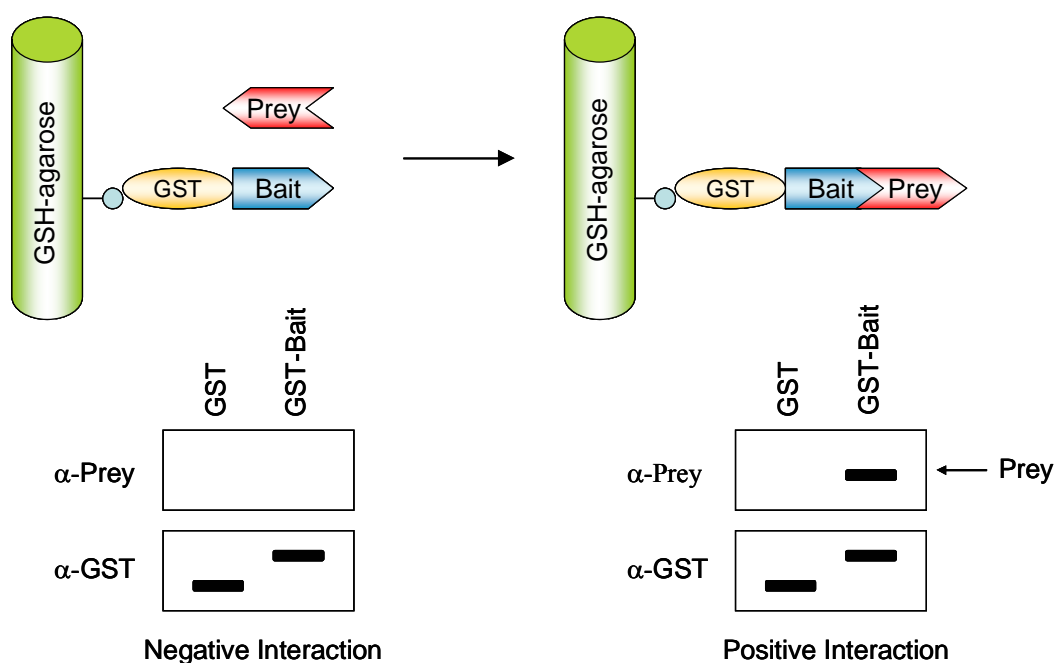
320 rpm. On the next day the O.N. culture was diluted in such a way that in 50 ml final volume a OD<sub>600nm</sub> of approximately 0.4 was achieved. The new culture was then incubated about 4 h at 30°C and 320 rpm, until a OD<sub>600nm</sub> of 0.8 - 1.0 was reached. Then, cells were harvested by centrifugation at 3000 x g for 5 min at RT and washed with 25 ml sterile water. Subsequently, 1 ml sterile H<sub>2</sub>O<sub>dd</sub> was added to the cells, transferred to 1.5 ml microcentrifuge tubes and centrifuged at 13000 x g, 30s at RT. The supernatant was discarded and the cells were taken up to 1 ml sterile H<sub>2</sub>O<sub>dd</sub>. The suspension was divided in tubes containing 100 µl each (ca. 10<sup>8</sup> cells). Per transformation a mix of 240 µl 50% PEG, 36 µl 1M LiAc, 50 µl salmon sperm carrier DNA (2 mg/ml) and 1 µg of each DNA of study was prepared. The carrier DNA was cooked before for 5 min in the water-bath and cooled briefly on ice. The mix was added to the tubes and mixed by vortex for posterior incubation for 40 min at 42°C in water-bath. Finally, the transformed cells were centrifuged (13,000 x g, 30 s, RT), washed once with 1 ml of sterile H<sub>2</sub>O<sub>dd</sub> and resuspended in a final volume of 50 µl. 3µl and 6 µl of each transformation was used to -UTL and -THULL plates, respectively.

#### **3.2.3.4. β-Galactosidase assay**

After transformation the plates were incubated at 30°C for 72h to allow the colonies to grow. The plates were then flooded with chloroform, immersing completely all the colonies, and placed under a fume hood for 5 min. The chloroform was then discarded, and plates were placed again under the fume hood to let them dry. Afterwards the plates were overlaid with 1% low melting agarose in 100 mM KH<sub>2</sub>PO<sub>4</sub>/ K<sub>2</sub>HPO<sub>4</sub> containing 1 mg/ml X-Gal. After the agarose hardened, the plates were inverted and incubated at 30°C for up to 24h (Duttweiler, 1996). To follow the development of blue color due to the progress of a positive reaction, pictures of the plates were taken at 4h and 24h.

### 3.2.4. Probing protein-protein interactions *in vitro* by pull-down assays

Pull-down assays allow the study of protein-protein interactions *in vitro* by co-sedimentation of the interacting partners. The condition is that one of the assayed proteins has to be a recombinant fusion to the glutathione-S-transferase (GST) protein. After incubation in the appropriate buffer, the complex is immobilized on glutathione agarose beads (GST pull-down assay), due to the affinity of GST to glutathione. The complex is afterwards resolved by SDS-PAGE and the presence of the proteins is assayed by Western blot employing the correspondent antibodies (Figure 3.2).



**Figure 3.2** A schematic diagram of the GST pull-down assay. The bait protein is bound to glutathione agarose beads and then the prey protein is added. After incubation and washing steps, the protein complex is resolved in a SDS-PAGE following a detection of the proteins by Western blot using the corresponding antibodies.

#### 3.2.4.1. Pull-down assays

For pull-down assays 5  $\mu$ g of purified GST-fused proteins or GST alone were bound to 50  $\mu$ l of glutathione-agarose beads, previously equilibrated with 1 X PBS, by an O.N. incubation at 4°C. After 3 washes steps of 10 min with 1ml of PD buffer (200 x g, 2 min, 4°C), 2.5  $\mu$ g of the corresponding Trx-fusion protein was added and the mixture was

---

incubated for 2 h at 4°C in PD buffer. Beads were then washed again 3 x 10 min with 1ml of PD buffer (200 x g, 2min, 4°C), resuspended in 40 µl of protein loading buffer and boiled for 5 min. The protein complexes were then resolved by SDS-PAGE electrophoresis and probed by Western blot using anti-P2X<sub>2</sub> antibody, anti-GST antibody or anti-Fe65-32 antibody as described above (section 3.2.2).

### **3.2.5. Characterization of protein-protein interaction *in vivo***

Immunoprecipitation (IP) is a widely used immunochemical technique that can be employed to identify protein complexes present in cell or tissue homogenates. A protein complex can be isolated by means of an appropriate antigen-antibody pair formation, due to the affinity of protein A or G for the Fc region of immunoglobulins. An antibody for one of the proteins, the antigen, believed to be in the protein-protein complex is incubated with the cell or tissue homogenate, followed by an isolation procedure of the protein-antigen-antibody complex by protein A- or G-agarose beads. After washing, proteins in the precipitate are resolved using SDS-PAGE and analyzed by western blot with the corresponding antibodies.

#### **3.2.5.1. Co-immunoprecipitation assays**

For total membrane protein brain extracts preparation, 8 or 21 days postnatal (P8 or P21) Spague Dawley rats were sacrificed and the complete brain was extracted and placed immediately on liquid nitrogen. Afterwards, two brains (c.a. 2 g each) were milled on a pestle with liquid nitrogen. The resulting powder was resuspended in 5 ml of 0.32 M glucose solution and subjected to a posterior cell lysis procedure by strokes on a Teflon homogenator, on ice. The homogenate was centrifuged at 800 x g for 20 min and the resultant supernatant was then ultracentrifuged at 54000 x g for 20 min to pellet the membrane extract. The pellet was then resuspended in 4 ml of Sol-buffer for an approximately concentration of 4 mg/ml protein. The protein concentration was determined using the Bio-Rad protein assay reagent.

---

For the immunoprecipitation assay 2 mg of total membrane protein brain extracts from P8 or P21 rats were pre-absorbed with 10  $\mu$ l of protein A/G Plus-agarose (Santa Cruz Biotechnology) for 30 min. The thus pre-cleared membrane protein extract was then incubated with 2  $\mu$ g of anti-P2X<sub>2</sub> antibody, anti-P2X<sub>7</sub> antibody, or anti-IgG from rabbit in 2 X LP buffer for 3 h at 4°C. Thereafter, 20  $\mu$ l of protein A/G Plus-agarose were then added to the samples and the mixtures were further incubated 45 min at 4°C. The protein-bead complexes were washed three times with 1 ml of 1X LP buffer (1000 x g, 30 s, 4°C) and the final pellet was resuspended in 40  $\mu$ l of protein loading buffer. The proteins were eluted by boiling for 5 min, analyzed by SDS-PAGE electrophoresis, and probed by Western blot using anti-P2X<sub>2</sub> antibody, anti-P2X<sub>7</sub> antibody or the Fe65-32 antibody, as described above (section 3.2.2).

### **3.2.6. Immunocolocalization assays**

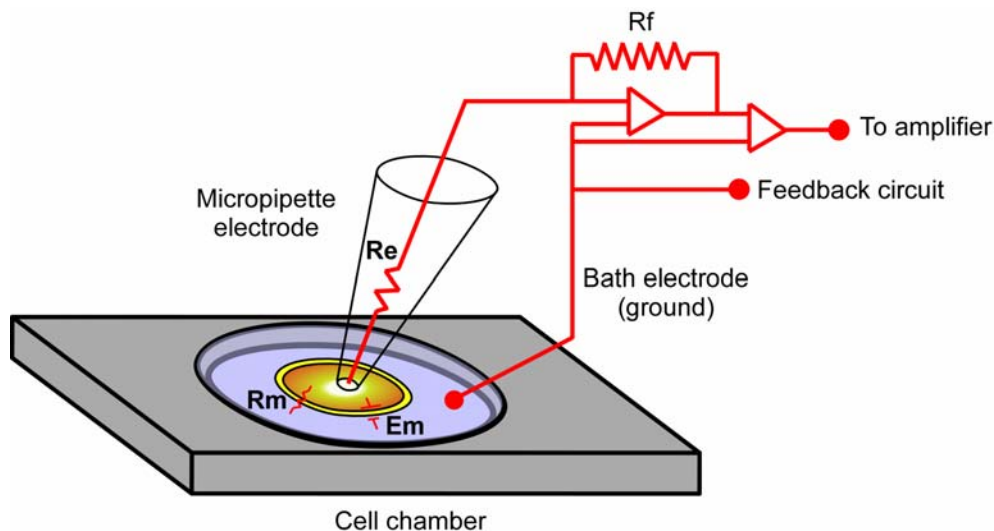
The immunocolocalization assays were performed by Maria Rubio, at Department of Physiology and Neurobiology, University of Connecticut at Storrs, USA.

For protocols see Rubio and Soto, 2001 and Masin *et al.*, 2006.

### **3.2.7. Electrophysiology**

#### **3.2.7.1. Whole cell Patch-clamp technique**

- **Generalities.** Whole cell patch clamping is an electrophysiological technique widely used to measure the average current across the entire surface area of one cell. A tight seal is achieved between the glass pipette and the membrane, and after ruptured of the membrane equilibrium is obtained between the pipette solution and the cell content, allowing the control of the composition of solutes on both sides of the membrane. Through the same pipette, an Ag/AgCl electrode allows the membrane potential of the cell to be held constant (clamped) while ion currents across the membrane are measured (Figure 3.3).



**Figure 3.3. Components of a whole cell voltage clamp.** After the tightly seal is formed between the cell and the pipette a rupture of the membrane patch allow the control of concentration of ions in both sides of the membrane. The membrane potential is clamped and the current necessary to maintain that potential is registered. Voltage control is established using feedback through an operation amplifier circuit. Em: membrane capacitance. Rm: membrane resistance. Re: electrode resistance. Rf: feedback resistance.

**-Cell transfection.** HEK-293 cells permanently expressing full length P2X<sub>2</sub> were co-transfected with full-length Fe65 cloned in pcDNA3.1/myc-His B and the empty vector pEGFP-C3 (the expression of the green fluorescent protein allows visualization and selection of co-transfected cells). The cells were normally cultured on D-MEM:F12 medium (Gibco) at 37°C in 75 mm<sup>2</sup> culture flasks. For transfection, cells were plated on six well plates at ~70-80% confluence in D-MEM:F12 medium (Gibco). One hour before transfection the culture medium was replaced by 2 ml of serum-free OptiMEM medium (Gibco). Appropriate DNA mix was prepared in a rate of 3:1 (µl FuGENE 6: µg DNA) in a total volume of 100 µl reached with OptiMEM medium, for each transfection. The transfection mix was incubated 15-30 min at room temperature and poured drop-wise onto cells and thus incubated for 4 to 5 h at 37°C. Thereafter, the medium was replaced for fresh normal culture medium for O.N. incubation. The next day, the cells were re-plated on poly-L-lysine coated coverslips (Ø10mm, Menzel-Glaser) in 40-50% confluence for posterior electrophysiological recording. Immunohistochemistry assays using an anti-myc antibody, recognizing a fusion tag to the



---

Fe65 protein, revealed that the transfection efficiency was higher than 90%. Cells were mock-transfected with both pcDNA3.1/myc-HisB and pEGFP-C3 vectors as control.

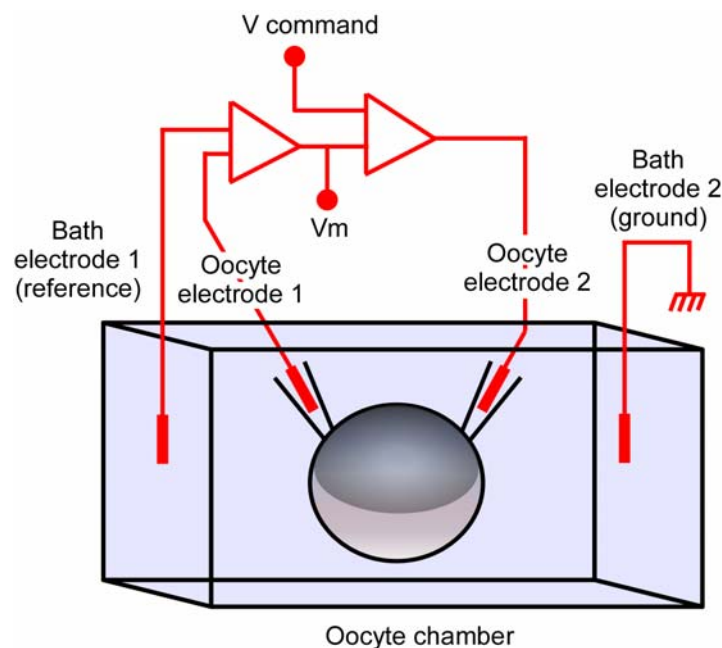
- **Measurements.** Standard whole-cell configuration of the patch-clamp technique was used. Recordings were made with an EPC-9 amplifier and Pulse+Pulsefit software package. Pipettes were made of borosilicate glass PG52165-4 IBBL capillaries (World Precision Instruments) pulled in two steps to the appropriate length and size in a vertical temperature controlled pipette puller L/M-3P-A (List medicals). Resulting pipettes had resistances of 1-2 M $\Omega$  when filled with the intracellular solution. For dose-concentration recordings the pipette solution contained 115 mM KCl, 1 mM MgCl<sub>2</sub>, 5mM EGTA, 5 mM BAPTA, 10 mM HEPES and 15 mM sucrose, pH 7.2, and the external solution 140 mM NaCl, 5 mM KCl, 2 mM CaCl<sub>2</sub>, 10 mM glucose and 10 mM HEPES, pH 7.4. A stock solution of ATP 10 mM in 100 mM HEPES (pH 7.2) was prepared and dilutions of it in the internal solution were performed to obtain different ATP concentrations (5, 10, 25, 50, 75 and 100  $\mu$ M) and thus attain the dose-concentration curve-points. For measurements of permeability to monovalent cations patch pipettes were filled with 160 mM NaCl, 10 mM HEPES and 11 mM EGTA, pH 7.3. Normal extracellular solution contained: 147 mM NaCl, 2 mM KCl, 1 mM MgCl<sub>2</sub>, 2 mM CaCl<sub>2</sub>, 10 mM HEPES and 12 mM glucose, pH 7.3. After achieving whole cell configuration the external solution was changed to 154 mM NMDG, 10 mM HEPES and 12 mM glucose. Currents-voltage relations were obtained by voltage ramps (-90 to 0 mV over 500 ms) using 100  $\mu$ M ATP prepared from the stock solution as well.

Typical holding potential was -70 mV, and the ATP solution was rapidly applied using a DAD-12 application system (ALA Scientific Instruments, Westbury, NY, USA). The time constant ( $\tau$ ) of the application system calculated using an open tip pipette was less than 1 ms.

---

### 3.2.7.2. Two-electrode voltage clamp

- **Generalities.** The Two-electrode voltage clamp (TEVC) is a method employed extensively for the study of functional properties of ion channels expressed in oocytes (Stuhmer, 1992). This method allows an accurate measurement of the ionic current under adequate control of the membrane potential. When opening of a channel is induced, the ionic flux alters the membrane potential. Under TEVC control, one intracellular electrode (the voltage electrode) is used for continuous measurement of the actual membrane potential, while the second (the current electrode) is used to pass the current necessary to keep the potential at the desired value (Figure 3.4). This is achieved using a feedback circuit, which is the main component of the voltage clamp. The amount of current that passes through the current electrode is the measured parameter.



**Figure 3.4.** A schematic diagram of the main components of a two-electrode voltage clamp. The difference in potential between the bath and the potential electrode (left),  $V_m$ , is compared to the command potential,  $V_{comm}$  and determines the amount of current injected into the oocyte through the current electrode (right).

- **Preparation of *Xenopus laevis* oocytes.** For oocyte extraction *Xenopus laevis* frogs were surgically opened under anesthesia (20-30 min in 1.25 g/l of Tricaine solution). After isolation of oocytes the incision was closed immediately and frogs were returned to water.

---

The follicular cell layer was removed from oocytes by 2-3 hours of incubation in collagenase type 2 solution (Worthington Biochemical Corporation) at 18°C. After inhibition of the enzymatic reaction by thoroughly washing the oocytes with Barth medium (88 mM NaCl, 1 mM KCl, 2.4 mM NaHCO<sub>3</sub>, 0.82 mM MgSO<sub>4</sub>, 0.33 mM Ca(NO<sub>3</sub>)<sub>2</sub>, 0.41 mM CaCl<sub>2</sub>, 7.5 mM Tris-HCl) oocytes in stages V-VI were separated with fine forceps for cRNA injection.

- **cRNA Synthesis.** P2X<sub>2</sub> cDNA subcloned in pcDNA1 and Fe65 or P2X<sub>7</sub> cDNA subcloned in pSGEM vector were used to synthesize capped complementary RNA by *in vitro* transcription. pSGEM clones were linearized with *PacI* (Biolabs) and P2X<sub>2</sub> in pcDNA1 was linearized using *NotI* enzyme (Biolabs), the reaction was performed at 37°C during 4h. A typical restriction reaction contained 10 µg of corresponding cDNA, 0.5 U/µl restriction enzyme, 1 X buffer (NEB1 buffer and H-buffer for *PacI* and *NotI*, respectively) in a final volume of 100 µl. The linearization product was treated 2 times with one volume of phenol/chloroform and 1 time with chloroform, vortexed and spinned at 14.000 x g for 5 min at 4°C. DNA was precipitated for 1h at -70°C with 1/10 v/v of 4 M LiAc (pH 6) and 2,5 v/v of EtOH 100% and spin down (20 min, 14.000 x g, at 4°C). The pellet was washed with ice cold 80% EtOH, dried and resuspended in 21 µl of DEPC-H<sub>2</sub>O. An agarose gel was performed with 1 µl of linearized DNA to check for an appropriate linearization and concentration. The transcription was performed employing the following reaction mixture: 10 µg of linearized DNA, 1 X transcription optimized buffer (Promega), 10 mM DTT (Promega), 0.5 mM ATP, 0.5 mM CTP, 0.5 mM UTP, 0.1 mM GTP, 0.4 mM m<sup>7</sup>G(5')ppp(5')G (Boehringer Mannheim), 1.1 units/µl RNAsin (Promega), 0.4 units/µl T7 polimerase (Startagene). The mixture was incubated at 37°C during 1.5 h. Thereafter, 0.06 unit/µl of DNaseI RNase free (Promega) were added to the mixture and further incubated at 37°C for 15 min.

---

The resultant cRNA was purified by a phenol-chloroform extraction and ethanol precipitation. For this approach 70 µl of DEPC-H<sub>2</sub>O and 30 µl of 2M NaAc (pH 6) were added to get a final volume of 200 µl, then the sample was treated 2 times with one volume of phenol/chloroform and 1 time with one volume of chloroform, vortexed and spinned at 14.000 x g for 5 min at 4°C. Then, the cRNA was treated with 3 volumes of EtOH 100% and subjected to precipitation O.N. at -20°C. On the next day the precipitated cRNA was spinned down (14.000 x g, 5 min at 4°C) washed with 1 ml EtOH 80%, dried by speed vac and resuspended in 50 µl of DEPC-H<sub>2</sub>O. A new precipitation step was performed with 30 µl 2M NaAc (pH 6), 121µl DEPC-H<sub>2</sub>O and 600 µl EtOH 100% overnight at -20°C. The precipitated cRNA was spinned down at 14.000 x g for 5 min at 4°C, washed with 1 ml EtOH 80%, dried by speed vac and resuspended in 50 µl of DEPC-H<sub>2</sub>O. The samples were aliquoted and stored at -70°C.

The quality of the purified cRNA was evaluated by agarose gel electrophoresis. Gel electrophoresis of RNA was performed on denaturing agarose gels, in the presence of 5% formaldehyde. For gel preparation, 0.6 g of agarose was dissolved in 2.4 ml of 20 x MOPS-buffer and 55 ml of DEPC-H<sub>2</sub>O and boiled in the microwave. After cooling to about 50°C, 10.2 ml of formaldehyde (37%) was added, stirred and poured into a gel chamber. For loading de gel, 5 µl of each RNA samples as well as RNA-molecular weight markers (Invitrogen) were mixed with 25 µl of RNA loading buffer and denatured for 15 min at 65°C. Samples were chilled on ice, loaded on the gel and allowed to run at 50 V for 3 hours.

- ***Injection of *Xenopus laevis* oocytes.*** Defolliculated oocytes were injected with approximately 50 nl of cRNA per oocyte, at a 25 ng/µl concentration for either P2X<sub>2</sub>, P2X<sub>7</sub> and/or Fe65 cRNAs, using an automatic Drummond injector (Nanoject II). Microinjection needles were pulled from glass capillaries (Drummond 3-000-203-G/X) using a standard vertical pipette puller PIP5 (HEKA). Afterwards, the tip was broken under microscope and

---

fire polished to avoid rough rim that might lesion the oocyte. Injected oocytes were incubated at 18°C in Barth medium containing antibiotics for 2-4 days prior to electrophysiological analysis. The antibiotics used were Gentamicin (0.05 mg/ml, Sigma) and Penicillin/Streptomycin (100 U/ml, Gibco). Alternation of antibiotics was performed in order to avoid the development of resistance.

- **Measurements.** Microelectrodes were made from borosilicate filament glass capillaries (Hilgenberg). After having been cut to the appropriate length, they were pulled in two steps to the appropriate length and size in a vertical temperature controlled pipette puller PIP5 (HEKA). After pulling, the very tip of the microelectrodes was broken under a microscope in order to decrease the resistance of them to 0.5-1 MΩ. Oocytes were superfused with standard Mg<sup>2+</sup> Ringer solution (98 mM NaCl, 1 mM MgCl<sub>2</sub> and 5 mM HEPES, pH 7.35-7.4) with the exception of the concentration-response curves that were obtained using an extracellular solution containing 115 mM NaCl, 2.8 mM KCl, 1.8 mM MgCl<sub>2</sub>, and 10 mM HEPES, pH 7.35-7.4. ATP solutions were prepared as described above for whole cell patch-clamp recordings. Oocytes were voltage-clamped at -60 mV, currents were filtered at 100 Hz and sampled at 500 Hz. In the experiments designed to determine ionic selectivity, equimolar substitution of NMDG<sup>+</sup> for Na<sup>+</sup> was employed in the superfused solution. The applied pulse protocol consisted on four segments, 50 ms at -60mV, 50 ms at -90 mV, 250 ms ramp from -90 to 0 mV, and finally 125 ms at -90 mV. The first segment was used to determine the time course of the current at -60 mV in NMDG<sup>+</sup>. When the reversal potential in Mg<sup>2+</sup> Ringer solution was determined, the ramp was performed between -40 and +40 mV. For this measurements a 100 μM ATP solutions was used. Data were acquired at 1 kHz and sampled at 5 kHz. All experiments were performed at room temperature. Data were analyzed using Pulse+Pulsefit (HEKA) or Igo Pro (Wavemetric).

---

Ion permeability ratios were calculated from the shift of the reversal potential using the equation  $P_{\text{NMDG}}/P_{\text{Na}} = \exp(\Delta E_{\text{rev}}F/RT)$ , where  $P_{\text{NMDG}}$  is the permeability to NMDG<sup>+</sup>,  $P_{\text{Na}}$  is the permeability to Na<sup>+</sup> and  $\Delta E_{\text{rev}}$  is the shift in reversal potential (Khakh *et al.*, 1999). Data are presented as mean  $\pm$  S.E. from n experiments. Statistical comparisons were performed using Student's t-test. The differences were considered significant if  $p < 0.02$ .

---

## 4. RESULTS

### 4.1. Isolation of proteins interacting with the C-terminus of the P2X<sub>2</sub> receptor

In order to identify potential interaction partners of P2X<sub>2</sub> receptors, a rat brain cDNA library (postnatal day 8) (Okamoto and Sudhof, 1997) was screened by the yeast two-hybrid (Y2H) technique (Fields and Song, 1989), employing the intracellular C-terminus region of the P2X<sub>2</sub> subunit (P2X<sub>2</sub>CD) as bait (Figure 4.6A). For this purpose the sequence coding for the P2X<sub>2</sub>CD was cloned in the plasmid pLexN (Hollenberg *et al.*, 1995) and the cDNA library from rat brain, namely prey, was cloned into the pVP16-3 vector (Okamoto and Sudhof, 1997). The P2X<sub>2</sub>CD-pLexN vector codes for a fusion of the bait protein with the *E. coli* DNA-binding domain of the bacterial protein LexA, while the population of pVP16-3 vectors code for the cDNAs from the library fused to the VP16 transactivation domain from the Herpes simplex virus.

A positive interaction between the prey and bait proteins will place the LexA DNA-binding domain in the vicinity of the VP16 transactivating domain. While the first protein will specifically bind to a promoter sequence on an engineered reporter gene in the employed yeast strain, the latter one will recruit the transcriptional machinery to this gene, thus the overall complex will efficiently activate transcription of the reporter(s) gene(s). The Y2H experiments described in this work were performed in the *S. cerevisiae* L40 strain, which shows auxotrophy for adenine, uracil, Trp, Leu and His. Therefore, efficiency on the transformation procedure and positive protein-protein interactions are determined by the ability of transformed colonies to grow in the absence of certain amino acids (prototrophy). Yeast cells that were successfully transformed with both vectors will grow in -UTL plates (without uracil, Trp and Leu), due to the selection markers provided by the vectors, *trp1* gene for pLexN and *leu2* gene for pVP16-4, allowing the growth in the absence of both Trp and Leu (Table 4.1). L40 cells contain the reporter genes *his3* and *lacZ* under the control of 4 and


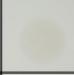

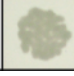
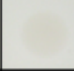

8 copies of the LexA operator from *E. coli*. Transformed L40 cells will grow in -THULL plates, lacking not only Trp and Leu, but also His and Lys, only when the fusion proteins contained in both vectors interact with each other (Table 4.1). Through the interaction, the DNA-binding domain and the transactivation domain come in close contact to activate the expression of *HIS3* gene that is under the control of LexA operators. An additional indicator of interaction is the activation of the *lacZ* gene, coding for  $\beta$ -Galactosidase. Thus, the measurement of  $\beta$ -Galactosidase activity on yeast that grew on -UTL plates is used to confirm an interaction between prey and bait proteins (Table 4.1).

	- UTL plate	- THULL plate	$\beta$ -Gal assay
VP16-prey +	Colony growth Successful transformation	Colony growth Positive interaction between prey and bait	Blue stain Positive interaction between prey and bait
LexA-bait	Absence of colonies Unsuccessful transformation	Absence of colonies No interaction between prey and bait	No stain No interaction between prey and bait

**Table 4.1. Schematic interpretation of expected Y2H results.** The growth of the yeast colonies on -UTL plates imply a successful transformation with both bait- and prey-containing plasmids. The growth of colonies on -THULL plates denote an interaction between prey and bait.  $\beta$ -gal assay is performed on colonies grew on -UTL plates. Blue stain comes from  $\beta$ -galactosidase activity reporting on a positive interaction between prey and bait.

In order to determine the usefulness of the P2X<sub>2</sub> construct used as bait in the Y2H screening, a number of control experiments had to be performed, mainly to evidence whether P2X<sub>2</sub>CD was able to self activate transcription or was interacting with the VP-16 protein. For this approach, P2X<sub>2</sub>CD fused to LexA was co-transformed in yeast both with an empty pVP16-4 vector or containing a non-related sequence (Figure 4.1). We employed the nuclear lamin protein A (lamin-pVP16-4) as a non-related sequence for these control experiments.



LexA-P2X <sub>2</sub> CD + VP16-	-UTL	-THULL	β-Gal
—			
Lamin			

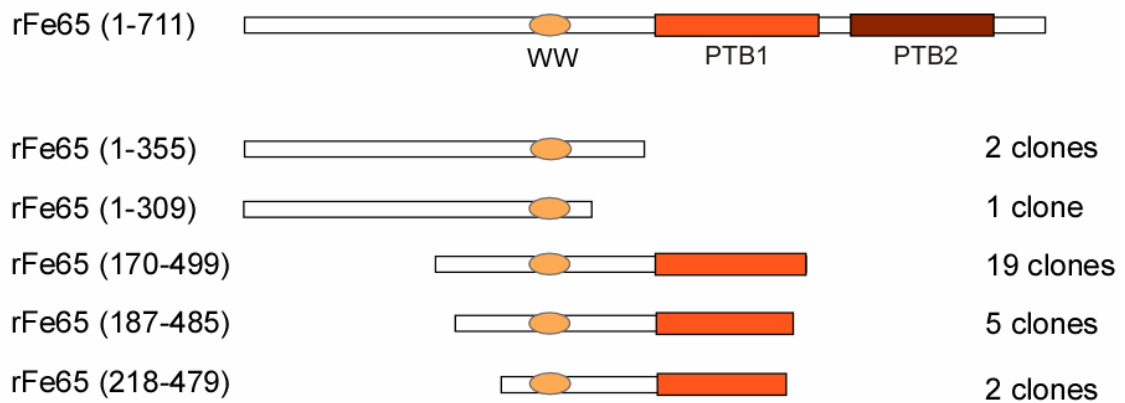
**Figure 4.1. The C-terminus of the P2X<sub>2</sub> receptor is not able to promote transcription unspecifically.** Y2H assay showing that the C-terminal domain of P2X<sub>2</sub> does not interact with VP16 (row 1) or Lamin-VP16 (row 2) when they are used as prey.

These results validate the use of P2X<sub>2</sub>CD as a tool in a Y2H screening since it displays no self-transactivation and does not interact with the VP-16 protein directly.

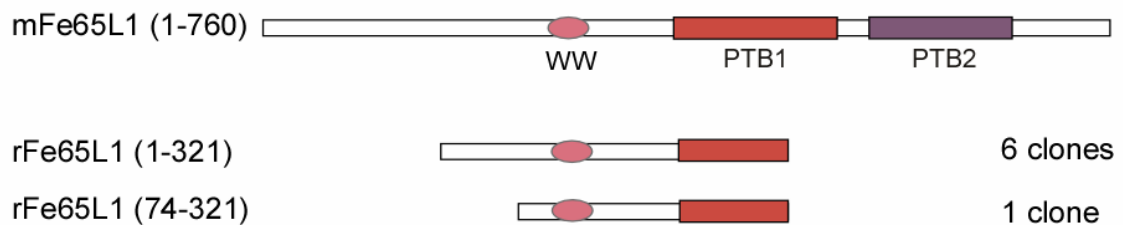
Approximately one million clones were screened by the Y2H procedure. Of them, 212 induced transcription of LexA-driven reporter genes for both histidine prototrophy and β-galactosidase activity. The positive clones were picked up, amplified by PCR, cloned in the pGEM-T easy vector, and sequenced.

In order to find the identity of the proteins interacting with P2X<sub>2</sub>CD, the sequences of the isolated clones were subjected to a data base search at ENTREZ, employing the Blast search engine (<http://www.ncbi.nlm.nih.gov/entrez/>). The most abundant cDNA isolated was represented by 29 clones (5 independent cDNAs; Figure 4.2A) that showed overlapping sequences identical to the adapter protein Fe65 from rat (gi:13377731) (Duilio *et al.*, 1991). In the same screening seven clones were isolated (2 independent cDNAs) containing overlapping sequences that were 96% identical to the human Fe65-like 1 cDNA (hFe65L1; gi:50083291) (Guenette *et al.*, 1996; McLoughlin and Miller, 1996), indicating they may represent its previously unidentified rat orthologue (Figure 4.2B). The isolation of multiple overlapping clones of two homologous proteins lends additional credibility to their interaction with the P2X<sub>2</sub> subunit.

**A**



**B**







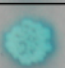
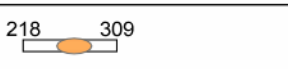





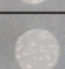
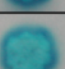
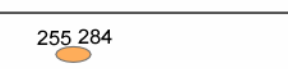


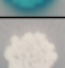






**Figure 4.2. The region comprising the WW domain and the first PTB domain from Fe65 or Fe65-like 1 interacts with the C-terminus of the P2X<sub>2</sub> receptor.** (A) Domain composition of full length rat Fe65 protein compared with Fe65 cDNA clones isolated in the Y2H screening. Numbers in brackets refers to amino acid position in the full length Fe65 sequence. The WW domain is highlighted in orange, the first PTB domain in red, and the second PTB domain in dark red. All Fe65 cDNAs isolated in the Y2H screening contained the complete WW domain, while only three of them also included part of the PTB1 domain, and none the PTB2 domain. The number of isolated clones for each cDNA sequence is noted at the right side. (B) Comparison of full length domain architecture of mouse Fe65-like1 (mFe65L1) protein with Fe65-like 1 (rFe65L1) cDNA clones isolated in the screening. The WW domain is highlighted in dark pink, the first PTB domain in purple, and the second PTB domain in indigo. Similarly to Fe65 cDNAs, all Fe65L1 cDNAs isolated in the Y2H screening contained the complete WW domain and part of the PTB1 domain, but none featured the PTB2 domain. The number of clones isolated for each cDNA sequence is shown on the right. The number between brackets for rFe65L1 clones are arbitrary, and respond to the sequence isolated in the screening. Please refer to the Appendix for full nucleotide and amino acids sequences of rFe65 and rFe65-like 1.

## 4.2. Studying the interaction between Fe65 and P2X<sub>2</sub> cytoplasmic domain by a direct Y2H assay

One of the isolated Fe65 cDNA clones, coding for amino acids 218 to 479 (Fe65<sub>218-479</sub>, named Fe65-202), was used to confirm the interaction with the P2X<sub>2</sub>CD in the Y2H system. In addition, to further delimit the region of interaction by this method, several deletions of the Fe65-202 clone were generated. For this approach all Fe65 constructs were cloned in pVP16-4 vector and used as prey in a direct Y2H assay, while P2X<sub>2</sub>CD was employed as bait, mirroring the condition implemented in the screening.

As shown on figure 4.4, we first confirmed the interaction between Fe65 and P2X<sub>2</sub>CD, as evidenced by histidine prototrophy (growth in –THULL plates) and presence of β-Galactosidase activity (blue color reaction) when the Fe65-202 construct was employed as prey (row 2). Different deletions on this construct provided insights into which domains of Fe65 are driving the interaction, and in line with the findings on the Y2H screening, a positive result was only evidenced with those constructs harboring the WW domain (Figure 4.3).

	LexA-P2X <sub>2</sub> CD + VP16-	-UTL	-THULL	β-Gal
	—			
	<b>Fe65 (218-479)</b>			
	<b>Fe65 (218-309)</b>			
	<b>Fe65 (218-284)</b>			
	<b>Fe65 (255-284)</b>			
	<b>Fe65 (285-479)</b>			

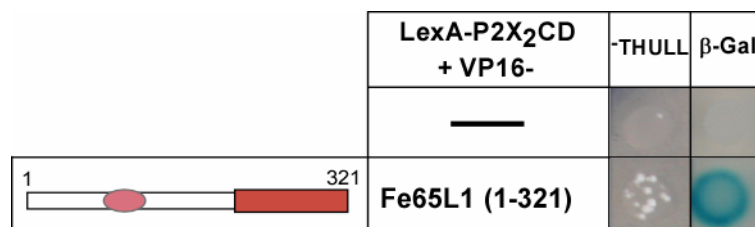
**Figure 4.3. The WW domain from Fe65 is sufficient for the interaction with the C-terminus of the P2X<sub>2</sub> receptor.** Y2H assay of the interaction between the C-terminal domain of P2X<sub>2</sub> and different deletions of Fe65. The interaction between Fe65-202 (218-479) and P2X<sub>2</sub>CD, observed in the Y2H screening, is confirmed by the Y2H direct assay (row 2). The interaction with deletions of Fe65 delimits which domains of Fe65 are responsible for the interaction (rows 3 to 6). Constructs are

as follows: Fe65(218-309), construct isolated from the Y2H screening lacking the PTB1 domain, row 3; Fe65(218-284), construct displaying the WW domain plus the N-terminus flanking sequence, row 4; Fe65(255-284), WW domain of Fe65, row 5; Fe65(285-479), construct lacking the WW domain, row 56. Highlighted in orange and red are the WW domain and the PTB1 domain, respectively. A negative control shows co-transformation of LexA-P2X<sub>2</sub>CD with an empty pVP16-4 vector (row 1).

We thus identified the WW domain of Fe65 as both necessary and sufficient for the binding to the C-terminus of P2X<sub>2</sub>. Interestingly, the growth in histidine deficient medium was accelerated, when the sequence 5' to the WW domain of Fe65 (Fe65<sub>218-254</sub>) was present, indicating that this part of the protein may stabilize the complex. Constructs containing only the PTB1 domain and sequences 3' to the WW domain were not able to induce histidine prototrophy or β-Galactosidase activity by themselves, arguing that this part of the sequence cannot sustain the interaction with P2X<sub>2</sub>. Nevertheless, since a significant reduction of the strength of the interaction was observed when the PTB1 domain was absent, we believe that this domain may have a supporting role in the binding event.

#### 4.2.1. Confirming the interaction between Fe65-like 1 and the cytoplasmic tail of P2X<sub>2</sub> subunit by a direct Y2H assay

In order to confirm the interaction between Fe65-like 1 and P2X<sub>2</sub>CD evidenced in the Y2H screening, the longer isolated Fe65L1 clones, coding for amino acids 1 to 321 (Fe65L1<sub>1-321</sub>), was subjected to a direct Y2H assay with P2X<sub>2</sub>CD. For the assay, the Fe65L1<sub>(1-321)</sub> construct was cloned in pVP16-4 and was co-transformed in yeast with the P2X<sub>2</sub>CD in pLexN vector (Figure 4.4).



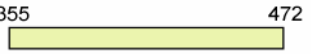

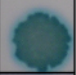

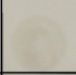


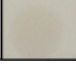



**Figure 4.4. Fe65-like 1 interacts with the C-terminus of the P2X<sub>2</sub> receptor.** Y2H assay confirming the interaction between the C-terminal domain of P2X<sub>2</sub> and Fe65-like 1 (Fe65L1) (row 2). Negative control was obtained by co-transforming LexA-P2X<sub>2</sub>CD with an empty pVP16-4 vector (row 1). The numbers in the brackets for Fe65L1 are arbitrary, and correspond to the amino acidic sequence of the clones isolated in the screening.

With this result we corroborate the interaction between Fe65L1 and P2X<sub>2</sub>CD as found in the screening.

#### 4.2.2. Probing the specificity of the interaction between Fe65 and P2X<sub>2</sub>CD by a direct Y2H assay

The P2X receptor family includes, besides P2X<sub>2</sub> subunits, six additional members mainly differing at the C-terminal sequence, thus the open question as whether Fe65 interacts with other P2X<sub>2</sub> subunits. The P2X<sub>4</sub> subunit is present, together with P2X<sub>2</sub>, in hippocampus and cerebellum at the postsynaptic specialization (Rubio and Soto, 2001), thus being exposed to the same cytoplasmic proteins as P2X<sub>2</sub>. On the other hand, P2X<sub>7</sub> carries the longest C-terminal domain among the seven P2X subunits, and forms a macromolecular assembly at the membrane level that accounts for almost eleven proteins including cytoskeletal proteins, chaperones, signaling and scaffolding proteins, many of them interacting with its C-terminus (Kim *et al.*, 2001). Hence we hypothesized that both P2X<sub>4</sub> and P2X<sub>7</sub> subunits are the most likely candidates to mimic P2X<sub>2</sub> behavior concerning its interaction with Fe65. In order to answer that question a direct Y2H assay using Fe65-202 as prey and cytoplasmic domains from both P2X<sub>4</sub> (P2X<sub>4</sub>CD) and P2X<sub>7</sub> (P2X<sub>7</sub>CD) as baits was performed (Figure 4.5).

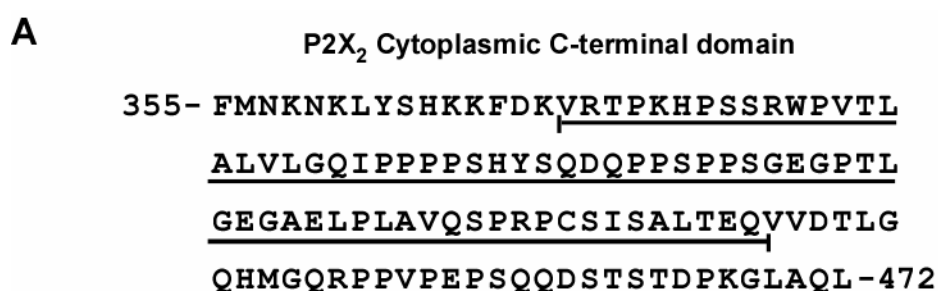
	VP16-Fe65-202 + LexA-	THULL	β-Gal
	—		
355  472	P2X <sub>2</sub> CD(355-472)		
360  388	P2X <sub>4</sub> CD(360-388)		
359  478	P2X <sub>7</sub> CD(359-478)		

**Figure 4.5. Fe65 interacts neither with P2X<sub>4</sub> nor with P2X<sub>7</sub> C-terminal domains.** Y2H assay showing that Fe65 fails to bind the cytoplasmic C-terminal tails from P2X<sub>4</sub> (in brown, row 3) or P2X<sub>7</sub> (in green, row 4) subunits. The positive interaction between P2X<sub>2</sub>CD and Fe65-202 is shown on row 2 for comparison (in yellow). Negative control was obtained by co-transforming VP16-Fe65-202 with an empty pLexN vector (row 1).

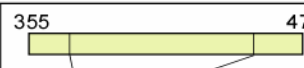


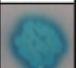


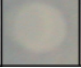

These results show that both P2X<sub>4</sub>CD and P2X<sub>7</sub>CD are not able to interact with Fe65, suggesting a high specificity for the interaction between P2X<sub>2</sub> receptors and Fe65.

#### 4.2.3. Probing the interaction between Fe65 and the splice variant of P2X<sub>2</sub> subunit by a direct Y2H assay

Three cDNAs encoding splice variants of the canonical P2X<sub>2</sub> subunit are known. Only one of these, the P2X<sub>2(b)</sub> subunit, was found to be functional, and interesting it is expressed in brain in a comparative level to the full-length subunits (Brandle *et al.*, 1997). The P2X<sub>2(b)</sub> subunit presents a shorter C-terminal region with a 207 base pairs-fragment spliced out. This corresponds to a deletion of 69 amino acids on this domain (underlined in Figure 4.6A). The loss of this region has indeed some physiological consequences for the P2X<sub>2(b)</sub> receptor, therefore it seemed very interesting to test whether Fe65 was also able to bind the splice variant form of P2X<sub>2</sub>.



**B**

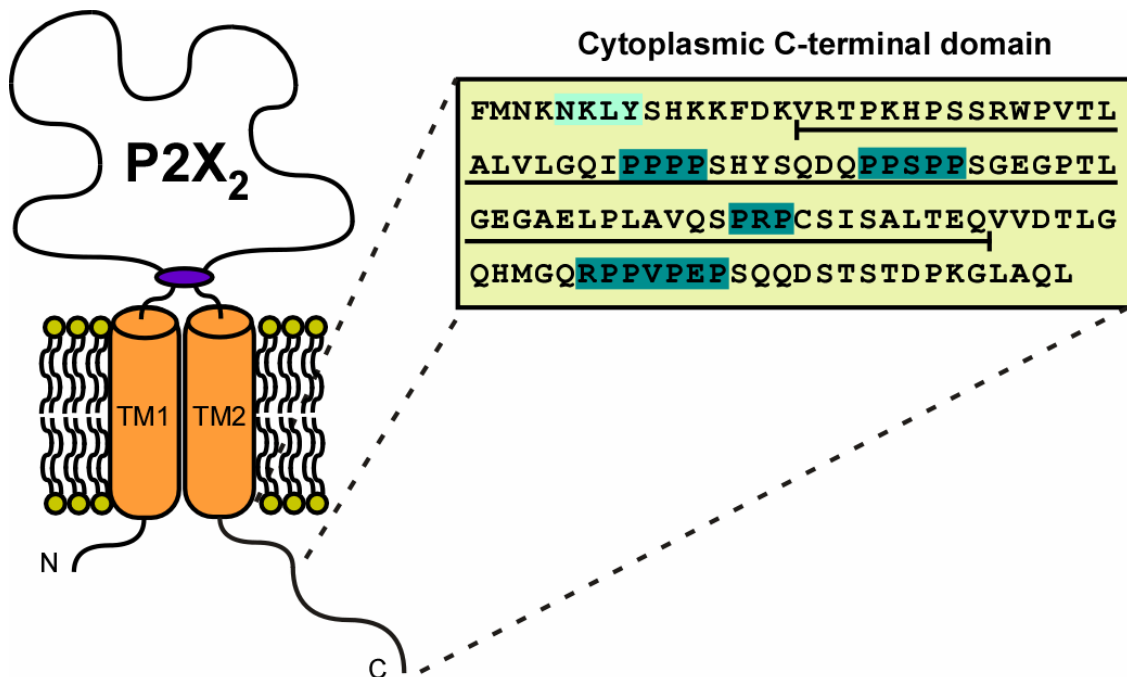
	VP16-Fe65-202 + LexA-	-UTL	THULL	β-Gal
	<b>P2X<sub>2</sub>CD(355-472)</b>			
	<b>P2X<sub>2(b)</sub>CD(355-403)</b>			

**Figure 4.6. The splice variant P2X<sub>2(b)</sub> does not interact with Fe65.** (A) Amino acidic sequence of the C-terminal tail of P2X<sub>2</sub> subunit. The amino-acids not present in the P2X<sub>2(b)</sub> splice variant are underlined. (B) Y2H assay of the interaction between the splice variant of the P2X<sub>2</sub> receptor (P2X<sub>2(b)</sub>CD) and Fe65-202. No positive interaction between P2X<sub>2(b)</sub>CD and Fe65 was observed, as evidenced in the bottom row of the figure. The positive interaction between P2X<sub>2</sub>CD and Fe65-202 is showed in the first row.

When the cytoplasmic domain of the P2X<sub>2</sub> splice variant (P2X<sub>2(b)</sub>CD) was employed as bait on a direct Y2H assay with Fe65 as prey, no interaction was found, both in the metabolic or the enzymatic assay (Figure 4.6B). These results suggest that alternative splicing might be a regulatory mechanism for the interaction between Fe65 and the P2X<sub>2</sub> subunit.

#### 4.2.4. Delimiting residues of P2X<sub>2</sub> responsible for the interaction

On the previous experiments we found that region of Fe65 important for the interaction is the WW domain while the first PTB domain might play a supporting role on the interaction. It is known that WW domains interact with proline-rich domains or proline-containing ligands (Sudol *et al.*, 1995), while the PTB domain may recognize the non-conserved sequence NPXY. We identified on the cytoplasmic domain of P2X<sub>2</sub> four proline-rich domains (<sub>393</sub>PPPP<sub>396</sub>, <sub>404</sub>PPSPP<sub>408</sub>, <sub>428</sub>PRP<sub>430</sub>, <sub>449</sub>RPPVPEP<sub>455</sub>), and one putative PTB-binding site (<sub>359</sub>NKLY<sub>362</sub>) (Figure 4.7).



**Figure 4.7. The P2X<sub>2</sub> C-terminal tail presents four Pro-rich domains and one putative PTB binding domain.** The proline-rich domain sequences and the putative PTB-binding domain are highlighted in blue and light blue respectively. Amino-acids not present in the P2X<sub>2(b)</sub> splice variant are underlined.

---

All together, this information prompted us to investigate whether the WW domain of Fe65 was interacting with any of the four proline-rich domains of P2X<sub>2</sub>CD. We already had at this point some information on this matter, since the splice variant of the P2X<sub>2</sub> receptor, which lacks the first three proline-rich domains, is not able to interact with Fe65 (Figure 4.6B), suggesting that the fourth proline-rich domain of P2X<sub>2</sub>CD may not be involved in binding to the WW domain of Fe65.

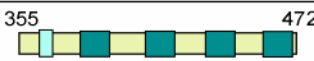
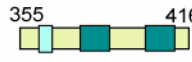
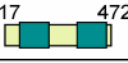
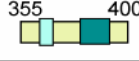
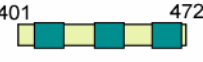
Constructs bearing deletions and point mutations of both P2X<sub>2</sub> and Fe65, as well as Y2H assays summarized on the two following two sections, were carried out by Anja Bremm under my supervision.

#### **4.2.4.1. The first proline-rich domain of P2X<sub>2</sub>CD is necessary for the interaction with Fe65.**

As a first attempt to elucidate which of the four proline-rich domains of P2X<sub>2</sub>CD is interacting with the WW domain of Fe65, two constructs, carrying either the first two or the last two proline-rich domains of P2X<sub>2</sub>CD, were generated. In order to probe the interaction, a direct Y2H assay using this constructs as bait and Fe65 as prey was performed.

The results, summarized on figure 4.8, demonstrated that neither the third nor the fourth proline-rich domain of P2X<sub>2</sub>CD interact with Fe65. Thus, to further investigate which of the first two proline-rich domains of P2X<sub>2</sub>CD are responsible for the interaction with the WW domain, two additional constructs were created. In this case, one construct contained the first proline-rich domain and the other includes the last three. Both constructs were assayed as baits in a direct Y2H assay using Fe65-202 as prey. A positive result for the interaction was evidenced on the construct that harbors the first proline-rich domain, while the construct containing the last three proline-rich domains was not able to interact with Fe65-202 (Figure 4.8).



	VP16-Fe65-202 + LexA-	Results
	P2X <sub>2</sub> CD(355-472)	Positive interaction
	P2X <sub>2</sub> CD(355-416)	Positive interaction
	P2X <sub>2</sub> CD(417-472)	No interaction
	P2X <sub>2</sub> CD(355-400)	Positive interaction
	P2X <sub>2</sub> CD(401-472)	No interaction

**Figure 4.8. The first proline rich domain of P2X<sub>2</sub>CD drives the interaction with Fe65.** Results obtained by Y2H assay on different deletions on the C-terminus of P2X<sub>2</sub> receptor. Binding to Fe65 by the full length P2X<sub>2</sub>CD to (row 1) was only reproduced on constructs containing the first proline-rich domain, as stated on rows 2 and 4. The last three proline-rich domains of P2X<sub>2</sub>CD are not required for the interaction with Fe65, as noted on rows 3 and 5. Proline rich domains are highlighted in dark blue, while the putative PTB binding motif is highlighted in light blue. Full results are provided in Anja Bremm diploma thesis.

#### 4.2.4.2. Structural integrity of the WW domain is required for Fe65 binding to the first proline-rich domain of P2X<sub>2</sub>CD.

WW domains are the smallest, naturally occurring, known protein modules, composed of 30 to 40 amino acids. The name refers to two signature tryptophan (W) residues that are spaced 20-22 amino acids apart and are present in most WW domains (Bork and Sudol, 1994). They fold into three beta sheets strands, stabilized by inter-strand hydrogen bonds. Besides the two hallmark Trp residues, many hydrophobic amino acids play an essential role in binding the Pro-rich ligand, and in particular those composing the second  $\beta$ -sheet strand (Tyr<sub>260</sub>, Tyr<sub>261</sub> and Trp<sub>262</sub> in Fe65). In order to further prove whether the binding event on the studied interaction was indeed a specific recognition of the first Pro-rich domain in P2X<sub>2</sub> by the WW domain in Fe65, a construct of Fe65-202 with point mutations on these three key residues (Tyr<sub>260</sub>Ala, Tyr<sub>261</sub>Ala and Trp<sub>262</sub>Tyr) was generated. The mutated construct was used as prey in a Y2H assay with P2X<sub>2</sub>CD as bait. This experiment shows that the interaction between Fe65 and P2X<sub>2</sub>CD was abolished in the absence of the YYW-motif, which supports the importance of the WW domain in driving the interaction. This result also

---

sustains compelling evidence on the key role that these hydrophobic residues play on binding to the target sequence in a more general WW domain-proline-rich motif interaction (Cao and Sudhof, 2001).

#### **4.2.5. Drawbacks of the yeast two hybrid assay.**

In sections 4.1 and 4.2 the isolation of Fe65 as an interacting partner of P2X<sub>2</sub> receptor and the characterization of that interaction were studied in detail. The results, based on the Y2H technique, indicate that the WW domain of Fe65 interacts with the first proline-rich domain of P2X<sub>2</sub> C-terminus, and that the PTB domain of Fe65 could improve the interaction through the putative PTB-binding site of P2X<sub>2</sub>CD. Y2H is a powerful technique to screen libraries and isolate interacting partners of the studied protein. However, the Y2H system accounts for many drawbacks that raise concerns on the results derived from such a method. In particular, it exist the possibility that an additional protein from yeast could help in the formation of the complex between both studied proteins. To discard such possibility we studied the interaction between P2X<sub>2</sub>CD and Fe65 by GST pull-down. Moreover the existence of the interaction *in vivo* was studies using co-immunoprecipitation approaches.

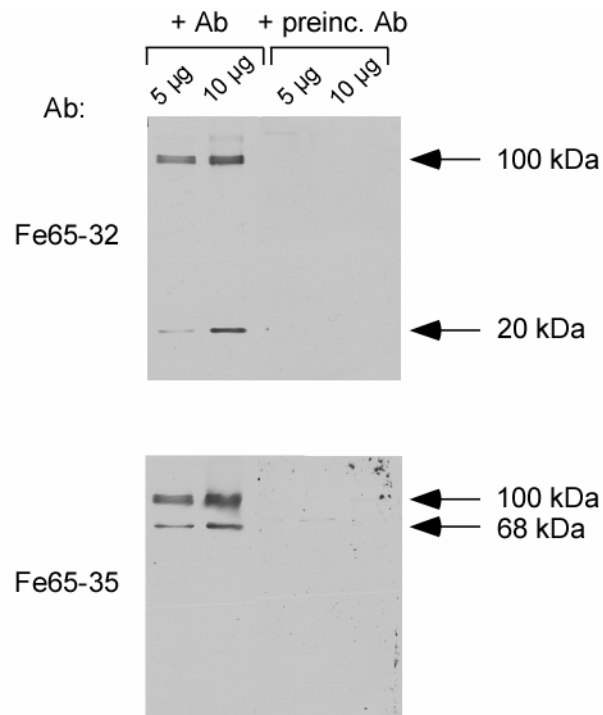
---

### 4.3. Generation and Western blot characterization of Fe65 antibodies

For a successful study on the interaction between Fe65 and P2X<sub>2</sub> both *in vitro* (GST pull-down assay) and *in vivo* (immunoprecipitation assays), and most importantly to assess whether these proteins co-localize and interact in rat brain, we had to obtain antibodies against Fe65. The commercially available antibodies were not specific enough for the planned experiments. Thus, antibodies were raised in rabbits against two different peptide sequences situated on regions at the N-terminus from the WW domain of Fe65 (Fe65<sub>197-255</sub> and Fe65<sub>40-100</sub>). Immunization of the rabbits (2 animals per antigen) was performed by Eurogentec (Seraing, Belgium) with recombinantly expressed GST- Fe65<sub>197-255</sub> or GST-Fe65<sub>40-100</sub> fusion proteins produced in the laboratory. Four different sera (numbers 32, 33, 34 and 35), obtained in the final bleeding of the immunized rabbits, were tested in Western blots against the purified Trx-Fe65<sub>(197-255)</sub> and Trx-Fe65<sub>(40-100)</sub> fusion proteins. Two of the rabbits sera, 32 and 35, showing satisfactory performance in preliminary Western blots were further purified by affinity chromatography using the AminoLink Plus Immobilization Kit (Pierce) with Trx-fused proteins, by a procedure successfully applied in our laboratory for other proteins (Rubio and Soto, 2001; Nicke *et al.*, 2005). The resultant purified antibodies Fe65-32 (immunoreactive to Fe65<sub>197-255</sub>) and Fe65-35 (immunoreactive to Fe65<sub>40-100</sub>) were evaluated for their specificity properties using Western blot on rat brain (postnatal day 21) crude membrane preparations.

Both antibodies detected a thick protein band (~100 kDa) assigned to Fe65 and consisting of two sub-bands (Figure 4.9). The same finding has been reported with different Fe65 antibodies, both in brain and in transfected cells, and has been attributed to different phosphorylation states of Fe65 (Zambrano *et al.*, 1998). One of the antibodies to Fe65 (Fe65-35) recognized an additional band of approximately 68 kDa, which might correspond to the Fe65L2 variant. The Fe65-32 antibody did not recognize the 68 kDa protein, but labeled a

band of approximately 20 kDa, which could be due to protein degradation. No labeling was detected, when the primary antibodies were pre-incubated with the corresponding Trx-fusion protein (Figure 4.9), indicating specificity for the epitope.



**Figure 4.9. Characterization of the antibodies Fe65-32 and Fe65-35 by Western blot of rat brain homogenates.** 5 or 10 µg of crude membrane protein fraction were loaded per lane. Both polyclonal antibodies recognize a band of approximately 100 kDa corresponding to Fe65. When Western blots were performed using antibodies pre-absorbed with the corresponding fusion protein no signal was detected indicating the specificity of the antibodies for the epitope.

Due to the evident specificity of the antibodies and their proper characteristics, both antibodies were used in Western blots for the following experiments.

---

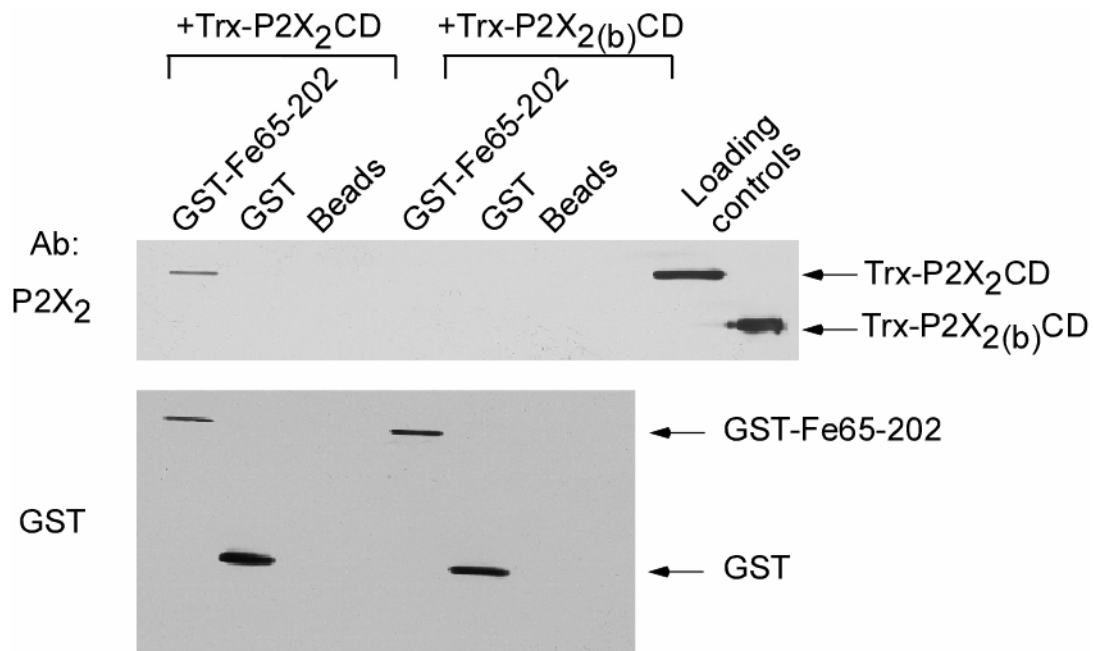
#### **4.4. The complex between Fe65 and P2X<sub>2</sub> is formed by direct interaction of the proteins *in vitro***

Pull-down assays allow the study of protein-protein interactions *in vitro* by co-sedimentation of the interacting partners. The condition is that one of the assayed proteins has to be a recombinant fusion to the glutathione-S-transferase (GST) protein. After incubation in the appropriate buffer, the complex is immobilized on glutathione agarose beads (GST pull-down assay), due to the affinity of GST to glutathione. The complex is afterwards resolved by SDS-PAGE and the presence of the proteins is assayed by Western blot employing the correspondent antibodies.

For this assay, Fe65-202 and P2X<sub>2</sub>CD were expressed as both GST and Trx fusion proteins in bacteria, purified by affinity chromatography and used to confirm the direct interaction between them. Glutathione-agarose beads, both alone or bound to GST, served as negative controls for the assay.

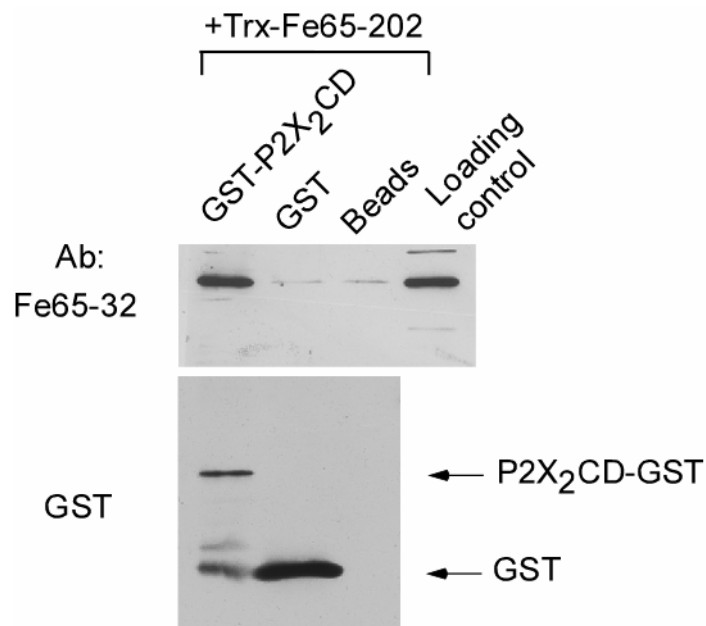
Using immobilized GST-Fe65-202 on glutathione-agarose beads, the C-terminal domain of P2X<sub>2</sub> (Trx-P2X<sub>2</sub>CD) was detected bound to the complex beads-GST-Fe65-202 by Western blot with an antibody specific for P2X<sub>2</sub> (Figure 4.10). The binding of GST-Fe65-202 to the beads was detected with an anti-GST antibody. Importantly, no P2X<sub>2</sub> immunoreactivity was detected in the negative controls, meaning that P2X<sub>2</sub> interacts neither with the agarose beads nor with GST alone. This result confirms that the interaction between Fe65 and the cytoplasmic domain of the P2X<sub>2</sub> receptor is direct, i.e. not mediated by any other protein present in yeast cells.

In the same experiment the resin was incubated with the C-terminal domain of the P2X<sub>2</sub> splice variant (Trx-P2X<sub>2(b)</sub>CD), and, confirming the findings from the Y2H assay (Figure 4.6B), Fe65-202 did not interact with the C-terminal domain of the P2X<sub>2(b)</sub> (Figure 4.10).



**Figure 4.10. Fe65 directly interacts with the cytoplasmic domain of P2X<sub>2</sub> (I).** GST pull-down assays between Fe65<sub>(218-479)</sub> fused to GST (GST-Fe65-202) and the C-terminal domain of P2X<sub>2</sub> fused to Trx (Trx-P2X<sub>2</sub>-CD). *Upper panel:* GST-Fe65-202 was bound to Glutathione agarose beads and incubated with recombinantly expressed Trx-P2X<sub>2</sub>-CD or Trx-P2X<sub>2</sub>(b)CD (splice variant). Glutathione agarose beads alone or bound to GST were used as negative control. Western blot of the co-sedimented proteins using an antibody against P2X<sub>2</sub> evidenced the presence of P2X<sub>2</sub>CD but not P2X<sub>2</sub>(b)CD when GST-Fe65-202 was bound to the resin. Four hundreds ng of Trx-P2X<sub>2</sub>-CD or Trx-P2X<sub>2</sub>(b)CD were loaded directly on the gels and used as positive control. *Lower blot:* An antibody directed to GST was used to verify the amount of GST-fused proteins bound to the beads.

To validate these results, we performed a pull-down experiment in the reverse orientation. In this case, GST-P2X<sub>2</sub>CD was immobilized on Glutathione-agarose beads and Trx-Fe65-202 was then incubated with the resultant resin (Figure 4.11). The Western blot using Fe65-32 antibody revealed co-sedimentation of Fe65-202 on the agarose-GST-P2X<sub>2</sub>CD resin, in line with the previous results. Glutathione-agarose beads alone or bound to GST used as a control also retained a detectable but small amount of Trx-Fe65-202, probably due to a direct interaction of Fe65-202 with the resin.



**Figure 4.11. Fe65 directly interacts with the cytoplasmic domain of P2X<sub>2</sub> (II).** GST pull-down assays in reverse orientation as shown in Figure 4.10. *Upper panel:* Pull-down assay performed with GST-P2X<sub>2</sub>CD bound to glutathione-agarose beads and incubated with Trx-Fe65-202. Western blot of the co-sedimented proteins using the Fe65-32 antibody only showed strong signal when GST-P2X<sub>2</sub>CD was bound to the agarose beads. *Lower blot:* An antibody directed to GST was used to probe the amount of GST-fused proteins bound to the beads. Four hundreds ng of Trx-Fe65-202 were loaded directly on the gel and used as positive control.

Together, these findings demonstrate that the interaction *in vitro* between Fe65 and P2X<sub>2</sub> is both specific and not mediated by any other protein, validating the results obtained by Y2H assays.

---

#### 4.5. Occurrence *in vivo* of the complex between Fe65 and the P2X<sub>2</sub> receptor

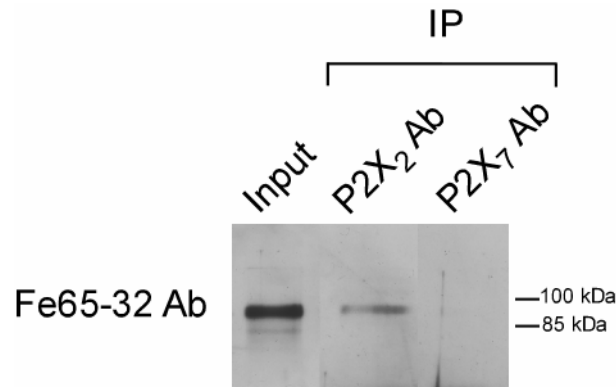
Up to now, we showed that the WW domain of Fe65 interacts *in vitro* with the cytoplasmic domain of P2X<sub>2</sub>. However, there is always the question on whether this interaction also occurs *in vivo*. In addition, both methods employed for detecting the interaction on the previous sections rely extensively on the use of chimeric proteins. This always represents a potential risk, since the fusion might change the actual conformation of the bait and/or prey proteins and consequently alter their complex formation.

Therefore we decided to implement a co-immunoprecipitation assay to study the occurrence of this protein-protein interaction in the proper environment, i.e. in the native tissue where both proteins are present. P2X receptor subunits are found throughout the body, whereas primarily P2X<sub>2</sub>, P2X<sub>4</sub> and P2X<sub>6</sub> subunits are expressed in the brain (Kidd *et al.*, 1995; Soto *et al.*, 1996; Kanjhan *et al.*, 1999; Rubio and Soto, 2001). It is also known that Fe65 is a brain-enriched protein (Bressler *et al.*, 1996), thus we seek to determine whether P2X<sub>2</sub> subunits associate with Fe65 in rat brain by co-immunoprecipitation.

Co-immunoprecipitation experiments were performed on P8 and P21 detergent-treated crude rat brain membrane fractions by capturing the putative P2X<sub>2</sub>-Fe65 complex with a specific antibody against the P2X<sub>2</sub> subunit coupled to a protein A/G agarose resin. The captured complex was resolved by SDS-PAGE and visualization of the protein components was performed by Western blot using antibodies against both Fe65 and P2X<sub>2</sub>.

We found that P2X<sub>2</sub> antibody co-immunoprecipitate Fe65 both in P8 and P21 brain extracts, since this protein was found on the captured complex, as determined by Western blot using the Fe65-32 antibody (Figure 4.12 and Figure 4.13A). Importantly, Fe65 was not detected when the brain membranes were incubated with a commercially available P2X<sub>7</sub> antibody, in line with parallel results obtained by Y2H that showed that Fe65-202 does not interact with the C-terminal domain of the P2X<sub>7</sub> receptor subunit (Figure 4.5).

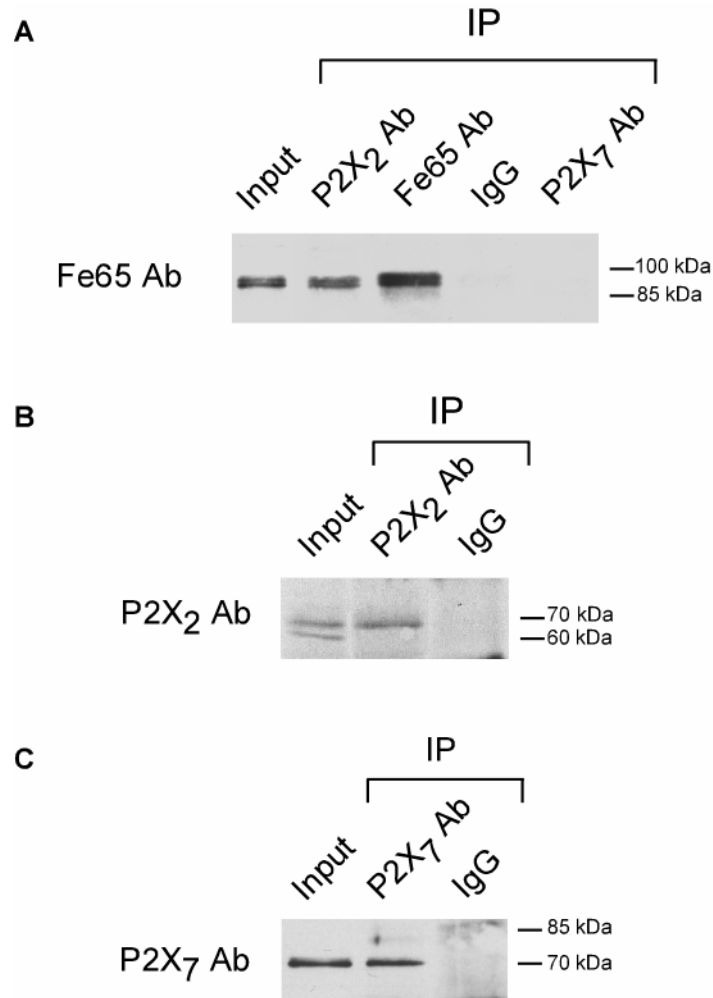




**Figure 4.12. Interaction of Fe65 with P2X<sub>2</sub> *in vivo* (I).** P21 Brain crude membrane fractions were used for co-immunoprecipitation with P2X<sub>2</sub> and P2X<sub>7</sub>, antibodies. The detection was performed using the Fe65-32 antibody. A band of approximately 100 kDa corresponding to Fe65 was detected in the brain membrane fraction (5  $\mu$ g of protein) as well as when the P2X<sub>2</sub> antibody was used for co-immunoprecipitation (2 mg of protein). Fe65 could not be detected when the brain membrane fractions (2 mg of protein) were incubated with a P2X<sub>7</sub> antibody.

As an additional negative control for the experiment, the co-immunoprecipitation was performed using a rabbit IgG, which also did not show any immunoreactivity when probed with the Fe65 antibody, providing stronger evidence for the specificity of the molecular complex investigated (Figure 4.13A).

To further prove the specificity of the antibodies, the co-immunoprecipitated complexes were probed against their target antigen, using anti-P2X<sub>2</sub> anti-P2X<sub>7</sub> antibodies (Figure 4.13B and C) or anti-Fe65 antibodies (Figure 4.13A). These Western blots show that P2X<sub>2</sub>, P2X<sub>7</sub> subunits and the Fe65 adapter protein were co-immunoprecipitated with their corresponding antibodies, and in the case of P2X<sub>2</sub> it confirms that the capture of Fe65 was because of the presence of P2X<sub>2</sub>, and not because of unspecific association of Fe65 with them.

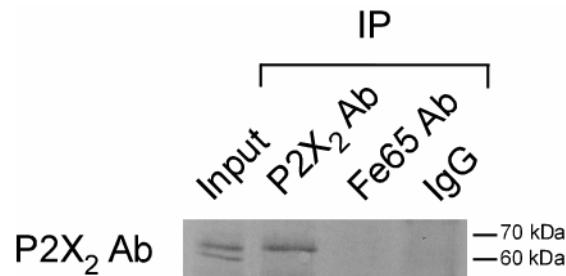


**Figure 4.13. Interaction of Fe65 with P2X<sub>2</sub> *in vivo* (II).** (A) P8 Brain crude membrane fractions were used for co-immunoprecipitation with P2X<sub>2</sub>, P2X<sub>7</sub>, rabbit IgG or Fe65-32 antibodies. The detection was performed using the Fe65-32 antibody. A band of approximately 100 kDa corresponding to Fe65 was detected in the brain membrane fraction (5 µg of protein) as well as when the P2X<sub>2</sub> or the Fe65-32 antibodies were used for co-immunoprecipitation (2 mg of protein). Fe65 could not be detected when the brain membrane fractions (2 mg of protein) were incubated with a P2X<sub>7</sub> antibody. (B) The P2X<sub>2</sub> antibody treated membrane fractions were additionally probed by Western blot using the P2X<sub>2</sub> antibody, in order to show co-immunoprecipitation of the corresponding protein. (C) same as (B) for the P2X<sub>7</sub> antibody.

The co-immunoprecipitation in the opposite direction, using a Fe65 antibody and detecting P2X<sub>2</sub>, did not result in detectable levels of the receptor in Western blots (Figure 4.14). In contrast to P2X<sub>2</sub>, Fe65 is very abundant in rat brain, and has been described to interact with several proteins that are also abundant (e.g. APP). As a consequence, we think that the amount of P2X<sub>2</sub> may constitute a small fraction of the total precipitated protein in

---

these experiments and thus might evade detection by Western blot with the available P2X<sub>2</sub> antibodies. Another possible explanation for these findings is that the region of Fe65, against which Fe65 antibodies were generated, is close to the WW domain and could be hindered.



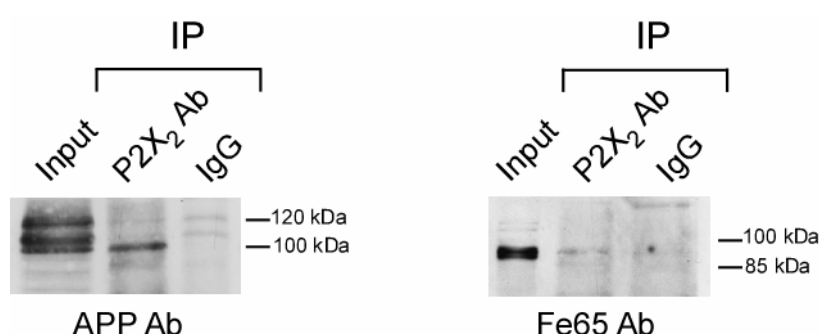
**Figure 4.14. Interaction of Fe65 with P2X<sub>2</sub> *in vivo* (III).** P8 Brain crude membrane fractions were used for co-immunoprecipitation with P2X<sub>2</sub>, Fe65 and IgG, antibodies. The detection was performed using the P2X<sub>2</sub> antibody. P2X<sub>2</sub> was detected in the brain membrane fraction (5 µg of protein) as well as when the P2X<sub>2</sub> antibody was used for co-immunoprecipitation (2 mg of protein), but P2X<sub>2</sub> was not detected when Fe65 antibody was used for co-immunoprecipitation (2 mg of protein).

---

#### 4.6. The Amyloid precursor protein may take part of the macromolecular complex between Fe65 and P2X<sub>2</sub>.

The membrane-located amyloid precursor protein (APP) has a major role in the occurrence of amyloid plaques that extracellularly deposit in Alzheimer's disease patients, since the A $\beta$  peptide is derived from abnormal proteolytic cleavage of this protein (Hardy, 1997). It is known that Fe65 binds APP at the cellular membrane, via an interaction between its PTB2 domain and the C-terminal cytoplasmic tail of APP (Sabo *et al.*, 1999). Since Fe65 binds to the C-terminus of P2X<sub>2</sub> through its WW domain, the formation of a triple molecular complex P2X<sub>2</sub>CD-Fe65-APP could be, in principle, feasible. We therefore investigated whether P2X<sub>2</sub> subunits may be associating with both Fe65 and APP at the membrane level.

Co-immunoprecipitation assays on rat brain membrane extracts with an antibody against P2X<sub>2</sub> showed that both APP and Fe65 could be isolated as interaction partners *in vivo* for the receptor (Figure 4.15). The occurrence of the interaction between P2X<sub>2</sub> and APP is presumably driven by the presence of Fe65, but we cannot discard yet an association between both membrane proteins by their own means. On going research in our lab is focused on the study of this triple protein complex.



**Figure 4.15. APP may form a triple protein complex with Fe65 and P2X<sub>2</sub> *in vivo*.** Brain crude membrane extracts were employed for co-immunoprecipitation with P2X<sub>2</sub> and rabbit IgG. The visualization of the proteins was performed using the Fe65-32 antibody or a commercial anti-APP antibody. *Right panel:* Three bands on the region from 110 to 120 kDa corresponding to APP were detected in the brain membrane fraction (5  $\mu$ g of protein), but only the band with the lower molecular mass was observed when the anti-P2X<sub>2</sub> antibody was used for co-immunoprecipitation (2 mg of protein). APP was not detected when the brain membrane fractions (2 mg of protein) were incubated with rat IgG. *Left panel:* As reported in 4.13, Fe65 was isolated when membrane fractions were treated with the P2X<sub>2</sub>, but not when IgG was used.

---

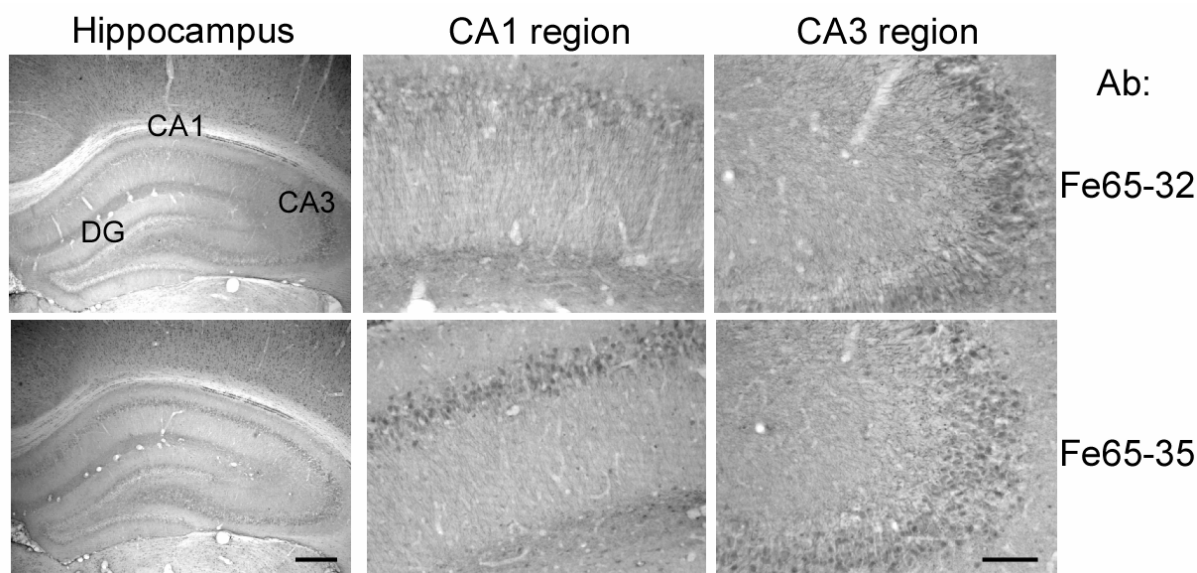
## 4.7. Fe65 and P2X<sub>2</sub> colocalize in excitatory postsynaptic specializations of the hippocampus.

All the experiments reported on section 4.7 were performed by Maria Rubio, at Department of Physiology and Neurobiology, University of Connecticut at Storrs, USA.

### 4.7.1. Characterization of the Fe65 antibodies by peroxidase immunostaining.

First we had to evaluate the level of detection on rat brain slices for the home-made Fe65-32 and Fe65-35 antibodies (section 4.3).

By light microscopy, immunoreactivity with identical patterns for both antibodies, and in a variety of brain areas, was found. In the hippocampus, pyramidal cells in the CA1 and CA3 regions, as well as granule cells of the dentate gyrus, showed immunostaining for Fe65 (Figure 4.16). In CA1 neurons labeling extended from the soma to the distal dendrites in the stratum radiatum. Similarly, in mouse brain, immunoreactivity to Fe65 antibodies has been found widely distributed with a high expression level described for the hippocampal region (Kesavapany *et al.*, 2002).

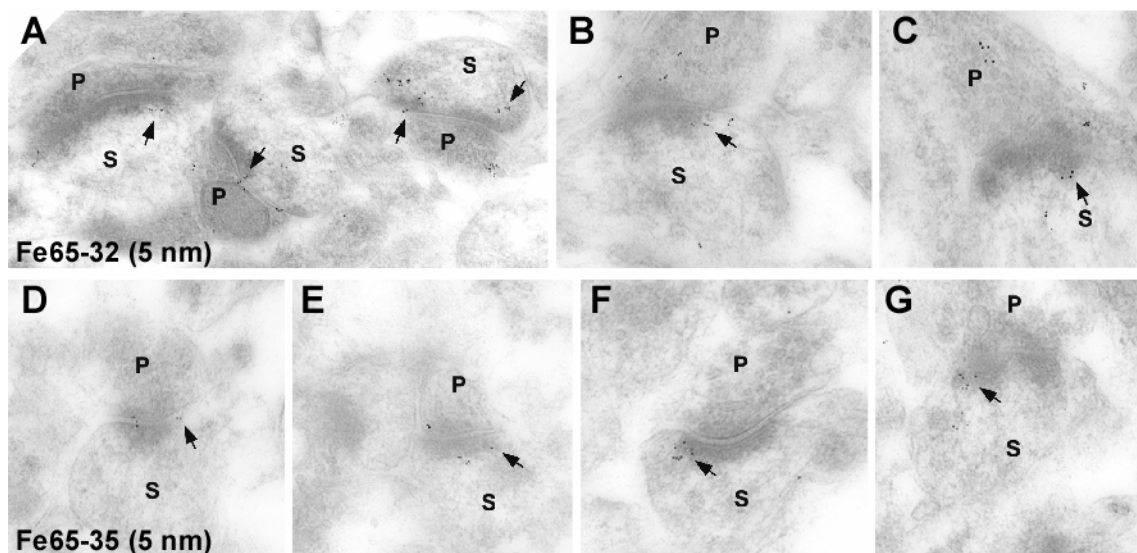


**Figure 4.16. Immunoreactivity for Fe65-32 and Fe65-35 antibodies in the hippocampus.** Light microscopy micrographs showing both in CA1 and CA3 regions immunohistochemical reaction for Fe65 extending from the cell body to the dendrites. Scale bars: 600  $\mu$ m (hippocampus); 300  $\mu$ m (CA1 and CA3).

---

#### 4.7.2. Fe65 is present at excitatory synapses in the hippocampus.

Up to our knowledge, the subcellular localization of Fe65 in the brain has not been described so far, but immunofluorescence labeling of cultured neurons detected Fe65 in both growth cones and in dendrites (Sabo *et al.*, 2003). P2X<sub>2</sub> subunits are present in many brain regions, including the hippocampus (Kanjhan *et al.*, 1999; Rubio and Soto, 2001), and have been localized in excitatory postsynaptic specializations of cerebellum and hippocampus (Rubio and Soto, 2001). To determine, whether Fe65 localization was synaptic, we performed postembedding immunogold labeling on CA1 hippocampal regions. The pattern of immunogold labeling at hippocampal excitatory CA1 synapses apposed to Schaffer collaterals was similar for both Fe65 antibodies (Figure 4.17A-G).



**Figure 4.17. The adapter protein Fe65 is present in hippocampal synapses.** (A-G) Immunogold localization of Fe65 using Fe65-32 (A-C) or Fe65-35 (D-G) antibodies. Gold particles were found both at the pre- and postsynaptic specialization of excitatory hippocampal synapses. Arrows indicate the presence of immunogold-labelled Fe65 in the outer portion of the postsynaptic density, precisely where P2X<sub>2</sub> receptor subunits are known to be found. (s) dendritic spine (p) presynaptic terminal. Scale bar: 200 nm.

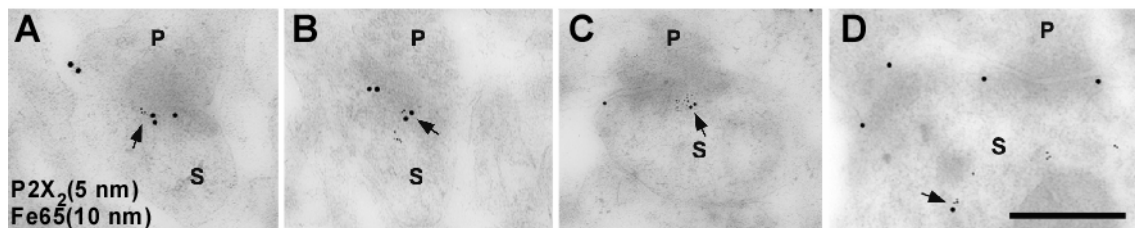
Gold particles were present at both the presynaptic terminal (p) and dendritic spines (s). Notably, on spines, immunogold particles were preferentially located at the edge of the postsynaptic specialization (marked by arrows in Figure 4.17), where P2X<sub>2</sub> receptor subunit immunoreactivity has previously been detected (Rubio and Soto, 2001).

---

By the use of both Fe65 antibodies combined with immunostaining in brain slices, it was possible to detect the presence of Fe65 in hippocampal synapses, and allowed for the first time the description of the subcellular localization of Fe65 in rat brain.

#### **4.7.3. Fe65 and P2X<sub>2</sub> co-localize in excitatory postsynaptic specializations of the hippocampus.**

As showed in the previous result, Fe65 is present in the outer portion of the postsynaptic density, exactly where P2X<sub>2</sub> receptor subunits are predominantly found (Rubio and Soto, 2001). To determine if Fe65 and the P2X<sub>2</sub> subunits are indeed present at the same synapses, we performed sequential immunogold labeling using two different sizes of gold particles (10nm for Fe65 and 5nm for P2X<sub>2</sub>).



**Figure 4.18. Fe65 and P2X<sub>2</sub> subunits co-localized in the postsynaptic specialization.** (A-D) Electron micrographs showing double immunogold labeling for P2X<sub>2</sub> subunits (5 nm) and Fe65 (10 nm). Only the postsynaptic specialization of CA1 synapses presented labeling for both proteins. Arrows in A-C indicate the presence of both Fe65 and P2X<sub>2</sub> receptor subunits in the outer portion of the postsynaptic density. Arrow in D indicates the presence of P2X<sub>2</sub> and Fe65 at the ER. (s) dendritic spine (p) presynaptic terminal. Scale bar: 200 nm

The corresponding results showed that the two proteins co-localize at the postsynaptic specialization, remarkably close to the edge of the postsynaptic density (Figure 4.18A-C, arrows), which argues that Fe65 could regulate synaptic receptor function. In addition, immunogold labeling corresponding to both P2X<sub>2</sub> and Fe65 was also found, although less frequently, colocalized at endoplasmic reticulum membranes (Figure 4.18D, arrow).

---

#### **4.8. Fe65 inhibits the ATP-induced pore dilation of P2X<sub>2</sub> channels.**

Evidenced that the interaction between Fe65 and P2X<sub>2</sub> occurs *in vivo* and since both proteins are co-localized at postsynaptic specializations, it became essential to study the functional consequences of the complex, in terms of modulation of the channel properties. In order to evaluate changes on the function of the P2X<sub>2</sub> receptor upon interaction with Fe65, the electrophysiological properties of the P2X<sub>2</sub> receptor were analyzed both in the presence and absence of Fe65.

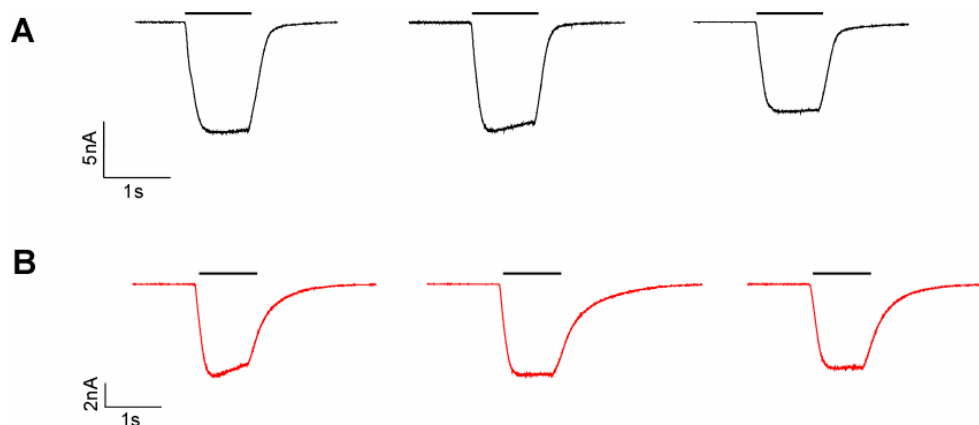
##### **4.8.1. Electrophysiology whole cell recordings.**

Human embryonic kidney 293 (HEK-293) cells permanently transfected with full length P2X<sub>2</sub> (kindly provided by Drs. Annmarie Surprenant and Dr. Alan North) (P2X<sub>2</sub> cells) were transiently transfected with full length Fe65 (P2X<sub>2</sub>-Fe65 cells) and the properties of the currents under patch clamp configuration were measured.

##### ***Current amplitude, desensitization and current recovery***

Transfected cells were measured under the patch clamp configuration at a constant membrane potential of -70 mV. Under these conditions, the fast application of 100 μM ATP elicited currents through P2X<sub>2</sub> receptors that varied in amplitude from -2 to -15 nA (n=25) for P2X<sub>2</sub> cells and from -1.5 to -12 nA (n=20) for P2X<sub>2</sub>-Fe65 cells. Application of higher concentrations of ATP (250 and 500 μM) elicited currents of the same amplitude, indicating that 100 μM is the supramaximal agonist concentration both for P2X<sub>2</sub> and P2X<sub>2</sub>-Fe65 receptors. Currents obtained did not desensitize during the application period of 1-3 seconds, but the channel did close when the application of ATP was discontinued, both for P2X<sub>2</sub> and P2X<sub>2</sub>-Fe65 receptors. After a washing time of 2 minutes in the absence of the agonist, the current was recovered to 70-100 % of the initial current. Elicited currents from P2X<sub>2</sub> and P2X<sub>2</sub>-Fe65 receptors obtained under three consecutive applications of 100 μM ATP followed by washing steps of 2 min are shown in figure 4.19.



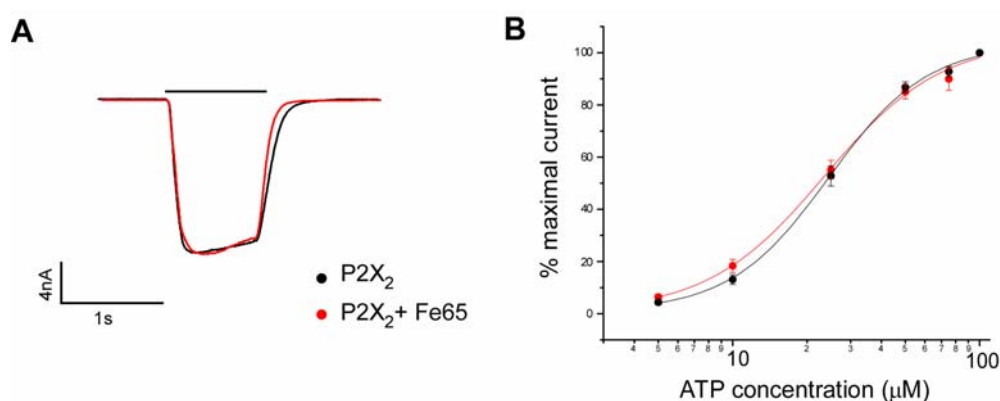


**Figure 4.19. Representative currents of P2X<sub>2</sub> and P2X<sub>2</sub>-Fe65 receptors.** Whole cell recordings of P2X<sub>2</sub> and P2X<sub>2</sub>-Fe65 cells. (A) Currents evoked by P2X<sub>2</sub> cells upon application of 100 μM ATP during 1s with 2 min wash steps between each application (B) Currents evoked by P2X<sub>2</sub>-Fe65 cells subjected to application of 100 μM ATP during 1s with 2 min wash steps between applications.

Once the initial conditions for recording of the currents were obtained, concentration-response and current-voltage relationships were measured.

*Sensitivity to ATP, concentration-response curves.*

Response to ATP for P2X<sub>2</sub> subunits in the absence and presence of Fe65 (P2X<sub>2</sub> receptors and P2X<sub>2</sub>-Fe65 receptors, respectively) was first studied by applying different concentration of ATP (5, 10, 24, 50, 75 and 100 μM ATP) in order to determine the amount of ATP that elicited 50% of the maximal current obtained at 100 μM ATP, the so-called EC<sub>50</sub> value (Figure 4.20).



**Figure 4.20. Interaction with Fe65 does not change the current kinetics or the ATP sensitivity of P2X<sub>2</sub> receptors.** Whole cell recordings of P2X<sub>2</sub> and P2X<sub>2</sub>-Fe65 cells. (A) currents evoked by 100 μM ATP on P2X<sub>2</sub> (black) or P2X<sub>2</sub>-Fe65 cells (red). (B) concentration-response curves for ATP in P2X<sub>2</sub> (black) or P2X<sub>2</sub>-Fe65 cells (red). A concentration-response curve was fitted to the data using IgorPro software. The EC<sub>50</sub>s obtained are 23.7 ± 1.6 and 24.4 ± 0.9 μM, for P2X<sub>2</sub> and P2X<sub>2</sub>-Fe65 respectively. Hill slopes for P2X<sub>2</sub> is 2.1 ± 0.1 and 1.8 ± 0.2 for P2X<sub>2</sub>-Fe65. Data are mean ± S.E.M.

---

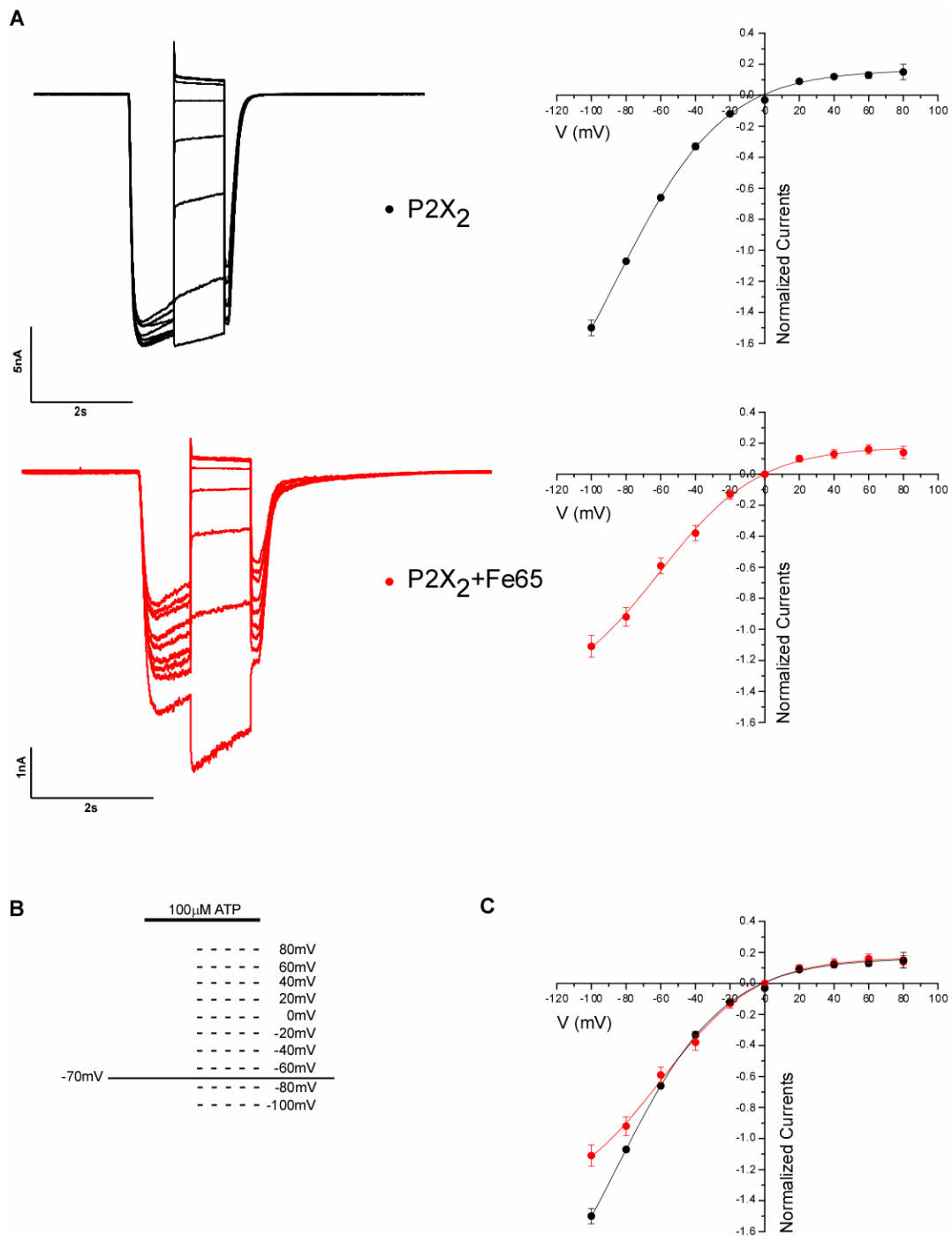
The results revealed equal pharmacological properties between P2X<sub>2</sub> receptors alone or in the presence of Fe65. Thus, no differences in ATP EC<sub>50</sub> values were found:  $23.7 \pm 1.6$  and  $24.4 \pm 0.9$   $\mu$ M with Hill slopes of  $2.1 \pm 0.1$  and  $1.8 \pm 0.2$ , for P2X<sub>2</sub> receptors and P2X<sub>2</sub>-Fe65 receptors respectively. In addition, similar current amplitude and kinetics were observed (Figure 4.20). Thus, the formation of the complex between Fe65 and P2X<sub>2</sub> does not change the response of the receptor to ATP, its natural ligand.

***Current-voltage relationship.***

Additionally, measurements of currents-voltage (I-V) relationships of ATP-gated currents were carried out. To determine the I-V relations curves, P2X<sub>2</sub> cells or P2X<sub>2</sub>-Fe65 cells were maintained at a initial holding potential of -70mV and during the 100  $\mu$ M ATP application, the cells were clamped at various holding potentials from -100 to 80 mV, in 20 mV steps (Figure 4.21B) . This protocol allows the evaluation of the potential where the inward and outward currents through the channel are identical so there is net zero current flowing to the channel. This is the so called reversal potential ( $E_{rev}$ ) of the current, and depends on the permeability of the channel to the different ions present in the intra- and extracellular solution. The shape of the I-V curve gives an idea on the gating of the channel at the different voltages.

As observed in figure 4.21, both in the presence and absence of Fe65, the P2X<sub>2</sub> receptor displays a similar behavior concerning its current-voltage dependence. Only at very negative voltages (-70 to -100 mV), the binding of Fe65 seems to exert a slight decrease (15 to 30 % reduction) in the amount of current that it is being carried through the channel. As expected the obtained reversal potentials in both cases were close to zero,  $-2.7 \pm 0.2$  mV (n=12) for P2X<sub>2</sub> receptors, and  $-2.4 \pm 2.0$  mV (n=10) for the complex P2X<sub>2</sub>-Fe65, respectively. Notably, both exhibited a similar degree of inward rectification as previously

reported (Evans *et al.*, 1996), supporting the notion that the response to ATP a different holding voltages essentially not affected (Figure 4.21).



**Figure 4.21. P2X<sub>2</sub> present similar current-voltage relationships in the presence and the absence of Fe65.** (A) I-V relation curves from voltage steps (-100 to 80 mV, in 20 mV steps) of P2X<sub>2</sub> receptors (black, top panel) and P2X<sub>2</sub>-Fe65 receptors (red, lower panel). On the left, representative currents evoked by one cell when the I-V protocol showed in (B) was applied. (B) Voltage steps protocol, the cells were voltage-clamped at the indicated holding potential during ATP application. (C) I-V relation curves in (A) but displayed together for comparison.

---

The absence of changes in the functional properties so far investigated upon formation of the complex between Fe65 and P2X<sub>2</sub>, pointed our attention towards a recent discovery on the mechanism by which P2X<sub>2</sub> channels undergo permeability changes. It was found that P2X channels open to a small pore in a second or less, and during maintained or repetitive ATP applications, they open a larger pore (Khakh *et al.*, 1999; Virginio *et al.*, 1999). Results suggest that the selectivity filter in these channels is dynamic, and that the channel has to necessary undergo conformational rearrangements to switch its preference between ions. What was recently observed is that motions on the cytosolic domain of P2X<sub>2</sub> may control ion channel permeability, which was indeed prevented by immobilization of the C-terminal domain (Fisher *et al.*, 2004). Consequently it is possible that Fe65 binding restrains the mobility of the P2X<sub>2</sub> C-terminus and alters the changes in ionic selectivity of the channel.

In order to measure permeability changes that might indicate a pore dilation, extracellular Na<sup>+</sup> was substituted by *N*-methyl-D-glucamine (NMDG<sup>+</sup>), a bulky organic cation which permeates poorly through P2X<sub>2</sub> because it is larger than the narrowest part of the channel pore (Evans *et al.*, 1996). It was shown that NMDG<sup>+</sup> was only uptaken by P2X<sub>2</sub> receptors upon prolonged exposure to ATP (Virginio *et al.*, 1999), so we attempted to measure permeability changes on HEK293 cells transfected with P2X<sub>2</sub> receptors in the presence or absence of Fe65.

When we attempted to measure NMDG<sup>+</sup> uptake in HEK293 cells, a significant leak, higher than 25% of the total current, was detected, which made measurements not reliable. This feature could be attributed to the effect that the absence of Ca<sup>+2</sup> provokes on the homeostasis of the membrane from cultured cells. Unfortunately, this was an important limitation that prompts us to change the method of choice for recording the electrophysiological properties of the channel. Instead of HEK293 cells we had to employ

---

two electrode voltage-clamp recordings in *Xenopus laevis* oocytes, which are easier to measure in the absence of extracellular  $\text{Ca}^{2+}$ .

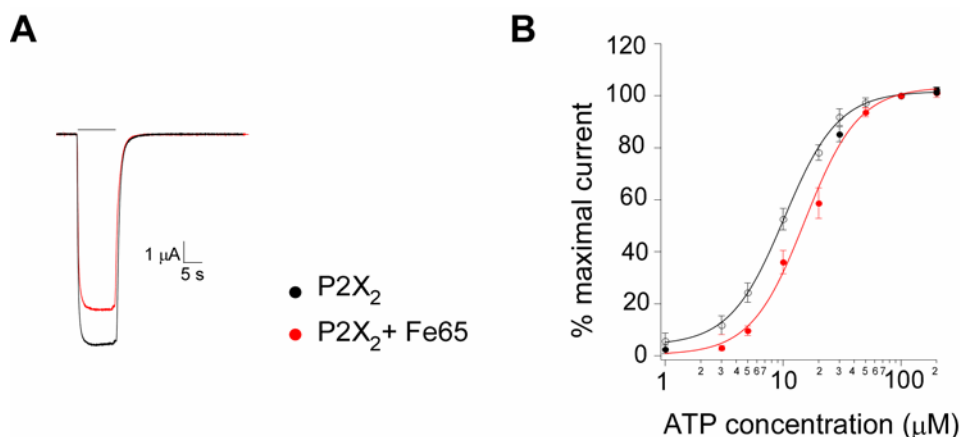
#### **4.8.2. Two electrode voltage-clamp recordings in *Xenopus laevis* oocytes**

For this approach *X. laevis* oocytes were injected with P2X<sub>2</sub> cRNA alone or with a mixture of cRNAs encoding for P2X<sub>2</sub> and Fe65, and the ATP-elicited currents were compared in both cases. Essentially, the same recordings as the ones performed for HEK293 cells were performed on oocytes.

##### ***Sensitivity to ATP, concentration-response curves.***

Since we changed the studied system from HEK293 cells to *X. laevis* oocytes, we had first to verify the similar dependence on ATP concentration for the P2X<sub>2</sub> receptor, both in the presence and absence of Fe65.

In line with what was observed in HEK293 cells, the currents obtained for P2X<sub>2</sub> or P2X<sub>2</sub>-Fe65 receptors in oocytes, with the two electrode voltage-clamp technique, showed comparable basic properties. They presented similar current amplitude (Table 4.2), kinetics (Figure 4.22A) and ATP EC<sub>50</sub> values:  $10.2 \pm 0.3$  and  $15.3 \pm 1.2$   $\mu\text{M}$  with Hill slopes of  $1.9 \pm 0.1$  and  $1.9 \pm 0.3$ , for P2X<sub>2</sub> and P2X<sub>2</sub>-Fe65, respectively (n=3-15), (Figure 4.22B). Under our experimental set up, it is expected that a change in the EC<sub>50</sub> would have to be close to one order of magnitude to be considered as significant.



**Figure 4.22. Fe65 does not substantially change the current kinetics or the ATP sensitivity of P2X<sub>2</sub> receptors.** Two electrode voltage clamps on *X. laevis* oocytes expressing P2X<sub>2</sub> (black) or P2X<sub>2</sub> and Fe65 (red). (A) currents evoked by 10 μM ATP on oocytes expressing P2X<sub>2</sub> or P2X<sub>2</sub>-Fe65 receptors. No apparent changes in current kinetics were observed upon co-expression. (B) concentration-response curves for ATP in oocytes expressing P2X<sub>2</sub> or P2X<sub>2</sub>-Fe65 receptors. Concentration-response curves were fitted to the data using IgorPro software. Values obtained for the EC<sub>50</sub>s were 10.2 ± 0.3 and 15.3 ± 1.2 μM for P2X<sub>2</sub> and P2X<sub>2</sub>-Fe65, respectively. Data are mean ± S.E.M. of 4 to 15 experiments from 2 different batches of oocytes.

#### *Current-voltage relationship.*

We performed current-voltage relation measurements with extracellular Na<sup>+</sup> solutions for P2X<sub>2</sub> and P2X<sub>2</sub>-Fe65 receptors expressed in *X. laevis* oocytes. As mentioned before, P2X<sub>2</sub> receptors display a time- and activation-dependent increase in the permeability to bulky organic cations (Khakh *et al.*, 1999; Virginio *et al.*, 1999), and measurements of fluorescence resonance energy transfer (FRET) have revealed that restriction of cytosolic channel motions are associated with the impairment of pore dilation. This is a plausible scenario to investigate physiological consequences for the binding event of Fe65 to the C-terminus of P2X<sub>2</sub>.

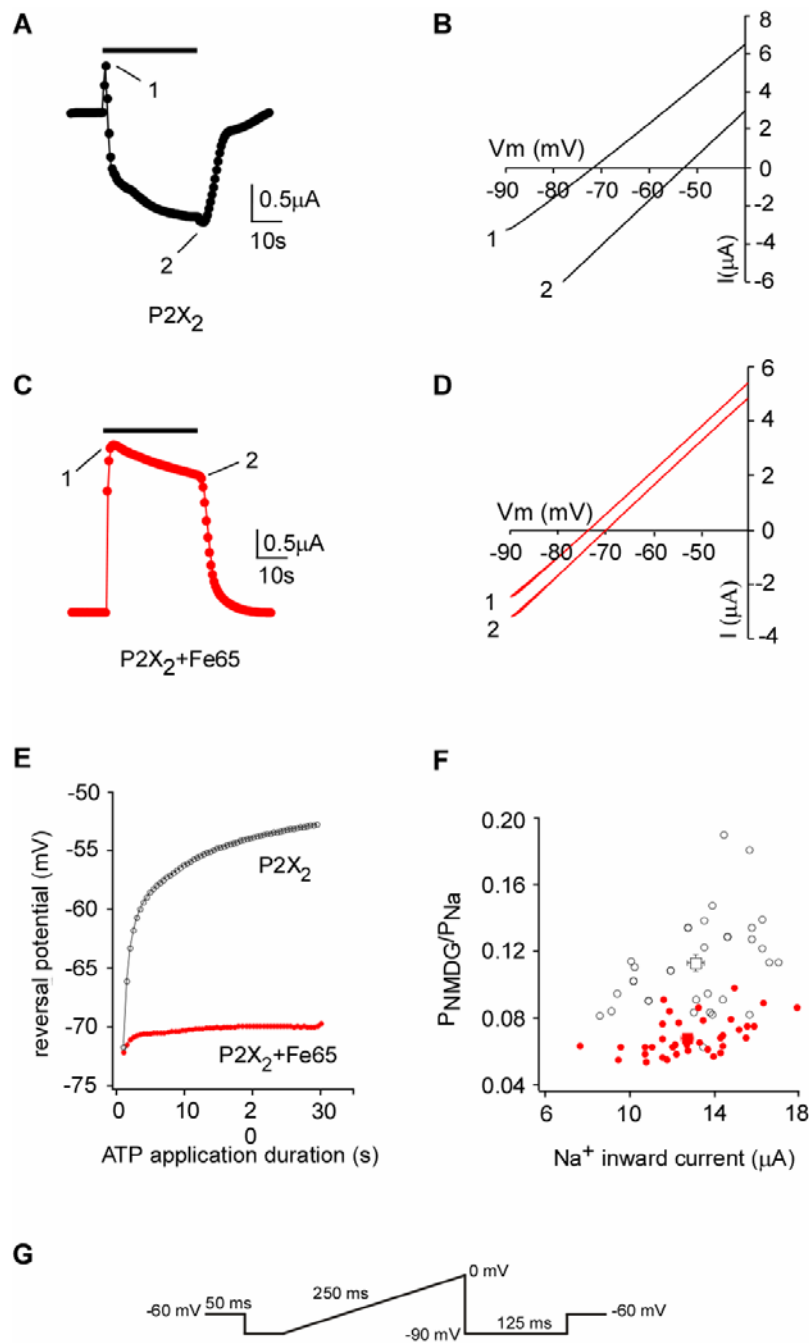
Therefore, we measured selectivity changes in oocytes expressing P2X<sub>2</sub> alone or in the presence of Fe65. We observed the shifts in the reversal potential of currents ( $E_{rev}$ ) recorded during prolonged exposure to ATP, in an extracellular solution containing the organic cation NMDG<sup>+</sup> as sole permeant ion. A voltage ramp protocol consisting of four segments, 50 ms at -60mV, 50 ms at -90 mV, 250 ms ramp from -90 to 0 mV, 125 ms at -90 mV, was applied (Figure 4.23G). The first segment was used to determine the time course of the current at -60 mV in NMDG<sup>+</sup> (Figure 4.23A and C). By repeatedly applying ramp pulses

---

we observed a time-dependent shift in the reversal potential of the current as previously described for P2X<sub>2</sub> receptors expressed in *Xenopus* oocytes (Eickhorst *et al.*, 2002). This change was drastically reduced in oocytes expressing P2X<sub>2</sub>-Fe65 receptors (Figure 4.23B and D). Thus, the mean reversal potential ( $E_{rev}$ ) of the current at 1 second ( $I_1$ ) and 30 seconds ( $I_2$ ) after the start of ATP application changed from  $-72.2 \pm 0.6$  mV (at  $I_1$ ) to  $-56.5 \pm 0.9$  mV (at  $I_2$ ; n=47) for P2X<sub>2</sub> receptors and from  $-74.7 \pm 0.5$  mV (at  $I_1$ ) to  $-67.8 \pm 0.6$  mV (at  $I_2$ , n=48) for P2X<sub>2</sub>-Fe65 receptors (Table 4.2). The corresponding  $P_{NMDG}/P_{Na}$  permeability ratios changed from  $0.057 \pm 0.001$  (at  $I_1$ ) to  $0.107 \pm 0.004$  (at  $I_2$ ; n=47) and from  $0.052 \pm 0.001$  (at  $I_1$ ) to  $0.068 \pm 0.002$  (at  $I_2$ , n=48) for P2X<sub>2</sub> and P2X<sub>2</sub>-Fe65 receptors, respectively.

Thus a notable decrease in the permeation to NMDG<sup>+</sup> in P2X<sub>2</sub>-Fe65 receptors with respect to P2X<sub>2</sub> receptors is observed. The time course of the changes in  $E_{rev}$  upon ATP application for the oocytes expressing P2X<sub>2</sub> or P2X<sub>2</sub>-Fe65 receptors are depicted in figure 4.23B and D is shown in figure 4.23E.

These measurements show the first drastic physiological difference for P2X<sub>2</sub> receptors in the presence and absence of Fe65. Importantly, these results were repeated in all of four batches of oocytes tested, supporting the reproducibility of the observed effect. In addition, P2X<sub>2</sub> and P2X<sub>2</sub>-Fe65 receptors presented similar current amplitudes (Table 4.2), ruling out differences in the expression level as a confounding factor on the analysis. Representative currents to supramaximal concentrations of ATP (100  $\mu$ M) in NMDG<sup>+</sup> solution at a holding potential of -60 mV for P2X<sub>2</sub> and P2X<sub>2</sub>-Fe65 receptors are shown in figure 4.23A and C, respectively.



**Figure 4.23. The interaction with Fe65 hinders the time- and activation-dependent change in pore selectivity presented by P2X<sub>2</sub> receptors.** Two electrode voltage clamps on *X. laevis* oocytes expressing P2X<sub>2</sub> (black) or P2X<sub>2</sub> and Fe65 (red). (A) steady state current obtained upon activation of oocytes expressing the P2X<sub>2</sub> receptor with 100 μM ATP at a holding potential of -60 mV in NMDG<sup>+</sup> containing solutions. (B) ATP was applied during 30 second-ramps (-90 to 0 mV; 250 ms), in NMDG<sup>+</sup> extracellular solution. Time points 1 and 2 represent the current-voltage relationships taken after 1 and 30 seconds of ATP application, respectively. (C-D) same data as in (A-B) recorded for oocytes co-injected with P2X<sub>2</sub> and Fe65. (E) time-dependence of the E<sub>rev</sub> shift for oocytes presented in (B) and (D), respectively. (F) correlation between the expression level of P2X<sub>2</sub> receptors and the permeability ratio at 30 seconds after the beginning of ATP application, for oocytes injected with P2X<sub>2</sub> cRNA alone (Black; n=34) or with P2X<sub>2</sub>+Fe65 cRNA (red; n=41). (G) Voltage ramp protocol, it consists of four segments, 50 ms at -60mV, 50 ms at -90 mV, 250 ms ramp from -90 to 0 mV, 125 ms at -90. The squares represent the mean ± S.E.M values of permeability *versus* current.



In order to determine the specificity of the regulation of P2X<sub>2</sub> receptor function by Fe65, we performed the same functional experiments by co-expressing Fe65 and P2X<sub>7</sub> receptor subunits. Similarly to P2X<sub>2</sub> receptors, P2X<sub>7</sub> receptors undergo changes in permeability upon exposure to agonist (Surprenant *et al.*, 1996; Khakh *et al.*, 1999). However, P2X<sub>7</sub> subunits do not seem to interact with Fe65 as we observed by Y2H and by co-immunoprecipitation experiments (Figure 4.5 and 4.12-4.13A, respectively).

By repeatedly applying ramp pulses (Figure 4.23G), we observed a time-dependent shift in the reversal potential of P2X<sub>7</sub> receptor expressed in *Xenopus* oocytes. Nevertheless, and in contrast to what we observed for P2X<sub>2</sub> receptors, the changes were of the same magnitude in oocytes expressing P2X<sub>7</sub>-Fe65 receptors. Thus, the mean reversal potential ( $E_{rev}$ ) of the current at 1 second ( $I_1$ ) and 45 seconds ( $I_2$ ) after start of ATP application changed from  $-68.4 \pm 0.6$  mV (at  $I_1$ ) to  $-48.1 \pm 0.9$  mV (at  $I_2$ ; n=25) and from  $-69.1 \pm 0.7$  mV (at  $I_1$ ) to  $-50.9 \pm 1.4$  mV (at  $I_2$ , n=22) for P2X<sub>7</sub> and P2X<sub>7</sub>-Fe65 receptors, respectively (Table 4.2).

	$I_1$		$I_2$		$I_{Na}$	
	$E_{rev}$ (mV)	$P_{NMDG}/P_{Na}$	$E_{rev}$ (mV)	$P_{NMDG}/P_{Na}$	maximal current ( $\mu$ A)	$E_{rev}$ (mV)
P2X <sub>2</sub>	$-72.2 \pm 0.6$ (n = 47)	$0.057 \pm 0.001$	$-56.5 \pm 0.6$	$0.107 \pm 0.004$	$-13.2 \pm 0.3$ (n = 34)	$-6.4 \pm 1.3$
P2X <sub>2</sub> +Fe65	$-74.7 \pm 0.5$ (n = 48)	$0.052 \pm 0.001$	$-67.8 \pm 0.6$	$0.068 \pm 0.002$	$-12.7 \pm 0.4$ (n = 41)	$-8.2 \pm 0.7$
P2X <sub>7</sub>	$-68.4 \pm 0.6$ (n = 25)	$0.065 \pm 0.002$	$-48.1 \pm 0.9$	$0.141 \pm 0.007$	$-6.17 \pm 0.9$ (n = 12)	$-6.9 \pm 0.4$
P2X <sub>7</sub> +Fe65	$-69.1 \pm 0.7$ (n = 22)	$0.065 \pm 0.003$	$-50.9 \pm 1.4$	$0.148 \pm 0.006$	$-5.2 \pm 0.7$ (n = 16)	$-5.5 \pm 0.5$

**Table 4.2. P2X<sub>2</sub> receptors show time- and activation-dependent changes in ionic selectivity that are hindered upon coexpression with Fe65.** Overall results obtained by two electrode voltage-clamp technique on P2X<sub>2</sub> and P2X<sub>7</sub> receptors after heterologous expression in *Xenopus* oocytes. Reversal potential ( $E_{rev}$ ) was measured and  $P_{NMDG}/P_{Na}$  was calculated 1 second ( $I_1$ ) and 30 (or 45) seconds ( $I_2$ ) after the beginning of 100  $\mu$ M (or 1 mM) ATP application in an extracellular solution containing NMDG<sup>+</sup> as the sole permeant ion.  $I_{Na}$  refers to the current obtained when the extracellular solution contained Na<sup>+</sup> as the sole permeant ion. The number of oocytes measured is represented by n.

---

The corresponding  $P_{\text{NMDG}}/P_{\text{Na}}$  permeability ratios changed from  $0.065 \pm 0.002$  (at  $I_1$ ) to  $0.141 \pm 0.007$  (at  $I_2$ ;  $n=25$ ) and from  $0.065 \pm 0.002$  (at  $I_1$ ) to  $0.148 \pm 0.006$  (at  $I_2$ ,  $n=22$ ) for  $P2X_7$  and  $P2X_7$ -Fe65 receptors, respectively. Also, no significant changes were observed in current amplitude or in reversal potential when  $\text{Na}^+$  was the main permeant ion (Table 4.2).

These data reveal that the interaction of Fe65 leads to a change in the function of the  $P2X_2$  receptor, and underline the importance of the C-terminal domain for the regulation of permeability changes on  $P2X_2$  receptors. Due to the co-localization of  $P2X_2$  and Fe65 in the post-synaptic specialization, these findings represent indeed a novel mechanism by which anchoring proteins in the cytoplasmic periphery of the neuronal membrane could control the function of synaptic receptors.

---

## 5. DISCUSSION

### 5.1. Synaptic signaling through protein-protein interactions

The mechanism by which extracellular signals are transmitted from the plasma membrane to specific intracellular sites is an essential aspect of cellular regulation. The responses of a cell to external and intrinsic signals are organized and coordinated through specific protein-protein, protein-DNA or protein-lipids interactions, among others. What has been a giant leap in the understanding of such cellular processes was the identification of highly conserved protein domains as main effectors of signaling pathways. It is now known that most protein-protein interactions strongly depend on a conserved module on one protein that specifically recognizes a target sequence on the second partner (Pawson and Scott, 1997).

As expected, protein-protein interactions also play a crucial role in synaptic transmission. The way neurons communicate with each other, at the synapse involves three main signaling events: first the generation of the message to sent, second the delivery of the message, and third the reception of the message. The last step involves the reception *per se* of the signal sent and the transduction of such a signal into a cellular response. Ionotropic receptors are neurotransmitter-gated ion channels that receive and process neuronal signals by transducing a chemical signal into a charge flux across the membrane.

Neurotransmitter-based electrical phenomena have devoted a great deal of attention to these receptors, and thus pharmacological and electrophysiological properties of the most abundant ionotropic receptors in the central nervous system have been largely studied. What has become clear not so long ago is that ionotropic receptors do not operate as free-floating entities in the plasma membrane, but more readily interact with specific cytoplasmic proteins forming macromolecular complexes.

---

Many membrane and intracellular proteins are now recognized as specific interacting partners of ionotropic receptors and thus regulating several aspects of their biological properties (Sheng and Pak, 2000). The elucidation of these interactions promises to shed more light on the function and regulation of ionotropic receptors. Indeed, major milestones in current research on ionotropic receptors are how their adequate localization is achieved and how are they involved in intracellular signaling cascades. From the signaling point of view, one way receptors may amplify their signaling is by the use of adapter or scaffolding proteins situated at the inner side of the plasma membrane, that provide additional docking sites for modular signaling proteins (Pawson and Scott, 1997). Certainly, it has been already found that interaction with intracellular proteins regulates the targeting, trafficking and signaling of certain ionotropic receptors as Glutamate, Acetylcholine,  $\gamma$ -aminobutyric and Glycine receptors (Sheng and Pak, 2000).

The P2X receptors are ionotropic receptors that have been shown to influence synaptic transmission and plasticity in different brain regions (Robertson *et al.*, 2001). Elucidation of the role of P2X receptors in neuronal function also requires an understanding of how P2X receptors are targeted to particular synapses and how this localization is regulated during development or synaptic activity. It is also important to find out how P2X receptor activation is coupled to the intracellular events responsible for a particular postsynaptic neuronal response and whether P2X receptor function is regulated by the interaction with intracellular proteins. From the seven different P2X subunits identified so far, P2X<sub>2</sub>, P2X<sub>4</sub> and P2X<sub>6</sub> subunits have been found at a very precise overlapping location of the postsynaptic density of excitatory synapses (Rubio and Soto, 2001). This might indicate that specific intracellular proteins interact with P2X receptors at this very active part of the synapse. From the three subunits, P2X<sub>2</sub> subunit was the most likely candidate to mediate interaction with intracellular proteins due to the length of the intracellular domains. Thus, we

---

employed a yeast two hybrid (Y2H)-based approach to identify proteins interacting in brain with the P2X<sub>2</sub> receptor.

By screening a rat brain cDNA library we isolated the adapter protein Fe65 as the main interacting partner of the P2X<sub>2</sub> cytoplasmic domain. Despite drawbacks of this technique, several lines of evidence acquired *in vitro* and *in vivo* confirmed the association between the P2X<sub>2</sub> subunit and Fe65. Firstly, distinct and overlapping partial cDNA sequences coding for Fe65 (section 4.1) together with the homologous gene Fe65 like 1, were identified in the Y2H screening, which lends strong sustain to their interaction with the P2X<sub>2</sub> subunit. Secondly, the interaction could be verified by co-sedimentation assays using immobilized GST-fused proteins (section 4.4), confirming that this interaction is specific and not mediated by any other protein from the yeast. Thirdly, both proteins were co-immunoprecipitated from rat brain crude membrane fractions (section 4.5), evidencing the occurrence *in vivo* of the interaction. Finally, P2X<sub>2</sub> and Fe65 present overlapping distribution in many brain areas including the hippocampus, where they co-localize at the postsynaptic specialization of excitatory synapses as evidenced by immunogold-labeling electron microscopy (seccion 4.7).

All together, this data unequivocally demonstrate that P2X<sub>2</sub> receptor directly interacts with the adapter protein Fe65, forming a complex at the membrane level. Nevertheless, in order to find out whether this complex could have functional characteristics in signaling pathways, it is first required to understand how this interaction is achieved, looking for common features with other signal transduction mechanisms. One then may be able to seek for physiological consequences of this interaction, as to whether localization or electrophysiological properties of the receptor are modulated by the interacting protein.

---

## 5.2. Dissecting the interaction between Fe65 and the P2X<sub>2</sub> receptor

Fe65 is a multidomain adapter protein that was recently reported to be required for neuronal positioning and the establishment of normal axonal projections during cortical development (Guenette *et al.*, 2006). It contains two different types of protein-protein interaction domains that are involved in protein signalling: one WW domain (amino acids 255 to 284) and two phosphotyrosine binding domains (PTB1, from residues 365 to 510, and PTB2, from 538 to 665).

WW domains are small protein modules (30-40 amino acids) that received their name from two conserved tryptophan residues located 20-22 amino acids apart (Kay *et al.*, 2000). PTB domains, on the other hand, are bigger and more divergent protein-recognition modules. They are found primarily as components of docking proteins that recruit additional signaling proteins to the vicinity of an activated receptor (Borg *et al.*, 1996). The WW domain of Fe65 has been shown to associate with Mena, a protein that regulates axonal growth cone motility (Sabo *et al.*, 2001). Through its PTB1 domain, Fe65 binds to the transcription factor CP2/LSF/LBP (Zambrano *et al.*, 1998), and via its PTB2 domain, it interacts with the amyloid precursor protein (APP), increasing its proteolytic processing to produce the neurotoxic  $\beta$ -amyloid peptide (Sabo *et al.*, 1999).

From the Y2H screening we found that the region of Fe65 that is responsible for the binding to P2X<sub>2</sub> comprised only the WW domain and the first PTB domain (residues 218 to 479), construct that we named Fe65-202 (section 4.1). Further deletions of this construct in its constitutive domains showed that the interaction is driven solely by the WW domain of Fe65 (section 4.2). Furthermore, when we compromised the integrity of the WW domain by mutating key hydrophobic residues the interaction was abolished, supporting the leading role of this protein-interacting domain on the interaction (section 4.2.4). Nevertheless, the presence of the PTB1 domain is very likely to be required for a more efficient interaction,

---

since constructs lacking this protein-interaction domain displayed a reduced binding to the target sequence.

Based on this information we searched the C-terminus of the P2X<sub>2</sub> receptor for motifs that could be responsible for the interaction with the protein-interacting modules of Fe65. We studied four proline-rich motifs (<sub>393</sub>PPPP<sub>396</sub>, <sub>404</sub>PPSPP<sub>408</sub>, <sub>428</sub>PRP<sub>430</sub>, <sub>449</sub>RPPVPEP<sub>455</sub>), and a putative PTB-binding site (<sub>359</sub>NKLY<sub>362</sub>). By means of deletion of domains, we were able to dissect the individual contribution of these motifs to the formation of the complex (section 4.2.4.). We found that the more N-terminal proline rich motif in the C-terminus of the P2X<sub>2</sub> subunit (<sub>393</sub>PPPP<sub>396</sub>) was both sufficient and necessary for the interaction with Fe65, given that in the absence of the first stretch of prolines, the more C-terminal domains did not display significant binding to the adapter protein.

WW domains are the smallest self-folding domains known in nature, and adopt a three beta sheet structure, whereas the central beta sheet ( $\beta$ 2) interacts with the proline-rich sequence. The WW domain of Fe65 belongs to the group II of WW domains, a subset that recognizes polyproline ligands containing PPLP cores, opposite to WW domains from group I that bind ligands with PPXY cores (Macias *et al.*, 2002). The main difference between group I and group II WW domains lies on the residues that are present on the central beta sheet. While group I domains present two consecutive aromatic amino acids in the central sequence, as the Yes-associated protein (YAP), group II domains contain three aromatic residues in the this position (residues Y260, Y261, W262 in Fe65). It was shown that placing a Trp as the third residue on the  $\beta$ 2 sheet in the WW1 domain of YAP was sufficient to shift its binding preferences from Group I to Group II ligands (Espanel and Sudol, 1999). In addition, there are two additional minor groups of WW domains, named III and IV, that bind the sequence PPPR and phospho-Ser or phospho-Thr proline-rich sequences, respectively (Sudol *et al.*, 2001).

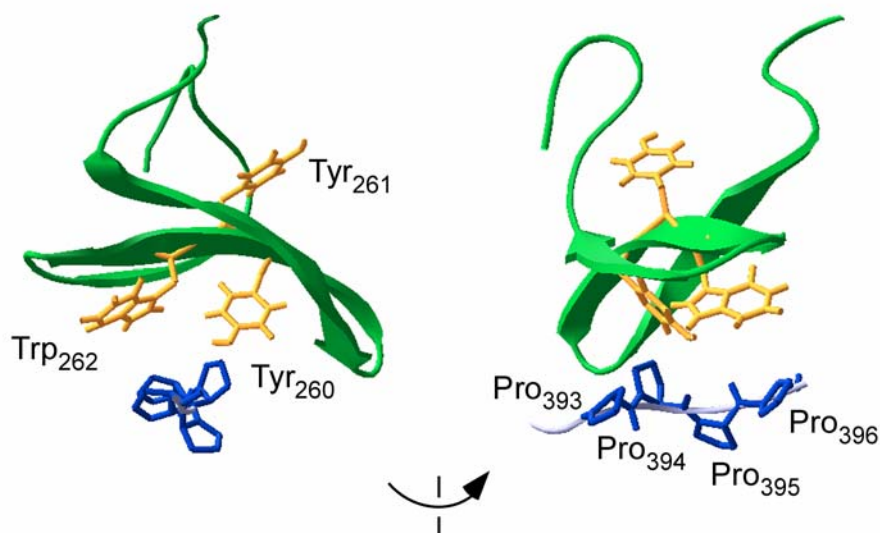
---

We found that the WW domain of Fe65 specifically recognizes the sequence PPPP in the C-terminus of the P2X<sub>2</sub> receptor, since mutations on the hydrophobic core of the  $\beta$ 2 sheet on the WW domain from Fe65 impair the formation of the complex. As mentioned before, it was reported that Fe65 binds the sequence PPLP in Mena, but this sequence is immersed in a longer sequence PPPPPPLPPPPPP, that is found several times on the protein (Ermekova *et al.*, 1997). Indeed by the spot synthesis technique employed on that work, strong binding to the target sequence was observed even in the absence of the central Leu residue. Later the same authors evidenced that the sequenced preferred by Fe65 is likely to be an hexapeptide with the form PPPPPR (Espanel and Sudol, 1999), which indeed contains the sequence PPPP that is found in the P2X<sub>2</sub> subunit. Due to its predilection for the PPPR type of sequences, the WW domain of Fe65 has only been recently included as part of the class III domains (Sudol *et al.*, 2001), which will nicely fit with the binding to a PPPP domain as the one found at the C-terminal domain of P2X<sub>2</sub> receptor subunits.

In order to determine how and why this ligand preference is achieved, it is instructive to comment on the molecular basis of such protein-protein interaction module. By homology with known WW domains architectures, we model the interaction of the WW domain of Fe65 with the Pro-rich PPPP sequence. This domain was fitted to the structure of a consensus WW domain reported by Macias *et al.* (2002), by employing the SWISS-MODEL Protein Modelling Server (Schwede *et al.*, 2003), as shown in figure 5.1.

The structure that we obtained seems to be consistent with the presence of the three beta sheet strands that face the ligand surface. As evidenced in our biochemical assays, both Tyr260 and Trp262 are directly involved in the interaction with the Pro-rich ligand, which is supported by the structural model. We are therefore in the presence of the formation of a molecular complex between a class II/III WW domain and a non-canonical proline rich motif of the type PPPP.





**Figure 5.1. Structural model for the Fe65-P2X<sub>2</sub> interaction.** Protein modelling result for the build-up of the WW domain of Fe65 based on the structure obtained for a consensus WW domain (Macias *et al.*, 2002). The proline-rich motif was oriented by comparison with different known and proposed structures for WW domain ligand-binding, in particular the one for the Npw38 WW domain. Swiss-Model server was employed for generating the structure (Schwede *et al.*, 2003), and the data was visualized by the PDB-viewer software.

In line with our findings, the Npw38 WW domain, which resembles the one from Fe65 since it possess the core Tyr-Tyr-Trp in the  $\beta$ 2 sheet, binds the non-canonical sequence PPGPPP (Komuro *et al.*, 1999). Together with our data, this suggests that the sole interaction between the proline residues and the hydrophobic binding pocket in the  $\beta$ -sheet face of the WW domain is very stable by itself. The role of flanking sequences could then be only required to define other features in the binding event, as for example the final orientation of the poly-proline peptide. Since the WW domain of Fe65 display a dual binding behavior, it is possible that this domain could accommodate ligands in a dual orientation, defining its preference towards Pro-rich sequences of the class II or III. This is the case of most SH3 domains, another protein interacting module that binds Pro-rich motifs, which can readily bind two distinct consensus sequences, each of which binds in a different orientation (Zarrinpar and Lim, 2000).

Opposite to the Pro-rich sequence, the involvement of the putative PTB binding motif of P2X<sub>2</sub> in the binding to Fe65 was not so clearly evidenced. From its location at the N-

---

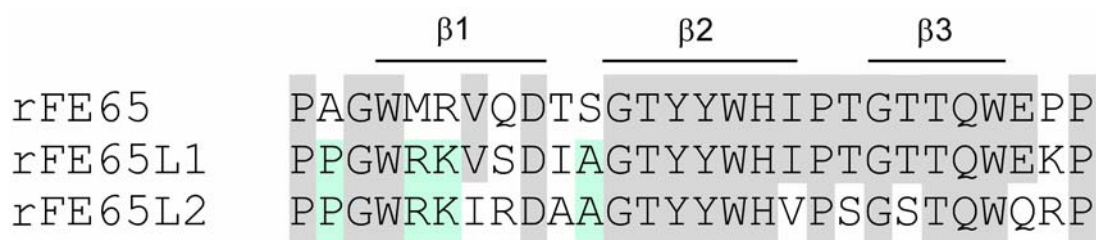
terminus, just 30 residues apart from the first Pro-rich domain, the cooperative binding between the WW domain and the PTB1 domain (distant 80 amino acids) is likely to occur. While the WW domain of Fe65 is conserved compared to those found in other proteins, both PTB domains significantly diverge from those found in other proteins. PTB domains bind the sequence NPXY, where X is any residue, and the Tyr sometimes is required to be phosphorylated for efficient binding (Zhou *et al.*, 1996). In the case of Fe65, phosphorylation is not required for binding to its target, since the first PTB domain lacks three key basic residues involved in the interaction with the negatively charged phosphate moiety (Russo *et al.*, 2002). The putative PTB binding domain in P2X<sub>2</sub> bears the sequence NKLY similar to NKSY, which is the interaction domain of Tip60, a protein recognized by the first PTB domain of Fe65 (Cao and Sudhof, 2001). However, as we determined by deletions on both the first PTB domain and the PTB binding motif, in the binding of Fe65 to P2X<sub>2</sub> the PTB1 domain is neither sufficient nor necessary. The change from a non-polar aliphatic residue as Leu to a polar smaller amino acid as Ser may have drastic consequences to the binding ability of the PTB1 domain. Further mutation analysis on the putative PTB binding motif at the C-terminus of P2X<sub>2</sub>, and evaluation of their impact on the binding event are required to validate this hypothesis.

### **5.3. The role of genetic variability in the interaction between Fe65 and the P2X<sub>2</sub> receptor**

The adapter protein Fe65 has, in humans, two isoforms named Fe65-like1 and Fe65-like2 (Fe65L1 and Fe65L2). Fe65L1 was isolated as an interactor of APP (Guenette *et al.*, 1996), while Fe65L2 was isolated from a cDNA library based on sequence homology to its rat orthologue (Tanahashi and Tabira, 1999). These two proteins contain the same three protein-protein interaction domains and, like Fe65, interact with APP through the PTB2 domain. The rat orthologue of Fe65L2 was early isolated from a rat-brain cDNA library

(Duilio *et al.*, 1998), but rat Fe65L1 has not been described so far. In our Y2H screening of a rat-brain cDNA library for proteins interacting with the C-terminus of P2X<sub>2</sub>, besides Fe65, we isolated a cDNA that showed 96 % homology with human Fe65L1. We believe that this cDNA represent the rat orthologue of this protein, named APBB2. We further performed a direct Y2H assay to corroborate its ability to interact with P2X<sub>2</sub>, and we found that this protein indeed binds the C-terminus of the receptor, in a similar fashion that the Fe65 protein.

Binding partners for the WW domain of Fe65L1 are not yet known, but a recent systematic wide screen approach has addressed binding preferences from the WW domains of Fe65 and the two isoforms Fe65L1 and Fe65L2, from human (Hu *et al.*, 2004). All the three proteins share the key conserved residues in its WW domain, including the Tyr-Tyr-Trp sequence in the  $\beta$ 2 sheet, thus they were expected to bind ligands with a proline-rich motif of the classes II and III. That study confirmed predilection for both Fe65 and Fe65L1 to the central sequence PPPP/K or PPPP/R, while Fe65L2 may bind to a more degenerate sequence G/PPPP/R. In this thesis work we found that the rat orthologue of Fe65L1 is able to bind the PPPP sequence at the C-terminus of P2X<sub>2</sub>, similarly to Fe65. In contrast to these two proteins, the rat orthologue of Fe65L2, although being highly expressed in brain, was not isolated in the Y2H screening, which in principle suggest that it is not able to bind to the poly-proline motif PPPP. Sequence comparison of this domain between Fe65 and Fe65L1 shows 75% conservation, while comparing to Fe65L2 shows only a 60% homology (Figure 5.2).



**Figure 5.2. Sequence homology for the WW domains for the rat Fe65 family.** Residues shared among Fe65 and its isoforms are highlighted in grey, while amino acids in light blue represent positions conserved between Fe65L1 and Fe65L2.

---

Notably, the sequence identity between rat Fe65 and Fe65L1 rises to 100% if we just consider the residues of the  $\beta 2$  and  $\beta 3$  strands of the WW domain, the ones directly involved in binding to the ligand, while comparison with Fe65L2 drops identity to 75%. This is very likely to explain the different binding behavior of the members of the family, and points once more towards the role that adjacent residues to key hydrophobic amino acids play on defining ligand predilection of WW domains. Our results are thus the first evidence for functional diversity for the WW domains of the Fe65 family of proteins.

Alternative splicing on the C-terminus of the P2X<sub>2</sub> subunit mRNA originates a shorter variant of this protein named P2X<sub>2(b)</sub>, that bears a 69-amino acid deletion. The loss of the region from residues Val<sub>371</sub> to Gln<sub>439</sub> is due to a 207 bp DNA fragment spliced out directly from the carboxyl-terminal exon 11 due to the presence of a cryptic splice site (Brandle *et al.*, 1997). This splice variant is expressed at high levels in neonatal rat brain, and its transcript is distributed in the central and peripheral nervous systems similarly to the P2X<sub>2</sub> subunit (Simon *et al.*, 1997). Activity of the receptor is not affected on the spliced variant, since ATP-evoked currents in P2X<sub>2(b)</sub> microinjected *X. laevis* oocytes were similar in size to those seen for the P2X<sub>2(a)</sub> receptor (Simon *et al.*, 1997), but the P2X<sub>2(b)</sub> subunit shows significant differences in desensitization kinetics and steady-state currents in the continuous presence of ATP (Brandle *et al.*, 1997; Simon *et al.*, 1997). In addition, it was recently suggested that alternative splicing of mouse P2X<sub>2</sub> receptor may regulate multimerization, since interactions between C-termini and between C- and N-termini of adjacent subunits were significantly enhanced in homomeric and heteromeric receptors containing P2X<sub>2(b)</sub> subunits (Koshimizu *et al.*, 2006).

Interestingly, we found by means of Y2H and pull-down assays that the P2X<sub>2(b)</sub> subunit is not able to interact with the adapter protein Fe65, which was anticipated due to the absence of the first proline rich domain (<sub>393</sub>PPPP<sub>396</sub>) at the C-terminus of this receptor. We

---

have discussed above how the first proline motif of P2X<sub>2</sub>CD was sufficient and necessary for the interaction with the WW domain of Fe65, and the behavior of the splice variant confirms once more our findings.

It was reported that ATP-activated currents mediated by the P2X<sub>2(b)</sub> receptor desensitized faster than P2X<sub>2</sub>-mediated currents, whereas the splice variant desensitized almost completely. When Ca<sup>+2</sup> uptake was evaluated, the P2X<sub>2(b)</sub> subunit did not mediate a steady Ca<sup>+2</sup> influx in the presence of ATP, which may reflect functional differences between cells expressing either of the two P2X<sub>2</sub> isoforms (Brandle *et al.*, 1997). This evidence points towards a potential role of the adapter protein Fe65 as regulator of desensitization kinetics of the P2X<sub>2</sub> receptor, feature that still needs experimental confirmation.

We demonstrate here that alternative splicing of the P2X<sub>2</sub> receptor is indeed an evolutionary mechanism by which neurons have impaired this interaction, while retaining some specific functionality features of the receptor. An analogous situation has been described for the NMDA receptor subunit NR1, where the alternative splicing of the C-terminal sequence C1 regulates the association with Yotiao and Neurofilament 1 (Sheng and Pak, 2000). Yotiao is an NR1-binding protein potentially involved in cytoskeletal attachment of NMDA receptors. Thus, alternative splicing of the NR1 subunit can act through splice-specific interactors such as yotiao to differentially localize or anchor distinct subsets of NMDA receptors. Differential subcellular localization by virtue of subunit-specific or splice variant-specific interactions could be exploited to create glutamatergic synapses with distinct pharmacological and physiological properties within the same neuron (Rubio and Wenthold, 1997).

---

#### **5.4. Fe65 is present in hippocampal excitatory synapses where colocalize with P2X<sub>2</sub> receptors**

The distribution profile of Fe65 immunoreactivity was first described by Kesavapany and coworkers in mouse brain. Fe65 expression was found to be widespread in neurons in adult brain with areas of highest expression including regions of the hippocampus and cerebellum (Kesavapany *et al.*, 2002). These results were consistent with earlier *in situ* hybridization studies where a widespread expression of Fe65 mRNA in adult mouse brain was shown, with the strongest signals evident in regions with high density of neurons, including the hippocampus and cerebellum, olfactory bulb, cortex and medial habenular nucleus (Bressler *et al.*, 1996). In agreement with both works, we got immunoreactivity for Fe65 in several rat brain regions with strong immunostaining in hippocampus, in pyramidal cells in the CA1 and CA3 regions, as well as granule cells of the dentate gyrus.

The subcellular localization of Fe65 in the brain has not been described so far, and is only suggested from immunofluorescence labeling of cultured neurons, where Fe65 was detected in both growth cones and in dendrites (Sabo *et al.*, 2003). In this work, we were able to describe the subcellular localization of Fe65 using postembedding immunogold labeling at hippocampal excitatory synapses. Both antibodies used showed immunolabeling at the pre- and postsynaptic specialization in rat brain (section 4.7). Notably, on spines, immunogold particles were preferentially located at the edge of the postsynaptic specialization. Very recently, a double Fe65/Fe65L1 knockout mice (FE65<sup>-/-</sup>; FE65L1<sup>-/-</sup>) was extensively study by immunohistochemistry, and the authors suggested essential roles for Fe65 in brain development (Guenette *et al.*, 2006). The studies were performed mainly in cortex and hippocampus, where they found that several axonal projection pathways are aberrant in FE65<sup>-/-</sup>; FE65L1<sup>-/-</sup> mice. Silver staining of coronal sections also revealed defects in the mossy fiber pathway formed by dentate granule cell axons. In *wt* mice these abnormalities were not found

---

indicating thus both the presence of Fe65 in presynaptic specializations, in accordance with our findings, and a functional role of this protein in axon projection (Guenette *et al.*, 2006).

In line with our findings on the occurrence *in vivo* of the molecular complex between Fe65 and P2X<sub>2</sub>, we observed that both proteins are co-localized at the postsynaptic density as evidenced by double immunolabeling studies using two different sizes of gold particles (Section 4.7.3). The two proteins co-localize at the postsynaptic specialization, remarkably close to the edge of the postsynaptic density of excitatory hippocampal synapses in rat brain a location that was previously described for P2X<sub>2</sub> subunits (Rubio and Soto, 2001). The putative protein complex around P2X<sub>2</sub>-subunit-containing receptors seems to be of different nature than the complex network of proteins so far identified at the excitatory postsynaptic density that regulates targeting, anchoring, and coupling to intracellular signaling machinery of glutamate receptors. Thus, both the AMPA and NMDA type of ionotropic glutamate receptors, present at the same synapses than P2X<sub>2</sub> receptor, do not assemble with their interacting proteins via proline-rich sequences but rather bind via PDZ binding domains to PDZ-domain-containing adapter proteins (Sheng and Pak, 2000).

As many scaffold proteins at the synapse, the modular structure of Fe65 suggests that it might link P2X<sub>2</sub> subunits containing receptors to additional cytosolic proteins. Many interacting partners for Fe65 have been identified so far, and among them APP is of special interest since it is linked to Alzheimer's disease. Indeed, we were able to evidence a triple molecular complex between P2X<sub>2</sub>CD, Fe65 and APP by co-immunoprecipitation in rat brain with an anti-P2X<sub>2</sub> antibody (section 4.6). Nevertheless this result is just a first hint and more studies are necessary to elucidate if the participation of APP in the complex Fe65-P2X<sub>2</sub>-APP is driven by Fe65 or whether APP and P2X<sub>2</sub> subunits are able to interact without the participation of Fe65. It also remains a challenge inquiring the functional consequences of this triple complex both in physiological and pathological conditions.

---

### **5.5. Fe65 regulates the function of P2X<sub>2</sub> receptors by binding of its cytoplasmic domain**

Many studies have addressed the functional role of the cytoplasmic carboxy-terminal tail from purinergic receptors in the regulation of the channel's functionality. Activation, desensitization, pore formation and regulation of the interaction with intracellular proteins are just few examples of the variety of manners by which the C-terminus was found to modulate the receptor's activity. In figure 5.3 the amino acid sequences of the C-terminus of all P2X receptors are depicted (A) and motifs of functional relevance are highlighted (B).

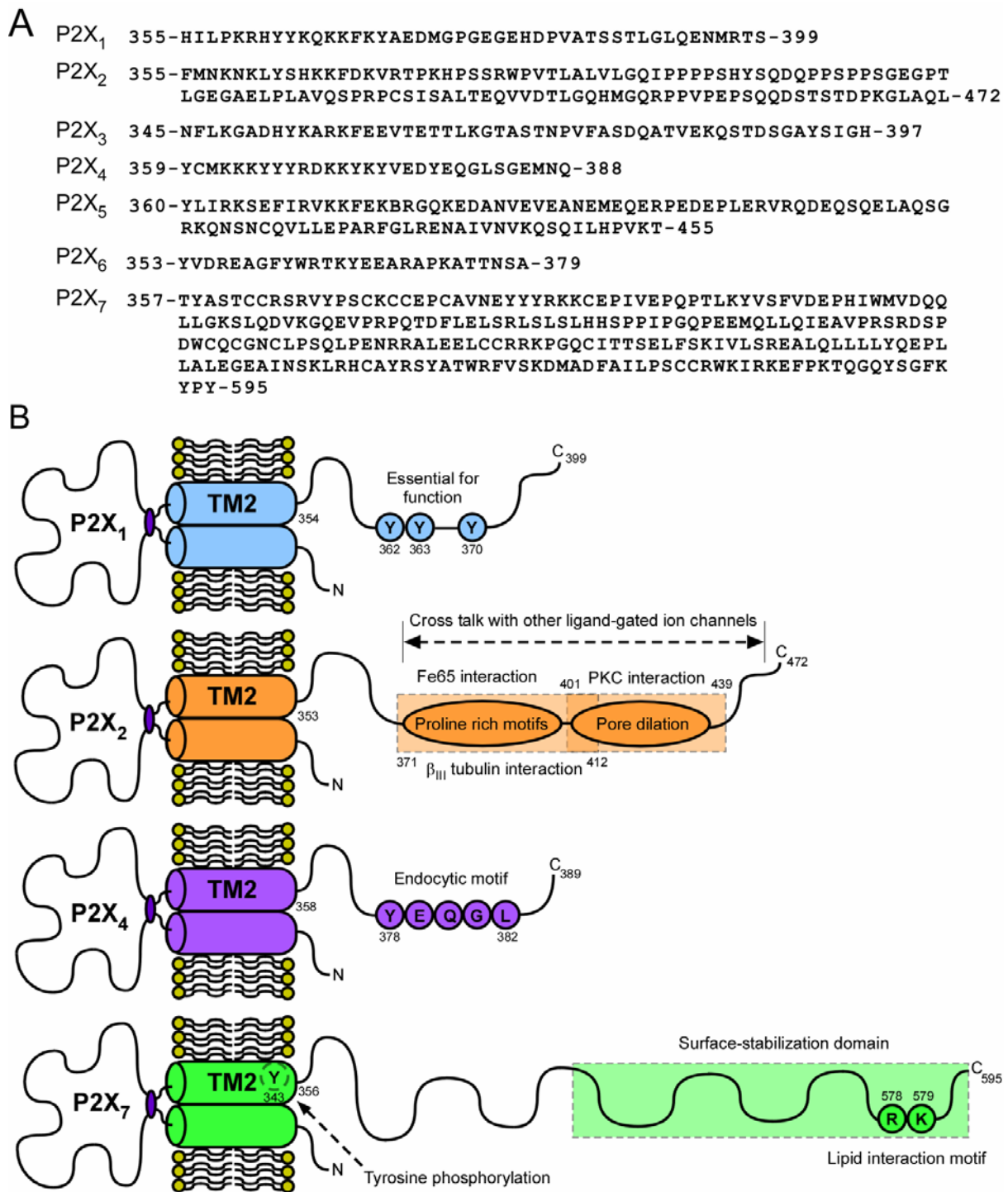
It has been shown that the C-terminal domain of P2X<sub>7</sub> is implicated in many regulatory pathways. An increase of the conductance to bigger cations by repeated application of ATP or BzATP was seen in macrophage-derived cells expressing P2X<sub>7</sub> receptors. That change in the permeability of the channel dropped when a truncated P2X<sub>7</sub> receptor, lacking most of the C-terminal tail, was analyzed (Surprenant *et al.*, 1996). In addition, by propidium iodide uptake assays designed to determine the pore dilation properties of P2X receptors upon activation with the agonist it was observed that the rate of uptake was greater for the rat P2X<sub>7</sub> than for the human P2X<sub>7</sub>. This variation was attributed to the differences in the C-terminal domains between the human and rat proteins, which was confirmed by the use of chimeras with exchanged C-terminal domains (Rassendren *et al.*, 1997b). When deactivation of the channel was studied on these chimeras, an involvement of the C-terminus on the rate of deactivation after removal of agonist was also observed, suggesting that this domain is a determinant of channel closing (Rassendren *et al.*, 1997b). In another study, the function of the human P2X<sub>7</sub> receptors was reported to be affected by a single missense mutation on its C-terminal domain. The change of a Glu to an Ala at position 496 impairs the activity of the P2X<sub>7</sub> in leukocytes, as evidenced by reduced Ba<sup>2+</sup> and ethidium uptake of the mutant (Gu *et al.*, 2001). This functional consequence, caused by the



---

lost of the negative charge in the C-terminus, suggests involvement of electrostatic interactions in immediate channel opening and properly assembly of the P2X<sub>7</sub> complex. In addition, P2X<sub>7</sub> subunits contain at the end of the C-terminal a conserved LBP-binding domain (Denlinger *et al.*, 2001) (Figure 5.3B). The authors could demonstrate that peptides derived from this P2X<sub>7</sub> sequence bind LPS *in vitro* and could disrupt this interaction by mutating two basic residues in the LPS-binding domain (Arg578Glu and Lys579Glu). The direct interaction with P2X<sub>7</sub> and subsequent possible effect on P2X<sub>7</sub> receptor function/signal transduction could explain the need of monocyte/macrophage priming by LPS to result in efficient caspase-1 activation by P2X<sub>7</sub> receptors. In contrast to the *wt* receptor, expression of P2X<sub>7</sub>-(R578E/K579E) mutant in heterologous systems failed to demonstrate surface immunoreactivity despite normal levels of total protein expression, indicating that the lipid binding domain might be involved in trafficking or stabilization of P2X<sub>7</sub> receptors in the membrane (Denlinger *et al.*, 2003).

A role for the cytosolic domain of the P2X<sub>4</sub> subunit in trafficking of the receptor has been studied. Royle and colleagues identified a non-canonical tyrosine-based sorting signal in the cytosolic C-terminus tail of P2X<sub>4</sub> subunits (Figure 5.3B) interacting with the protein AP-50. When the interaction was disrupted, an increase in the surface expression of P2X<sub>4</sub> receptors in transfected neurons was observed (Royle *et al.*, 2002; Royle *et al.*, 2005). In addition, P2X<sub>4</sub> receptors lacking the internalization signal evidenced not only a large increase in the amplitude of ATP-elicited current, but also a higher ionic permeability when compared to P2X<sub>4</sub> *wt* receptors (Toulme *et al.*, 2006).



**Figure 5.3. Carboxyl terminal tail of P2X receptor subunits.** (A) Sequence of the C-terminal domains of rat P2X receptor subunits. (B) Representation of the variation and regulating functions assigned to the C-termini of P2X<sub>1</sub>, P2X<sub>2</sub>, P2X<sub>4</sub>, and P2X<sub>7</sub> receptor subunits. Only the motifs with functional relevance are highlighted.

In the case of the P2X<sub>2</sub> receptor, desensitization rates in Ca<sup>2+</sup> responses following activation of *wt*, spliced, and mutant subunits was correlated with the presence of certain amino acid residues (<sub>371</sub>RTPKHP<sub>376</sub>) on the C-terminus of the channel (Koshimizu *et al.*,

---

1998; Koshimizu *et al.*, 1999). In line with these findings, Boue-Grabot and colleagues described a P2X<sub>2</sub> phenotype with fast kinetics and complete desensitization evidenced by a mutation of the conserved protein kinase C (PKC) consensus site TX(K/R) (Figure 5.3B), localized on the cytoplasmic N-terminal domain of the receptor. Interestingly, when they evaluated the action of the C-terminal domain on the desensitization of the channel in response to ATP, they observed that the fast desensitizing PKC mutant receptor was not altered by a C-terminal deletion, whereas the *wt* P2X<sub>2</sub> was either slowly desensitizing or had a biphasic phenotype. This suggests that the C-terminus plays not only a modulatory role in desensitization, but also a stabilizing role on the phosphothreonine-dependent slow phenotype, via a cross-talk with the N-terminus of the protein (Boue-Grabot *et al.*, 2000b). More direct evidence implicating the C-terminal domain in the kinetic properties of P2X receptors have been supplied from the characterization of the functional properties of the P2X<sub>2</sub> splice variant lacking either 69 amino acids (P2X<sub>2(b)</sub>) from the C-terminal domain. As mentioned above (section 5.3), the shorter splice variant desensitized faster than the P2X<sub>2</sub> homomeric receptor formed by the full-length subunit (P2X<sub>2(a)</sub>) (Brandle *et al.*, 1997). In the case of P2X<sub>2</sub>, a direct interaction with  $\beta$ -III tubulin has been observed (Gendreau *et al.*, 2003). Employing GST-pulldown assays, the tubulin binding motif was assigned to the first half of the cytoplasmic C-terminal tail of the receptor (Figure 5.3B). Interestingly, the P2X<sub>2</sub>SV and both the P2X<sub>5</sub> and the P2X<sub>7</sub> receptors failed to bind  $\beta$ -III tubulin, evidencing an evolutionary functional specification inside the C-terminus of the P2X family (Figure 5.3A). Although very speculative, the authors suggest that this interaction may play a role in receptor desensitization or in targeting and segregation of the channel. This interaction has not been demonstrated *in vivo* so far.

Likewise to P2X<sub>7</sub> receptors, the cytosolic C-terminal tail is also crucial in regulating the permeation properties of P2X<sub>2</sub> channels. As reported recently, the permeability changes

---

for rat and mouse P2X<sub>2</sub> receptors are substantially different, being higher for the rat P2X<sub>2</sub> than for the mouse P2X<sub>2</sub> (Eickhorst *et al.*, 2002). By constructing several mutant and chimeric channels it was observed that two amino acid residues of the C-terminal tail were responsible for this differential behavior. In addition, evidence for conformational changes in the cytosolic domain of P2X<sub>2</sub> channels was found. Employing a combination of electrophysiology and fluorescence resonance energy transfer (FRET) microscopy cytosolic channel motions associated with the pore dilation were observed, which were abolished by tethering the cytosolic domain to the membrane (Fisher *et al.*, 2004), proving once again that the C-terminal domain modulates permeability changes of P2X receptors.

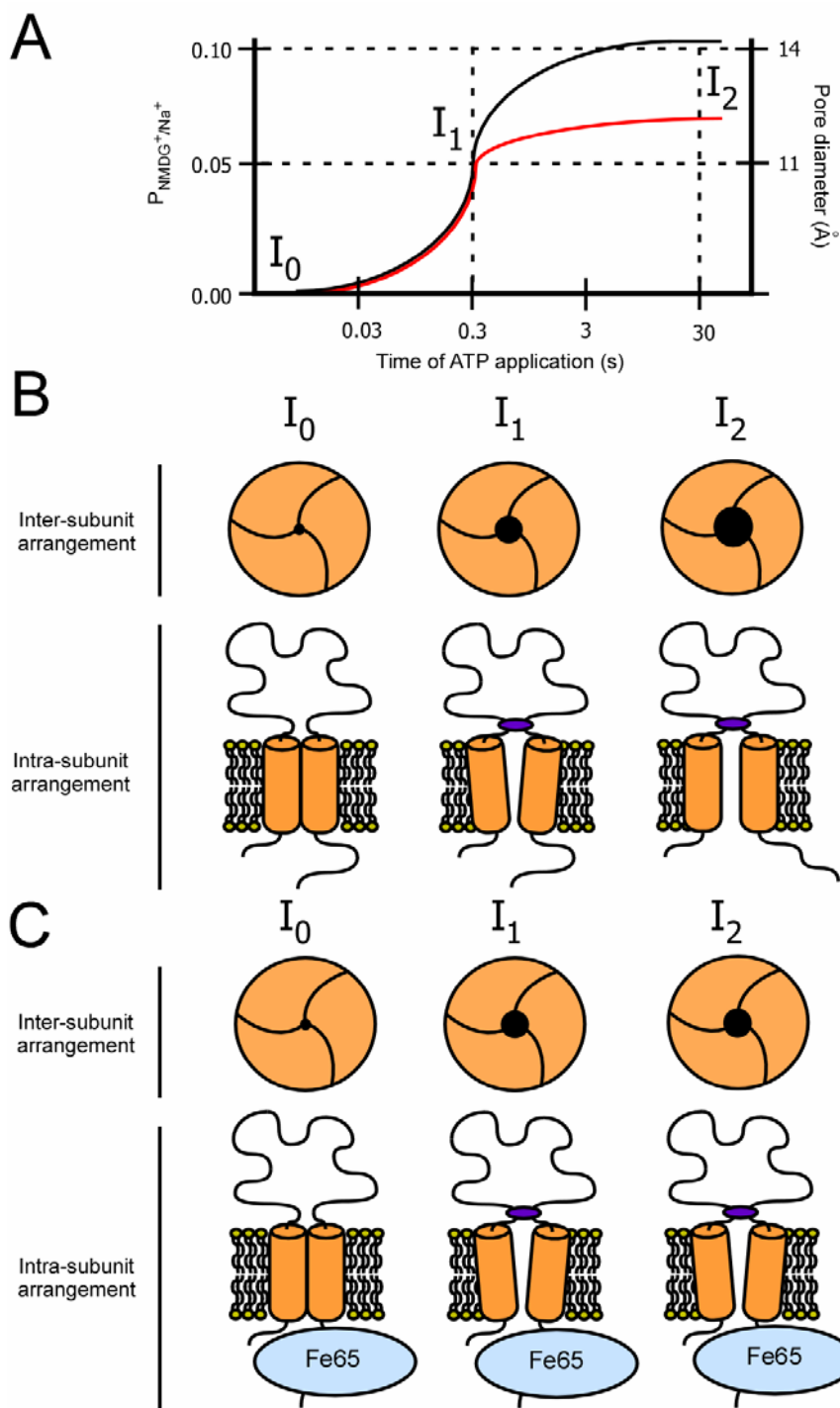
In accord with all these findings it is possible to postulate that a movement-permissive cytosolic domain is required for P2X<sub>2</sub> receptor to undergo permeability changes. Based on that we hypothesized, that Fe65 binding might restrain the P2X<sub>2</sub> C-terminus and alter the changes in ionic selectivity following agonist exposure. Two electrode voltage-clamp recordings in *Xenopus laevis* oocytes showed that P2X<sub>2</sub> receptors co-expressed with Fe65 do not change their permeability to the same extent as P2X<sub>2</sub> receptors, while other macroscopic properties including current activation, deactivation, permeability to monovalent cations and sensitivity to ATP are not changed by the assembly (section 4.8). In addition, it was observed a shift in the reversal potential of the current for P2X<sub>2</sub> receptors that was drastically reduced in oocytes expressing P2X<sub>2</sub>-Fe65 receptors.

Previous works have related changes in permeability to bulky organic cations with the opening mechanism of the channel's pore. Changes in P2X<sub>2</sub> pore size were characterized using reversal potential measurements and excluded field theory, and the pore diameter was found to be of approximately 11 Å in the I<sub>1</sub> state, permissive for Na<sup>+</sup> but not for NMDG<sup>+</sup> (Eickhorst *et al.*, 2002). Transition to the I<sub>2</sub> state, which is permissive to both Na<sup>+</sup> and NMDG<sup>+</sup>, increases the diameter of the receptor by at least 3 Å, resulting in an expansion of

---

the pore area by at least 60-72 Å<sup>2</sup>. Permeability ratios may also be related to such structural changes, since they directly report on the ability of the channel to allow the flow of small or bulky cations.

We can nicely correlate our findings on the functional consequences of the Fe65-P2X<sub>2</sub> complex with that previous report. Our measurements indicate that  $P_{\text{NMDG}}/P_{\text{Na}}$  permeability ratios changed from  $0.057 \pm 0.001$  (at I<sub>1</sub>) to  $0.107 \pm 0.004$  (at I<sub>2</sub>; n=47) for the P2X<sub>2</sub> receptor, but for the P2X<sub>2</sub>-Fe65 complex they only shifted from  $0.052 \pm 0.001$  (at I<sub>1</sub>) to  $0.068 \pm 0.002$  (at I<sub>2</sub>, n=48) (section 4.8.2). If we combine our data and refer it to those previous results, it is possible to describe the pore diameter increase for P2X<sub>2</sub> in the presence or absence of Fe65 (Figure 5.4A). According to kinetic measurements, the change from the I<sub>0</sub> to the I<sub>1</sub> state in P2X<sub>2</sub> takes place very rapidly, occurring within 0.5 seconds at 100 μM ATP. Our experimental setup does not allow evaluating the effect of the complex with Fe65 on the kinetic changes to achieve this first opened state, but since both permeability to monovalent cations and sensitivity to ATP are not affected by such assembly, we can predict that this event may not interfere with this first structural re-arrangement. In addition, the  $P_{\text{NMDG}}/P_{\text{Na}}$  ratios characterizing the I<sub>1</sub> state are practically identical for the receptor both in the presence and absence of Fe65, which allow us to assume that the pore may easily dilate up to 11 Å (Figure 5.4A).



**Figure 5.4. Summary of P2X<sub>2</sub> permeability changes in the presence of Fe65.** (A) Changes of channel permeation upon continued application of ATP are related with opening of the channel's pore. Representation of data measured for P2X<sub>2</sub> receptor alone (black curve) or in the presence of Fe65 (red curve). (B) The cartoon shows P2X<sub>2</sub> channels in closed and open states of differing diameter across the narrowest region (the gate). In the I<sub>0</sub> and I<sub>1</sub> state the C-terminal domain is displayed in a non-permissive state with respect to permeability changes. While the pore dilates, permeability changes are increased, which is correlated with conformational changes on the C-terminal tail. (C) Our findings support a model where binding to Fe65 allows fast conformational changes on P2X<sub>2</sub> subunits to reach a I<sub>1</sub> state but tethers the C-terminus in such a way that a I<sub>2</sub> state can not be attained. Adapted from Eickhorst *et al.*, 2002.

---

The opening to the second state is much more gradual, and depends on a continued agonist application over dozens of seconds. In our hands P2X<sub>2</sub> achieved the I<sub>2</sub> state with a biphasic mode, characterized with rate constants of 1.37 s<sup>-1</sup> and 0.10 s<sup>-1</sup> and attained a P<sub>NMDG</sub>/P<sub>Na</sub> ratio of 0.107. In the presence of Fe65, despite the fact that the second state reached a maximal P<sub>NMDG</sub>/P<sub>Na</sub> ratio of just 0.068, we did not find significant changes on the mechanism by which this pseudo-I<sub>2</sub> state is reached, which was also biphasic and characterized by time constants of 1.67 s<sup>-1</sup> and 0.12 s<sup>-1</sup>. The conservation of the mechanism by which the residual fraction of NMDG<sup>+</sup> is transported through the channel excludes a possible partial opened state of the pore upon interaction with Fe65. Thus binding to Fe65 may completely abolish the ability of P2X<sub>2</sub> to reach the I<sub>2</sub> state, and this attained pseudo-I<sub>2</sub> state likely reflects a fraction of channels where the binding of Fe65 to P2X<sub>2</sub> may not be occurring (approximately 30%).

A very intuitive model for the functional consequences of the formation of the molecular complex can therefore be derived from our findings. Upon continued activation with ATP, the P2X<sub>2</sub> receptor is capable of undergoing structural re-arrangement that permits the trafficking of bulky cations (Figure 5.4B). The two-state behavior of P2X<sub>2</sub> upon long-lasting exposures to ATP determines that the channel is able to move from a state with high ionic selectivity (I<sub>1</sub>) to a state that discriminates poorly between ions (I<sub>2</sub>). Interaction with the scaffolding protein Fe65, through a specific binding to the C-terminus of the receptor, alters the ability of this domain to trigger the conformational change required to attain the I<sub>2</sub> state, and keeps the channel in an I<sub>1</sub> state, characterized by a narrower pore size and high ionic selectivity (Figure 5.4C). The outcome of such a mechanism is reflected in the impairment of the channel's capability of allowing permeability changes and thus the flux of organic cations as NMDG<sup>+</sup>. Permeability changes on P2X<sub>7</sub> receptor have been associated with morphological changes, cell death, release of signaling molecules and vesicle shedding (Surprenant *et al.*,

---

1996; Rassendren *et al.*, 1997b; Virginio *et al.*, 1999; MacKenzie *et al.*, 2001; North, 2002). By analogy a physiological role for P2X<sub>2</sub> channel permeability may also be expected, and ATP-evoked morphological changes in dendrites have been described in hippocampal neurons expressing P2X<sub>2</sub>, indeed (Khakh, 2001). Another scenario that can be envisaged is that upon pore dilation intracellular solutes may leave the cell down their concentration gradients, disturbing cytoplasm homeostasis and causing cell injury. The formation of the complex between P2X<sub>2</sub> and Fe65 would sustain the ability of the channel to discriminate among ions and would permit neurons to overcome the ATP-evoked effects.

There is other aspect of particular interest about the time- and activation-dependent changes of ionic selectivity from P2X<sub>2</sub> receptors with respect to their assembly with Fe65. Permeability changes of P2X<sub>2</sub> receptors depend on the expression level, implicating interplay between neighboring P2X<sub>2</sub> receptors in the process. The association with Fe65 might interfere with this process, e.g. if it occupies a domain of the P2X<sub>2</sub> subunits required for the crosstalk between receptors. Thus, Fe65 seems capable of regulating the ionic selectivity of neuronal P2X<sub>2</sub> receptors by influencing either or both permeation or oligomerization, providing a novel mechanism for functional regulation of synaptic transmission.

Importantly, the specificity of the functional interaction of Fe65 with P2X<sub>2</sub> receptors was proven by the study of Fe65 effects on P2X<sub>7</sub> receptor function. P2X<sub>7</sub> receptor, similarly to P2X<sub>2</sub> receptors, show permeability changes upon prolonged or repetitive exposure to the agonist (Surprenant *et al.*, 1996; Khakh *et al.*, 1999). They also possess several proline rich motifs in the C-terminal domain (Kim *et al.*, 2001), but we failed to detect interaction between P2X<sub>7</sub> and Fe65, as determined both by Y2H or co-immunoprecipitation assays (sections 4.2 and 4.5). This makes P2X<sub>7</sub> receptors a relevant negative control for the functional effects evidenced on P2X<sub>2</sub> subunits. We verified indeed that permeability changes



---

of P2X<sub>7</sub> receptors were unmodified upon co-expression with Fe65 as showed by electrophysiological recording in *X. laevis* oocytes (Section 4.8.2).

## 5.6. Outlook

From the point of view of ATP signaling, physiological consequences for conformational changes in cytoplasmic domains of P2X receptors have been documented. Activation of intracellular signal transduction pathways mediated by neurotransmitter-evoked conformational re-arrangements would add a temporal dimension to ATP signaling that could outlast the surge of extracellular ATP (Fisher *et al.*, 2004). Intracellular responses are thus likely to be triggered by proteins that associate at the membrane level with the cytoplasmic domains of P2X receptors. In the case of P2X<sub>2</sub> and the adapter protein Fe65 a tight link with transcription regulation can be suggested, since Fe65 can be transported to the nucleus via interaction with the histone acetyltransferase Tip60 and the transcription factor CP2/LSF/LBP1 (Cao and Sudhof, 2001).

Fe65 also regulates gene transcription through interaction with APP protein family members (Cao and Sudhof, 2001; Bruni *et al.*, 2002; Scheinfeld *et al.*, 2002; Hass and Yankner, 2005). Furthermore, the Fe65/APP interaction regulates essential physiological processes at the neuromuscular junction (Zambrano *et al.*, 2002), and the complex may function in membrane extension and motility through their association with Mena (Sabo *et al.*, 2001). All these process could be, in principle, modulated by the formation of the trimeric complex between P2X<sub>2</sub>, Fe65 and APP, and future research should be focused on dissecting the link of ATP-gated receptors and the deposition of the A $\beta$  peptide in Alzheimer's disease. Disease-states have been linked to a very similar molecular complex, as for the WW domain of the E3 ubiquitin protein ligase Nedd4, which binds a proline-rich motif in the amiloride sensitive epithelial sodium channel (ENaC). Interaction between ENaC and Nedd4 targets the

---

channel to degradation (Bedford *et al.*, 1997) and mutations that disrupt this interaction cause a human hypertensive disorder, the Liddle's syndrome (Snyder *et al.*, 1995).

Overall, these results clearly show the involvement of the C-terminal domain of P2X receptors in the interaction with intracellular proteins that regulate activity of the channel.

---

## 6. CONCLUSIONS

The adapter protein Fe65 has been identified as a native binding partner of P2X<sub>2</sub> subunits at excitatory synapses, able to confer distinct functional characteristics to the receptor. This major finding of the present thesis work is supported by the following experimental evidence:

- Overlapping partial cDNA sequences coding for the protein Fe65 and the homologous protein Fe65 like 1 were identified in a Y2H screening for interacting partners of the C-terminal cytoplasmic domain of the P2X<sub>2</sub> subunit.

- Direct Y2H assays on deletions and mutants on both interacting partners identified the WW domain of Fe65 and the first proline rich sequence at the C-terminus of the P2X<sub>2</sub> subunit as key players for the interaction.

- The assembly could be verified by co-sedimentation assays using immobilized GST-fused proteins, revealing the direct interaction between Fe65 and P2X<sub>2</sub> subunits.

- Specificity of the interaction is sustained on the absence of binding to Fe65 by C-terminal cytoplasmic domains of P2X<sub>2(b)</sub>, P2X<sub>4</sub>, and P2X<sub>7</sub> receptor subunits.

- Both proteins were co-immunoprecipitated from rat brain crude membrane fractions, evidencing the occurrence *in vivo* of the interaction.

- P2X<sub>2</sub> and Fe65 present overlapping distribution in many brain areas including the hippocampus, where they co-localize at the postsynaptic specialization of excitatory synapses.

- Assembly with Fe65 modulates the agonist-induced permeability changes of P2X<sub>2</sub> receptors indicating that the complex assembly may provide a mechanism for regulation of ATP-mediated synaptic transmission.

---

## 7. REFERENCES

- Agboh, K. C., T. E. Webb, R. J. Evans and S. J. Ennion (2004). Functional characterization of a P2X receptor from *Schistosoma mansoni*. *J. Biol. Chem.* **279**(40): 41650-7.
- Bedford, M. T., D. C. Chan and P. Leder (1997). FBP WW domains and the Abl SH3 domain bind to a specific class of proline-rich ligands. *EMBO J.* **16**(9): 2376-83.
- Bedford, M. T., D. Sarbassova, J. Xu, P. Leder and M. B. Yaffe (2000). A novel pro-Arg motif recognized by WW domains. *J. Biol. Chem.* **275**(14): 10359-69.
- Bertrand, D., J. L. Galzi, A. Devillers-Thiery, S. Bertrand and J. P. Changeux (1993). Mutations at two distinct sites within the channel domain M2 alter calcium permeability of neuronal alpha 7 nicotinic receptor. *Proc. Natl. Acad. Sci. U S A.* **90**(15): 6971-5.
- Bo, X., L. H. Jiang, H. L. Wilson, M. Kim, G. Burnstock, A. Surprenant and R. A. North (2003). Pharmacological and biophysical properties of the human P2X<sub>5</sub> receptor. *Mol. Pharmacol.* **63**(6): 1407-16.
- Bockers, T. M., M. G. Mameza, M. R. Kreutz, J. Bockmann, C. Weise, F. Buck, D. Richter, E. D. Gundelfinger and H. J. Kreienkamp (2001). Synaptic scaffolding proteins in rat brain. Ankyrin repeats of the multidomain Shank protein family interact with the cytoskeletal protein alpha-fodrin. *J. Biol. Chem.* **276**(43): 40104-12.
- Borg, J. P., J. Ooi, E. Levy and B. Margolis (1996). The phosphotyrosine interaction domains of X11 and FE65 bind to distinct sites on the YENPTY motif of amyloid precursor protein. *Mol. Cell. Biol.* **16**(11): 6229-41.
- Bork, P. and M. Sudol (1994). The WW domain: a signalling site in dystrophin? *Trends Biochem. Sci.* **19**(12): 531-3.
- Boue-Grabot, E., M. A. Akimenko and P. Seguela (2000a). Unique functional properties of a sensory neuronal P2X ATP-gated channel from zebrafish. *J. Neurochem.* **75**(4): 1600-7.
- Boue-Grabot, E., V. Archambault and P. Seguela (2000b). A protein kinase C site highly conserved in P2X subunits controls the desensitization kinetics of P2X<sub>2</sub> ATP-gated channels. *J. Biol. Chem.* **275**(14): 10190-5.
- Brandle, U., P. Spielmanns, R. Osteroth, J. Sim, A. Surprenant, G. Buell, J. P. Ruppersberg, P. K. Plinkert, H. P. Zenner and E. Glowatzki (1997). Desensitization of the P2X<sub>2</sub> receptor controlled by alternative splicing. *FEBS Lett.* **404**(2-3): 294-8.
- Bressler, S. L., M. D. Gray, B. L. Sopher, Q. Hu, M. G. Hearn, D. G. Pham, M. B. Dinulos, K. Fukuchi, S. S. Sisodia, M. A. Miller, C. M. Disteche and G. M. Martin (1996). cDNA cloning and chromosome mapping of the human Fe65 gene: interaction of the conserved cytoplasmic domains of the human beta-amyloid precursor protein and its homologues with the mouse Fe65 protein. *Hum. Mol. Genet.* **5**(10): 1589-98.

- 
- Brown, S. G., A. Townsend-Nicholson, K. A. Jacobson, G. Burnstock and B. F. King (2002). Heteromultimeric P2X<sub>1/2</sub> receptors show a novel sensitivity to extracellular pH. *J. Pharmacol. Exp. Ther.* **300**(2): 673-80.
- Bruni, P., G. Minopoli, T. Brancaccio, M. Napolitano, R. Faraonio, N. Zambrano, U. Hansen and T. Russo (2002). Fe65, a ligand of the Alzheimer's beta-amyloid precursor protein, blocks cell cycle progression by down-regulating thymidylate synthase expression. *J. Biol. Chem.* **277**(38): 35481-8.
- Buell, G., C. Lewis, G. Collo, R. A. North and A. Surprenant (1996). An antagonist-insensitive P2X receptor expressed in epithelia and brain. *EMBO J.* **15**(1): 55-62.
- Burnstock, G. (1978). A basis for distinguishing two types of purinergic receptor. New York, Raven press.
- Burnstock, G. and C. Kennedy (1985). Is there a basis for distinguishing two types of P2-purinoceptor? *Gen. Pharmacol.* **16**(5): 433-40.
- Cao, X. and T. C. Sudhof (2001). A transcriptionally [correction of transcriptively] active complex of APP with Fe65 and histone acetyltransferase Tip60. *Science.* **293**(5527): 115-20.
- Chow, Y. W. and H. L. Wang (1998). Functional modulation of P2X<sub>2</sub> receptors by cyclic AMP-dependent protein kinase. *J. Neurochem.* **70**(6): 2606-12.
- Collo, G., R. A. North, E. Kawashima, E. Merlo-Pich, S. Neidhart, A. Surprenant and G. Buell (1996). Cloning of P2X<sub>5</sub> and P2X<sub>6</sub> receptors and the distribution and properties of an extended family of ATP-gated ion channels. *J. Neurosci.* **16**(8): 2495-507.
- Denlinger, L. C., P. L. Fiset, J. A. Sommer, J. J. Watters, U. Prabhu, G. R. Dubyak, R. A. Proctor and P. J. Bertics (2001). Cutting edge: the nucleotide receptor P2X<sub>7</sub> contains multiple protein- and lipid-interaction motifs including a potential binding site for bacterial lipopolysaccharide. *J. Immunol.* **167**(4): 1871-6.
- Denlinger, L. C., J. A. Sommer, K. Parker, L. Gudipaty, P. L. Fiset, J. W. Watters, R. A. Proctor, G. R. Dubyak and P. J. Bertics (2003). Mutation of a dibasic amino acid motif within the C terminus of the P2X<sub>7</sub> nucleotide receptor results in trafficking defects and impaired function. *J. Immunol.* **171**(3): 1304-11.
- Dubyak, G., R., and El-moatassim, C., (1993). Signal transduction via P2-purinergic receptors for extracellular ATP and other nucleotides. *Am. J. Physiol.* **264**: C577-C606.
- Duilio, A., R. Faraonio, G. Minopoli, N. Zambrano and T. Russo (1998). Fe65L2: a new member of the Fe65 protein family interacting with the intracellular domain of the Alzheimer's beta-amyloid precursor protein. *Biochem. J.* **330** ( Pt 1): 513-9.
- Duilio, A., N. Zambrano, A. R. Mogavero, R. Ammendola, F. Cimino and T. Russo (1991). A rat brain mRNA encoding a transcriptional activator homologous to the DNA binding domain of retroviral integrases. *Nucleic Acids Res.* **19**(19): 5269-74.

- 
- Duttweiler, H. M. (1996). A highly sensitive and non-lethal beta-galactosidase plate assay for yeast. *Trends Genet.* **12**(9): 340-1.
- Edwards, F. A. and A. J. Gibb (1993). ATP--a fast neurotransmitter. *FEBS Lett.* **325**(1-2): 86-9.
- Egan, T. M., J. A. Cox and M. M. Voigt (2000). Molecular cloning and functional characterization of the zebrafish ATP-gated ionotropic receptor P2X<sub>3</sub> subunit. *FEBS Lett.* **475**(3): 287-90.
- Egan, T. M., W. R. Haines and M. M. Voigt (1998). A domain contributing to the ion channel of ATP-gated P2X<sub>2</sub> receptors identified by the substituted cysteine accessibility method. *J. Neurosci.* **18**(7): 2350-9.
- Eickhorst, A. N., A. Berson, D. Cockayne, H. A. Lester and B. S. Khakh (2002). Control of P2X<sub>2</sub> channel permeability by the cytosolic domain. *J. Gen. Physiol.* **120**(2): 119-31.
- Ermekova, K. S., Chang, A., Zambrano, N., Candia, P., Russo, T., and Sudol, M. (1998). Proteins implicated in Alzheimer disease. The role of FE65, a new adapter which binds to  $\beta$ -amyloid precursor protein. *Adv. Exp. Med. Biol.* **446**: 161-180.
- Ermekova, K. S., N. Zambrano, H. Linn, G. Minopoli, F. Gertler, T. Russo and M. Sudol (1997). The WW domain of neural protein FE65 interacts with proline-rich motifs in Mena, the mammalian homolog of Drosophila enabled. *J. Biol. Chem.* **272**(52): 32869-77.
- Espanel, X. and M. Sudol (1999). A single point mutation in a group I WW domain shifts its specificity to that of group II WW domains. *J. Biol. Chem.* **274**(24): 17284-9.
- Evans, R. J., C. Lewis, G. Buell, S. Valera, R. A. North and A. Surprenant (1995). Pharmacological characterization of heterologously expressed ATP-gated cation channels (P2X purinoceptors). *Mol. Pharmacol.* **48**(2): 178-83.
- Evans, R. J., C. Lewis, C. Virginio, K. Lundstrom, G. Buell, A. Surprenant and R. A. North (1996). Ionic permeability of, and divalent cation effects on, two ATP-gated cation channels (P2X receptors) expressed in mammalian cells. *J. Physiol.* **497** ( Pt 2): 413-22.
- Fields, S. and O. Song (1989). A novel genetic system to detect protein-protein interactions. *Nature.* **340**(6230): 245-6.
- Fields, S. and R. Sternglanz (1994). The two-hybrid system: an assay for protein-protein interactions. *Trends Genet.* **10**(8): 286-92.
- Fisher, J. A., G. Girdler and B. S. Khakh (2004). Time-Resolved Measurement of State-Specific P2X<sub>2</sub> Ion Channel Cytosolic Gating Motions. *J. Neurosci.* **24**(46): 10475-10487.

- 
- Furukawa, H. and E. Gouaux (2003). Mechanisms of activation, inhibition and specificity: crystal structures of the NMDA receptor NR1 ligand-binding core. *EMBO J.* **22**(12): 2873-85.
- Garcia-Guzman, M., F. Soto, J. M. Gomez-Hernandez, P. E. Lund and W. Stuhmer (1997). Characterization of recombinant human P2X<sub>4</sub> receptor reveals pharmacological differences to the rat homologue. *Mol. Pharmacol.* **51**(1): 109-18.
- Garcia-Guzman, M., F. Soto, B. Laube and W. Stuhmer (1996). Molecular cloning and functional expression of a novel rat heart P2X purinoceptor. *FEBS Lett.* **388**(2-3): 123-7.
- Gendreau, S., J. Schirmer and G. Schmalzing (2003). Identification of a tubulin binding motif on the P2X<sub>2</sub> receptor. *J. Chromatogr. B Analyt. Technol. Biomed. Life Sci.* **786**(1-2): 311-8.
- Gietz, D., A. St Jean, R. A. Woods and R. H. Schiestl (1992). Improved method for high efficiency transformation of intact yeast cells. *Nucleic Acids Res.* **20**(6): 1425.
- Gu, B. J., W. Zhang, R. A. Worthington, R. Sluyter, P. Dao-Ung, S. Petrou, J. A. Barden and J. S. Wiley (2001). A Glu-496 to Ala polymorphism leads to loss of function of the human P2X<sub>7</sub> receptor. *J. Biol. Chem.* **276**(14): 11135-42.
- Guenette, S., Y. Chang, T. Hiesberger, J. A. Richardson, C. B. Eckman, E. A. Eckman, R. E. Hammer and J. Herz (2006). Essential roles for the FE65 amyloid precursor protein-interacting proteins in brain development. *EMBO J.* **25**(2): 420-31.
- Guenette, S. Y., J. Chen, P. D. Jondro and R. E. Tanzi (1996). Association of a novel human FE65-like protein with the cytoplasmic domain of the beta-amyloid precursor protein. *Proc. Natl. Acad. Sci. U S A.* **93**(20): 10832-7.
- Haines, W. R., G. E. Torres, M. M. Voigt and T. M. Egan (1999). Properties of the novel ATP-gated ionotropic receptor composed of the P2X<sub>1</sub> and P2X<sub>5</sub> isoforms. *Mol. Pharmacol.* **56**(4): 720-7.
- Hardy, J. (1997). The Alzheimer family of diseases: many etiologies, one pathogenesis? *Proc. Natl. Acad. Sci. U S A.* **94**(6): 2095-7.
- Hass, M. R. and B. A. Yankner (2005). A {gamma}-secretase-independent mechanism of signal transduction by the amyloid precursor protein. *J. Biol. Chem.* **280**(44): 36895-904.
- Haydon, P., G., (2001). Glia: listening and talking to the synapse. *Nat. Rev. Neurosci.* **2**: 185-193.
- Hille, B. (1992). Ionic channels of excitable membranes. Sunderland, Massachusetts.
- Hollenberg, S. M., R. Sternglanz, P. F. Cheng and H. Weintraub (1995). Identification of a new family of tissue-specific basic helix-loop-helix proteins with a two-hybrid system. *Mol. Cell Biol.* **15**(7): 3813-22.

- 
- Hu, H., J. Columbus, Y. Zhang, D. Wu, L. Lian, S. Yang, J. Goodwin, C. Luczak, M. Carter, L. Chen, M. James, R. Davis, M. Sudol, J. Rodwell and J. J. Herrero (2004). A map of WW domain family interactions. *Proteomics*. **4**(3): 643-55.
- Illes, P. and J. A. Ribeiro (2004). Neuronal P2 receptors of the central nervous system. *Curr. Top. Med. Chem.* **4**(8): 831-8.
- Jahr, C. E. and T. M. Jessell (1983). ATP excites a subpopulation of rat dorsal horn neurones. *Nature*. **304**(5928): 730-3.
- Jensen, M. L., A. Schousboe and P. K. Ahring (2005). Charge selectivity of the Cys-loop family of ligand-gated ion channels. *J. Neurochem.* **92**(2): 217-25.
- Jiang, L. H., F. Rassendren, V. Spelta, A. Surprenant and R. A. North (2001). Amino acid residues involved in gating identified in the first membrane-spanning domain of the rat P2X<sub>2</sub> receptor. *J. Biol. Chem.* **276**(18): 14902-8.
- Jiang, L. H., F. Rassendren, A. Surprenant and R. A. North (2000). Identification of amino acid residues contributing to the ATP-binding site of a purinergic P2X receptor. *J. Biol. Chem.* **275**(44): 34190-6.
- Kanjhan, R., G. D. Housley, L. D. Burton, D. L. Christie, A. Kippenberger, P. R. Thorne, L. Luo and A. F. Ryan (1999). Distribution of the P2X<sub>2</sub> receptor subunit of the ATP-gated ion channels in the rat central nervous system. *J. Comp. Neurol.* **407**(1): 11-32.
- Kay, B. K., M. P. Williamson and M. Sudol (2000). The importance of being proline: the interaction of proline-rich motifs in signaling proteins with their cognate domains. *Faseb J.* **14**(2): 231-41.
- Kesavapany, S., S. J. Banner, K. F. Lau, C. E. Shaw, C. C. Miller, J. D. Cooper and D. M. McLoughlin (2002). Expression of the Fe65 adapter protein in adult and developing mouse brain. *Neuroscience*. **115**(3): 951-60.
- Khakh, B. (2001). Molecular physiology of P2X receptors and ATP signalling at synapses. *Nat. Rev. Neurosci.* **2**(3): 165-174.
- Khakh, B. S., X. R. Bao, C. Labarca and H. A. Lester (1999). Neuronal P2X transmitter-gated cation channels change their ion selectivity in seconds. *Nat. Neurosci.* **2**(4): 322-30.
- Khakh, B. S. and T. M. Egan (2005). Contribution of transmembrane regions to ATP-gated P2X<sub>2</sub> channel permeability dynamics. *J. Biol. Chem.* **280**(7): 6118-29.
- Kidd, E. J., C. B. Grahames, J. Simon, A. D. Michel, E. A. Barnard and P. P. Humphrey (1995). Localization of P2X purinoceptor transcripts in the rat nervous system. *Mol. Pharmacol.* **48**(4): 569-73.



- 
- Kim, M., L. H. Jiang, H. L. Wilson, R. A. North and A. Surprenant (2001). Proteomic and functional evidence for a P2X<sub>7</sub> receptor signalling complex. *EMBO J.* **20**(22): 6347-58.
- King, B. F., A. Townsend-Nicholson, S. S. Wildman, T. Thomas, K. M. Spyer and G. Burnstock (2000). Coexpression of rat P2X<sub>2</sub> and P2X<sub>6</sub> subunits in *Xenopus oocytes*. *J. Neurosci.* **20**(13): 4871-7.
- Komuro, A., M. Saeki and S. Kato (1999). Npw38, a novel nuclear protein possessing a WW domain capable of activating basal transcription. *Nucleic. Acids. Res.* **27**(9): 1957-65.
- Koshimizu, T., M. Koshimizu and S. S. Stojilkovic (1999). Contributions of the C-terminal domain to the control of P2X receptor desensitization. *J. Biol. Chem.* **274**(53): 37651-7.
- Koshimizu, T., M. Tomic, M. Koshimizu and S. S. Stojilkovic (1998). Identification of amino acid residues contributing to desensitization of the P2X<sub>2</sub> receptor channel. *J. Biol. Chem.* **273**(21): 12853-7.
- Koshimizu, T. A., K. Kretschmannova, M. L. He, S. Ueno, A. Tanoue, N. Yanagihara, S. S. Stojilkovic and G. Tsujimoto (2006). Carboxy-terminal Splicing Enhances Physical Interactions between the Cytoplasmic Tails of Purinergic P2X Receptors. *Mol. Pharmacol.* **In press**.
- Lambrecht, G. (1996). Design and pharmacology of selective P2-purinoceptor antagonists. *J. Auton. Pharmacol.* **16**(6): 341-4.
- Le, K. T., K. Babinski and P. Seguela (1998). Central P2X<sub>4</sub> and P2X<sub>6</sub> channel subunits coassemble into a novel heteromeric ATP receptor. *J. Neurosci.* **18**(18): 7152-9.
- Lewis, C., S. Neidhart, C. Holy, R. A. North, G. Buell and A. Surprenant (1995). Coexpression of P2X<sub>2</sub> and P2X<sub>3</sub> receptor subunits can account for ATP-gated currents in sensory neurons. *Nature.* **377**(6548): 432-5.
- Li, Z., K. Migita, D. S. Samways, M. M. Voigt and T. M. Egan (2004). Gain and loss of channel function by alanine substitutions in the transmembrane segments of the rat ATP-gated P2X<sub>2</sub> receptor. *J. Neurosci.* **24**(33): 7378-86.
- Lodish, H., A. Berk, L. Zipursky, P. Matsudaira, D. Baltimore and J. Darnell (2000). *Molecular Cell Biology*. Fourth Edition. New York.
- Macias, M. J., S. Wiesner and M. Sudol (2002). WW and SH3 domains, two different scaffolds to recognize proline-rich ligands. *FEBS Lett.* **513**(1): 30-7.
- MacKenzie, A., H. L. Wilson, E. Kiss-Toth, S. K. Dower, R. A. North and A. Surprenant (2001). Rapid secretion of interleukin-1beta by microvesicle shedding. *Immunity.* **15**(5): 825-35.
- Madden, D. R. (2002). The structure and function of glutamate receptor ion channels. *Nat. Rev. Neurosci.* **3**(2): 91-101.

- 
- Masin, M., D. Kerschensteiner, K. Dumke, M. E. Rubio and F. Soto (2006). Fe65 interacts with P2X<sub>2</sub> subunits at excitatory synapses and modulates receptor function. *J. Biol. Chem.* **281**(7): 4100-8.
- Mayer, M. L. (2005). Glutamate receptor ion channels. *Curr. Opin. Neurobiol.* **15**(3): 282-8.
- McLoughlin, D. M. and C. C. Miller (1996). The intracellular cytoplasmic domain of the Alzheimer's disease amyloid precursor protein interacts with phosphotyrosine-binding domain proteins in the yeast two-hybrid system. *FEBS Lett.* **397**(2-3): 197-200.
- Newbolt, A., R. Stoop, C. Virginio, A. Surprenant, R. A. North, G. Buell and F. Rassendren (1998). Membrane topology of an ATP-gated ion channel (P2X receptor). *J. Biol. Chem.* **273**(24): 15177-82.
- Newman, E. A. (2003). Glial cell inhibition of neurons by release of ATP. *J. Neurosci.* **23**(5): 1659-66.
- Nicke, A., D. Kerschensteiner and F. Soto (2005). Biochemical and functional evidence for heteromeric assembly of P2X<sub>1</sub> and P2X<sub>4</sub> subunits. *J. Neurochem.* **92**(4): 925-33.
- Nicke, A., J. Rettinger, C. Buttner, A. Eichele, G. Lambrecht and G. Schmalzing (1999). Evolving view of quaternary structures of ligand-gated ion channels. *Prog. Brain Res.* **120**: 61-80.
- North, R. A. (1996). P2X receptors: a third major class of ligand-gated ion channels. *Ciba Found Symp.* **198**: 91-105; discussion 105-9.
- North, R. A. (2002). Molecular physiology of P2X receptors. *Physiol. Rev.* **82**(4): 1013-67.
- North, R. A. and E. A. Barnard (1997). Nucleotide receptors. *Curr. Opin. Neurobiol.* **7**(3): 346-57.
- Okamoto, M. and T. C. Sudhof (1997). Mints, Munc18-interacting proteins in synaptic vesicle exocytosis. *J. Biol. Chem.* **272**(50): 31459-64.
- Pawson, T. and J. D. Scott (1997). Signaling through scaffold, anchoring, and adaptor proteins. *Science.* **278**(5346): 2075-80.
- Ralevic, V. and G. Burnstock (1998). Receptors for purines and pyrimidines. *Pharmacol. Rev.* **50**(3): 413-92.
- Rassendren, F., G. Buell, A. Newbolt, R. A. North and A. Surprenant (1997a). Identification of amino acid residues contributing to the pore of a P2X receptor. *EMBO J.* **16**(12): 3446-54.
- Rassendren, F., G. N. Buell, C. Virginio, G. Collo, R. A. North and A. Surprenant (1997b). The permeabilizing ATP receptor, P2X<sub>7</sub>. Cloning and expression of a human cDNA. *J. Biol. Chem.* **272**(9): 5482-6.

- 
- Robertson, S. J., S. J. Ennion, R. J. Evans and F. A. Edwards (2001). Synaptic P2X receptors. *Curr. Opin. Neurobiol.* **11**(3): 378-86.
- Royle, S. J., L. K. Bobanovic and R. D. Murrell-Lagnado (2002). Identification of a non-canonical tyrosine-based endocytic motif in an ionotropic receptor. *J. Biol. Chem.* **277**(38): 35378-85.
- Royle, S. J., O. S. Qureshi, L. K. Bobanovic, P. R. Evans, D. J. Owen and R. D. Murrell-Lagnado (2005). Non-canonical YXXGPhi endocytic motifs: recognition by AP2 and preferential utilization in P2X<sub>4</sub> receptors. *J. Cell Sci.* **118**(Pt 14): 3073-80.
- Rubio, M. E. and F. Soto (2001). Distinct Localization of P2X receptors at excitatory postsynaptic specializations. *J. Neurosci.* **21**(2): 641-53.
- Rubio, M. E. and R. J. Wenthold (1997). Glutamate receptors are selectively targeted to postsynaptic sites in neurons. *Neuron.* **18**(6): 939-50.
- Ruppelt, A., B. T. Liang and F. Soto (1999). Cloning, functional characterization and developmental expression of a P2X receptor from chick embryo. *Prog. Brain Res.* **120**: 81-90.
- Ruppelt, A., W. Ma, K. Borchardt, S. D. Silberberg and F. Soto (2001). Genomic structure, developmental distribution and functional properties of the chicken P2X<sub>5</sub> receptor. *J. Neurochem.* **77**(5): 1256-65.
- Russo, C., V. Dolcini, S. Salis, V. Venezia, E. Violani, P. Carlo, N. Zambrano, T. Russo and G. Schettini (2002). Signal transduction through tyrosine-phosphorylated carboxy-terminal fragments of APP via an enhanced interaction with Shc/Grb2 adaptor proteins in reactive astrocytes of Alzheimer's disease brain. *Ann. N. Y. Acad. Sci.* **973**: 323-33.
- Russo, T., R. Faraonio, G. Minopoli, P. De Candia, S. De Renzis and N. Zambrano (1998). Fe65 and the protein network centered around the cytosolic domain of the Alzheimer's beta-amyloid precursor protein. *FEBS Lett.* **434**(1-2): 1-7.
- Sabo, S. L., A. F. Ikin, J. D. Buxbaum and P. Greengard (2001). The Alzheimer amyloid precursor protein (APP) and FE65, an APP-binding protein, regulate cell movement. *J. Cell. Biol.* **153**(7): 1403-14.
- Sabo, S. L., A. F. Ikin, J. D. Buxbaum and P. Greengard (2003). The amyloid precursor protein and its regulatory protein, FE65, in growth cones and synapses in vitro and in vivo. *J. Neurosci.* **23**(13): 5407-15.
- Sabo, S. L., L. M. Lanier, A. F. Ikin, O. Khorkova, S. Sahasrabudhe, P. Greengard and J. D. Buxbaum (1999). Regulation of beta-amyloid secretion by FE65, an amyloid protein precursor-binding protein. *J. Biol. Chem.* **274**(12): 7952-7.
- Scheinfeld, M. H., E. Ghersi, K. Laky, B. J. Fowlkes and L. D'Adamio (2002). Processing of beta-amyloid precursor-like protein-1 and -2 by gamma-secretase regulates transcription. *J. Biol. Chem.* **277**(46): 44195-201.

- 
- Schwede, T., J. Kopp, N. Guex and M. C. Peitsch (2003). SWISS-MODEL: An automated protein homology-modeling server. *Nucleic Acids Res.* **31**(13): 3381-5.
- Seguela, P., A. Haghghi, J. J. Soghomonian and E. Cooper (1996). A novel neuronal P2X ATP receptor ion channel with widespread distribution in the brain. *J Neurosci.* **16**(2): 448-55.
- Sheng, M. and D. T. Pak (2000). Ligand-gated ion channel interactions with cytoskeletal and signaling proteins. *Annu. Rev. Physiol.* **62**: 755-78.
- Shepherd, G. M. (1994). Discrimination of molecular signals by the olfactory receptor neuron. *Neuron.* **13**(4): 771-90.
- Silberberg, S. D., T. H. Chang and K. J. Swartz (2005). Secondary structure and gating rearrangements of transmembrane segments in rat P2X<sub>4</sub> receptor channels. *J. Gen. Physiol.* **125**(4): 347-59.
- Simeone, A., A. Duilio, F. Fiore, D. Acampora, C. De Felice, R. Faraonio, F. Paolocci, F. Cimino and T. Russo (1994). Expression of the neuron-specific FE65 gene marks the development of embryo ganglionic derivatives. *Dev. Neurosci.* **16**(1-2): 53-60.
- Simon, J., E. J. Kidd, F. M. Smith, I. P. Chessell, R. Murrell-Lagnado, P. P. Humphrey and E. A. Barnard (1997). Localization and functional expression of splice variants of the P2X<sub>2</sub> receptor. *Mol. Pharmacol.* **52**(2): 237-48.
- Smart, M. L., B. Gu, R. G. Panchal, J. Wiley, B. Cromer, D. A. Williams and S. Petrou (2003). P2X<sub>7</sub> receptor cell surface expression and cytolytic pore formation are regulated by a distal C-terminal region. *J. Biol. Chem.* **278**(10): 8853-60.
- Snyder, P. M., M. P. Price, F. J. McDonald, C. M. Adams, K. A. Volk, B. G. Zeiher, J. B. Stokes and M. J. Welsh (1995). Mechanism by which Liddle's syndrome mutations increase activity of a human epithelial Na<sup>+</sup> channel. *Cell.* **83**(6): 969-78.
- Soto, F., M. Garcia-Guzman, C. Karschin and W. Stuhmer (1996). Cloning and tissue distribution of a novel P2X receptor from rat brain. *Biochem. Biophys. Res. Commun.* **223**(2): 456-60.
- Soto, F., M. Garcia-Guzman and W. Stuhmer (1997). Cloned ligand-gated channels activated by extracellular ATP (P2X receptors). *J. Membr. Biol.* **160**(2): 91-100.
- Squire, L., F. Bloom, N. Spitzer, J. Roberts, M. Zigmond and S. McConnell (2002). *Fundamental Neuroscience*. Second Edition. San Diego, California, Academic press, Elsevier Science.
- Stromgaard, K. (2005). Natural products as tools for studies of ligand-gated ion channels. *Chem. Rec.* **5**(4): 229-39.
- Stuhmer, W. (1992). Electrophysiological recording from *Xenopus oocytes*. *Methods Enzymol.* **207**: 319-39.

- 
- Sudol, M., H. I. Chen, C. Bougeret, A. Einbond and P. Bork (1995). Characterization of a novel protein-binding module: the WW domain. *FEBS Lett.* **369**(1): 67-71.
- Sudol, M., K. Sliwa and T. Russo (2001). Functions of WW domains in the nucleus. *FEBS Lett.* **490**(3): 190-5.
- Surprenant, A., F. Rassendren, E. Kawashima, R. A. North and G. Buell (1996). The cytolytic P2Z receptor for extracellular ATP identified as a P2X receptor (P2X<sub>7</sub>). *Science.* **272**(5262): 735-8.
- Tanahashi, H. and T. Tabira (1999). Genome structure and chromosomal mapping of the gene for Fe65L2 interacting with Alzheimer's beta-amyloid precursor protein. *Biochem. Biophys. Res. Commun.* **258**(2): 385-9.
- Torres, G. E., T. M. Egan and M. M. Voigt (1998a). Topological analysis of the ATP-gated ionotropic [correction of ionotropic] P2X<sub>2</sub> receptor subunit. *FEBS Lett.* **425**(1): 19-23.
- Torres, G. E., T. M. Egan and M. M. Voigt (1999). Hetero-oligomeric assembly of P2X receptor subunits. Specificities exist with regard to possible partners. *J. Biol. Chem.* **274**(10): 6653-9.
- Torres, G. E., W. R. Haines, T. M. Egan and M. M. Voigt (1998b). Co-expression of P2X<sub>1</sub> and P2X<sub>5</sub> receptor subunits reveals a novel ATP-gated ion channel. *Mol. Pharmacol.* **54**(6): 989-93.
- Toulme, E., F. Soto, M. Garret and E. Boue-Grabot (2006). Functional properties of internalization-deficient P2X<sub>4</sub> receptors reveal a novel mechanism of ligand-gated channel facilitation by ivermectin. *Mol. Pharmacol.* **69**(2): 576-87.
- Unwin, N. (1993). Neurotransmitter action: opening of ligand-gated ion channels. *Cell.* **72** **Suppl**: 31-41.
- Valera, S., N. Hussy, R. J. Evans, N. Adami, R. A. North, A. Surprenant and G. Buell (1994). A new class of ligand-gated ion channel defined by P2X receptor for extracellular ATP. *Nature.* **371**(6497): 516-9.
- Villmann, C., L. Bull and M. Hollmann (1997). Kainate binding proteins possess functional ion channel domains. *J. Neurosci.* **17**(20): 7634-43.
- Virginio, C., A. MacKenzie, F. A. Rassendren, R. A. North and A. Surprenant (1999). Pore dilation of neuronal P2X receptor channels. *Nat. Neurosci.* **2**(4): 315-21.
- Wilson, H. L., S. A. Wilson, A. Surprenant and R. A. North (2002). Epithelial membrane proteins induce membrane blebbing and interact with the P2X<sub>7</sub> receptor C terminus. *J. Biol. Chem.* **277**(37): 34017-23.
- Yan, K. S., M. Kuti and M. M. Zhou (2002). PTB or not PTB -- that is the question. *FEBS Lett.* **513**(1): 67-70.

- 
- Zambrano, N., M. Bimonte, S. Arbucci, D. Gianni, T. Russo and P. Bazzicalupo (2002). *feh-1* and *apl-1*, the *Caenorhabditis elegans* orthologues of mammalian Fe65 and beta-amyloid precursor protein genes, are involved in the same pathway that controls nematode pharyngeal pumping. *J. Cell. Sci.* **115**(Pt 7): 1411-22.
- Zambrano, N., G. Minopoli, P. de Candia and T. Russo (1998). The Fe65 adaptor protein interacts through its PID1 domain with the transcription factor CP2/LSF/LBP1. *J. Biol. Chem.* **273**(32): 20128-33.
- Zarrinpar, A. and W. A. Lim (2000). Converging on proline: the mechanism of WW domain peptide recognition. *Nat. Struct. Biol.* **7**(8): 611-3.
- Zhou, M. M., and Fesik, S.W. (1995). Structure and function of the phosphotyrosine binding (PTB) domain. *Prog. Biophys. molec. Biol.* **64**(2/3): 221-235.
- Zhou, M. M., B. Huang, E. T. Olejniczak, R. P. Meadows, S. B. Shuker, M. Miyazaki, T. Trub, S. E. Shoelson and S. W. Fesik (1996). Structural basis for IL-4 receptor phosphopeptide recognition by the IRS-1 PTB domain. *Nat. Struct. Biol.* **3**(4): 388-93.

---

## II. APPENDIX

### II.I. Oligonucleotides.

Name	Sequence (5' → 3')	Template sequence
2155	CCGAATTCCTACCGGCTGGATGGATGAGG	rFe65
2156	CGGGATCCCTATGGGGGTTCCTACTGGGTGGT	rFe65
2157	CCGAATTCGGCCGGGCCTCCCCATCACAG	rFe65
2158	CGGGATCCCTACTTGATCCCTGGATTGGCGTT	rFe65
2159	CCGAATTCTGTTTCGCTGTGCGCTCCCTA	rFe65
2160	CGGGATCCCTAGGTGGCGATGTTCTTGGCAGG	rFe65
2161	CGGGATCCCTAAGCATTGCGCCGTTTCAGACAT	rFe65
2178	CCGAATTCTTCATGAACAAAAACAAGCTCTAC	rP2X <sub>2</sub>
2179	CGGGATCCCTACCCTTCTCCCAAAGTTGG	rP2X <sub>2</sub>
2180	CCGAATTCGCAGAGCTACCACTGGCTGTC	rP2X <sub>2</sub>
2181	CGGGATCCCTAAAGTTGGGCCAAACCTTT	rP2X <sub>2</sub>
2184	CTGGGATCCTTCATGAACAAAAACAAGCTCTAC	rP2X <sub>2</sub>
2185	GAGCGGCCGCATCTAAAGTTGGGCCAAACCTTT	rP2X <sub>2</sub>
2188	CTGGGATCCAGTGACGAGGACTCAAGCTGG	rFe65
2189	GAGCGGCCGCATCTACCCACACGCGAATG	rFe65
2196	CCGAATTCAGTGACGAGGACTCAAGCTGG	rFe65
2197	CGGGATCCCTACTAGGTCAGCTTATCTCGAGCTAC	rFe65
2206	CCGGATCCCAAGCCACAGCTGTGGTAC	rFe65
2207	GGAATAAGCTTTGCGGCTGGCCTCCTCCGC	rFe65
2208	CCGGATCCACAGATGGCCCCCGGGAAC	rFe65
2209	GGAATAAGCTTTGCATCGGAATCCGTCTCGAA	rFe65
2304	TGGCGGCCGCATGTCTGTTCCATCATCCCTG	rFe65

<b>Name</b>	<b>Sequence (5' → 3')</b>	<b>Template sequence</b>
2305	CCTCTAGACTTGGGGTCTGGGATCCTAG	rFe65
2217	GAGCGGCCGCATCTAGGTCAGCTTATCTCGAGCTAC	rFe65
2333	CGGGATCCCTACTGGGAGTAGTGACTAGG	rP2X <sub>2</sub>
2334	CCGAATTCGATCAGCCACCCAGCCCT	rP2X <sub>2</sub>
2358	CGGAATTCCAGCCTGGCCCAGGC	rFe65L1
2359	CGTCTAGACTACCTTGTGTCCTTGTCTCT	rFe65L1
2455	GCGGTGGCGGCCGCTCTAGAA	rFe65
2456	CTCGAACTCTCATCAAAGCCT	rP2X <sub>2</sub>
2468	GACTTGTCTGAATCAGAGTGC	rP2X <sub>2</sub>
2469	GATCTAGATTAGTGAGGATGAGATCAAAG	rP2X <sub>2</sub>
2474	TTAGTGAGGATGAGATCAAAG	rP2X <sub>2</sub>
2475	GAGGAGGACTTGTCTTCTCCT	rFe65
2476	TTCATTCTTTGGTGCTGG	rFe65



## II.II. Cloned constructs

<b>DNA-Construct</b>	<b>(PCR: Primer s/as)</b>	<b>Vector</b>	<b>Restriction sites</b>
Fe65 <i>full length</i>	2304/2305	pcDNA3.1/myc-His B	<i>NotI</i> / <i>XbaI</i>
Fe65 <i>full length</i>	----	pSGEM	<i>Sall</i>
Fe65(218-479)	2196/2197	pVP16-4	<i>EcoRI</i> / <i>BamHI</i>
Fe65(218-309)	2196/2158	pVP16-4	<i>EcoRI</i> / <i>BamHI</i>
Fe65(218-284)	2196/2156	pVP16-4	<i>EcoRI</i> / <i>BamHI</i>
Fe65(255-284)	2155/2156	pVP16-4	<i>EcoRI</i> / <i>BamHI</i>
Fe65(285-479)	2157/2197	pVP16-4	<i>EcoRI</i> / <i>BamHI</i>
Fe65L1(1-321)	2358/2359	pVP16-4	<i>EcoRI</i> / <i>BamHI</i>
Fe65(218-479)	2188/2217	pGEX-4T-1	<i>BamHI</i> / <i>NotI</i>
Fe65(218-479)	2188/2217	pET 32a(+)	<i>BamHI</i> / <i>NotI</i>
Fe65(197-255)	2208/2209	pGEX-4T-1	<i>EcoRI</i> / <i>BamHI</i>
Fe65(40-100)	2206/2207	pGEX-4T-1	<i>EcoRI</i> / <i>BamHI</i>
P2X <sub>2</sub> (355-472)	2178/2181	pLexN	<i>EcoRI</i> / <i>BamHI</i>
P2X <sub>2</sub> (355-416)	2178/2179	pLexN	<i>EcoRI</i> / <i>BamHI</i>
P2X <sub>2</sub> (417-472)	2180/2181	pLexN	<i>EcoRI</i> / <i>BamHI</i>
P2X <sub>2</sub> (355-400)	2178/2333	pLexN	<i>EcoRI</i> / <i>BamHI</i>
P2X <sub>2</sub> (401-472)	2334/2181	pLexN	<i>EcoRI</i> / <i>BamHI</i>
P2X <sub>2(b)</sub> (355-403)	2178/2181	pLexN	<i>EcoRI</i> / <i>BamHI</i>
P2X <sub>2</sub> (355-472)	2184/2185	pGEX-4T-1	<i>BamHI</i> / <i>NotI</i>
P2X <sub>2</sub> (355-472)	2184/2185	pET 32a(+)	<i>BamHI</i> / <i>NotI</i>
P2X <sub>2(b)</sub> (355-472)	2184/2185	pET 32a(+)	<i>BamHI</i> / <i>NotI</i>

### II.III. Nucleotide and amino acid sequence of rat P2X<sub>2</sub> receptor

1 atggtccggcgcttgccccgggctgctggtccgcgttctgggactacgagacgcctaag  
1 M V R R L A R G C W S A F W D Y E T P K  
61 gtgatcgtggtgcggaatcggcgccctgggattcgtgcaccgcatggtgcagcttctcatc  
21 V I V V R N R R L G F V H R M V Q L L I  
121 ctgctttacttctggtgtggtacgtcttcatcgtgcagaaaagctaccaggacagcgagacc  
41 L L Y F V W Y V F I V Q K S Y Q D S E T  
181 ggaccggagagctccatcatcaccaaagtcaaggggatcaccatgtcggaagacaaagtg  
61 G P E S S I I T K V K G I T M S E D K V  
241 tgggacgtggaggaatacgtaaagccccggaggggggcagtgtagtcagcatcatcacc  
81 W D V E E Y V K P P E G G S V V S I I T  
301 aggatcgaggttacccttcccagaccttgggaacatgccagagagcatgagggttccac  
101 R I E V T P S Q T L G T C P E S M R V H  
361 agctctacctgccattcagacgacgactgtattgccggacagctggacatgcaaggcaat  
121 S S T C H S D D D C I A G Q L D M Q G N  
421 gggattcgcacagggcactgtgtaccctattaccatggggactccaagacctgaggggtg  
141 G I R T G H C V P Y Y H G D S K T C E V  
481 tcagcctggtgccccggtggaggatggaacttctgacaaccattttctgggtaaaatggcc  
161 S A W C P V E D G T S D N H F L G K M A  
541 ccaaatttcaccatcctcatcaagaacagcatccactacccaagttcaagttctcaag  
181 P N F T I L I K N S I H Y P K F K F S K  
601 ggcaacattgcaagccagaagagtgactacctcaagcattgcacatttgatcaggactct  
201 G N I A S Q K S D Y L K H C T F D Q D S  
661 gaccatactgtcccacttccaggctgggtttcattggtgagaaggcaggagagaacttc  
221 D P Y C P I F R L G F I V E K A G E N F  
721 acagaactggcacacaagggcggtgtcattggagtcatcatcaactggaactgtgacctg  
241 T E L A H K G G V I G V I I N W N C D L  
781 gacttgtctgaatcagagtgcaaccccaaatattctttccggaggctcgacccaagtat  
261 D L S E S E C N P K Y S F R R L D P K Y  
841 gaccctgcctcctcaggctacaacttcaggtttgccaagtattacaagataaacggcact  
281 D P A S S G Y N F R F A K Y Y K I N G T  
901 accaccactcgaactctcatcaaagcctatgggattcgaatcgatgttatcgtgcatgga  
301 T T T R T L I K A Y G I R I D V I V H G  
961 caggcagggaaattcagtcctattcccaccatcatcaatctggccactgctctgacctcc  
321 Q A G K F S L I P T I I N L A T A L T S  
1021 atcgggggtgggctccttctgtgtgactggattttgttaacgttcatgaacaaaacaag  
341 I G V G S F L C D W I L L T F M N K N K  
1081 ctctacagccataagaagttcgacaagggtgcgtactccaagcactcctcaagtagatgg  
361 L Y S H K K F D K V R T P K H P S S R W

---

### Nucleotide and amino acid sequence of rat P2X<sub>2</sub> receptor (cont.)

```
1141 cctgtgacccttgcccttgtcttgggccagatccctccccacctagtcactactcccag
381 P V T L A L V L G Q I P P P P S H Y S Q
1200 gatcagccaccagccctccatcaggtgaaggaccaactttgggagaaggggcagagcta
400 D Q P P S P P S G E G P T L G E G A E L
1261 ccactggctgtccagtctcctgggccttgctccatctctgctctgactgagcaggtgggtg
421 P L A V Q S P R P C S I S A L T E Q V V
1321 gacacacttgccagcatatgggacaaagacctcctgtccctgagcctttcccaacaggac
441 D T L G Q H M G Q R P P V P E P S Q Q D
1381 tccacatccacggacccccaaaggtttggcccaactttga
461 S T S T D P K G L A Q L *
```

The putative PTB binding site is highlighted in light blue, while the four proline-rich domains are highlighted in dark blue. The nucleotides spliced out in P2X<sub>2(b)</sub> are delimited by black arrows.

---

## II.IV. Nucleotide and amino acid sequence of rat Fe65 protein (APBB1)

1 atgtctgttccatcatccctgagccagtcggccattaatgctaacagccacggaggccct  
1 M S V P S S L S Q S A I N A N S H G G P  
61 gcactcagcttcccccttcccccttgcatgctgcccataaccagctgctcaacgccaaagctg  
21 A L S F P F P L H A A H N Q L L N A K L  
121 caagccacagctgtggtacccaaggaccttcgaagtgccatgggagagggtagtgtgcct  
41 Q A T A V V P K D L R S A M G E G S V P  
181 gaaccaggccctgccaatgccaagtggttaaaggaaggccagaaccagcttcggaggggct  
61 E P G P A N A K W L K E G Q N Q L R R A  
241 gccacagcccatcgagaccagaaccgaaatgtgaccttgaccttgggcggaggaggccagc  
81 A T A H R D Q N R N V T L T L A E E A S  
301 caggaggctgagacagcacctttgggtcccaaggcttaatgcatctatactctgagctg  
101 Q E A E T A P L G P K G L M H L Y S E L  
361 gagctctcggcccacaatgcagccaaccgagggcttcatggatccgccttgatcatcaac  
121 E L S A H N A A N R G L H G S A L I I N  
421 acccagggactgggaccagatgaaggagaggagaaggcagcaggagaagttgaggaggag  
141 T Q G L G P D E G E E K A A G E V E E E  
481 gatgaagatgaggaggaagaggatgaggaggaggaggacttgtcttctcctcaagggcta  
161 D E D E E E E D E E E E D L S S P Q G L  
541 cctgagcctctggagaatgtggaagtccccctctggaccccaggctcctcacagatggcccc  
181 P E P L E N V E V P S G P Q V L T D G P  
601 cgggaacatagcaagagtgcctagcctctatittggcatgcgaacagctgcagccagtgac  
201 R E H S K S A S L L F G M R N S A A S D  
661 gaggactcaagctgggccaccttatcgcagggcagccccctctatggctctccggaggac  
221 E D S S W A T L S Q G S P S Y G S P E D  
721 acagattccttctggaacccccaacgctttcgagacggattccgatctaccggctggatgg  
241 T D S F W N P N A F E T D S D L P A G W  
781 atgaggggtccaagacacctcagggacctactactggcacatcccaacagggaccaccag  
261 M R V Q D T S G T Y Y W H I P T G T T Q  
841 tgggaacccccaggccgggctccccatcacaggggaacagtcccaagaagaggtcccag  
281 W E P P G R A S P S Q G N S P Q E E S Q  
901 ctcacctggactggctttgctcaccagaaggctttgaggaaggagagttttggaaggat  
301 L T W T G F A H Q E G F E E G E F W K D  
961 gaacctagtgaagagggccccaatggagttgggactgaaggacctgaggaggggacattg  
321 E P S E E A P M E L G L K D P E E G T L  
1021 cccttctcagctcagagcctcagcccagagccagtgccccaggaggaggagaatctgcc  
341 P F S A Q S L S P E P V P Q E E E N L P  
1081 caacgggaacgccaatccagggatcaagtgttttcgctgtgctccttaggctgggtagag  
361 Q R N A N P G I K C F A V R S L G W V E

## Nucleotide and amino acid sequence of rat Fe65 protein (APBB1) (cont.)

```

1141 atgactgaggaggagctggccccaggacgcagcagtggtggcagtcaacaattgtatccgc
381 M T E E E L A P G R S S V A V N N C I R
1200 cagctctcctaccacaaaaacaatctacatgatccgatgtctggaggctggggagagggga
400 Q L S Y H K N N L H D P M S G G W G E G
1261 aaggatctgctgctccagctggaggatgagacgctaaagtgggaggccacagaaccag
421 K D L L L Q L E D E T L K L V E P Q N Q
1321 acactgctgcatgccagcccacatcgctcagcattcgcggtgtggggcggtggggcgggacagt
441 T L L H A Q P I V S I R V W G V G R D S
1381 ggaagagagaggggactttgcctacgtagctcgagataagctgaccagatgctcaagtgc
461 G R E R D F A Y V A R D K L T Q M L K C
1441 cagtggtttcgctgtgaggacacctgccaagaacatcgccaccagcctgcatgagatctgc
481 H V F R C E A P A K N I A T S L H E I C
1500 tccaagatcatgtctgaacggcgcaatgctcgctgcttggtaaatggactctccctggac
500 S K I M S E R R N A R C L V N G L S L D
1561 cactctaaacttgtggatgtccctttccaagtgggaattcccagcaccacaagaatgaactg
521 H S K L V D V P F Q V E F P A P K N E L
1621 gtgcagaagtttcaagctctattacctagggaacgtgccctgtggcctaaccctgtgggta
541 V Q K F Q V Y Y L G N V P V A K P V G V
1681 gatgtgattaatggagccctggagtcagtcctgtcttccagtagtcgtgagcagtgacc
561 D V I N G A L E S V L S S S S R E Q W T
1741 ccaagtacgctcagcgtggcccccgccaccctcaccatcttgcaccagcagacagaagca
581 P S H V S V A P A T L T I L H Q Q T E A
1800 gtgctgggggagtgctcagtgcggttcctctccttccctggctgtgggcagagatgtgcac
600 V L G E C R V R F L S F L A V G R D V H
1861 acgttcgcattcatcatggctgccggcccagcctccttctgctgtcacatgttttgggtgc
621 T F A F I M A A G P A S F C C H M F W C
1921 gagcccaatgctgccagctctctcggaggctgtgcaggctgcatgcatgctccgctaccag
641 E P N A A S L S E A V Q A A C M L R Y Q
1981 aagtgtctggatgctcgttcccagacctccacctcctgcctcccagaccccccgaggag
661 K C L D A R S Q T S T S C L P A P P A E
2041 tcagttgagagcgtgtagggtggactgtccgcaggggtgttcagctctctgtggggttcc
681 S V A R R V G W T V R R G V Q S L W G S
2100 ctcaagcccaaacgtctaggatcccagaccccatga
701 L K P K R L G S Q T P *

```

The WW domain is highlighted in orange, the first PTB domain in red and the second PTB domain in dark red.

## II.V. Partial nucleotide and amino acid sequence of rat Fe65 Like 1 isolated in the Y2H screening (APBB2)

```

1  ttccagcctggcccaggccaggccccagtagtcattgggaatggtgacttgggtgccacag
1  F  Q  P  G  P  G  Q  A  P  V  V  I  G  N  G  D  L  V  P  Q
61  aaaccaaacaaaccccagtcagcccagaggatggccaagtagccacagtatcatccagc
21  K  P  N  K  P  Q  S  S  P  E  D  G  Q  V  A  T  V  S  S  S
121 ccagagaccaagaagaccaccctaaaacaggagccaaaaccgactgtgcactccatcgg
41  P  E  T  K  K  D  H  P  K  T  G  A  K  T  D  C  A  L  H  R
181 atccagaacctggcaccagtgatgaggaatccagctggacaacgctgtcccaagacagc
61  I  Q  N  L  A  P  S  D  E  E  S  S  W  T  T  L  S  Q  D  S
241 gcctccccagctccccagatgaaacagcagatatctggagtggtcactcatttcagaca
81  A  S  P  S  S  P  D  E  T  A  D  I  W  S  G  H  S  F  Q  T
301 gatccggatttgccgcctggctggaaaagagtcagtgacattgctgggacctattactgg
101  D  P  D  L  P  P  G  W  K  R  V  S  D  I  A  G  T  Y  Y  W
361 cacatcccaacagggagcactcagtgggaaacggcccgtctctatcccagcggatctccat
121  H  I  P  T  G  T  T  Q  W  E  R  P  V  S  I  P  A  D  L  H
421 ggttctaggaagggtcacttagctctgtaacgccatctcccaccagagaacggagaaa
141  G  S  R  K  G  S  L  S  S  V  T  P  S  P  T  P  E  N  E  K
481 cagccatggagtgatcttctgcttctgaatgggggaaagattaatagtgacatttggag
161  Q  P  W  S  D  F  A  V  L  N  G  G  K  I  N  S  D  I  W  K
541 gatttgcaagcagccacagtttaaccagaccccagtttaaagagtttgaaggagcaaca
181  D  L  H  A  A  T  V  N  P  D  P  S  L  K  E  F  E  G  A  T
601 ctgcgctatgcateccttgaactcagaaacgccctcatgccgatgacgatgattcttgt
201  L  R  Y  A  S  L  K  L  R  N  A  P  H  A  D  D  D  D  S  C
661 agtatcaacagtgaccagaagccagtgcttctgtgcttctctgggctgggtagag
221  S  I  N  S  D  P  E  A  K  C  F  A  V  R  S  L  G  W  V  E
721 atggcagaggaggaccttgccccgggaagagcagtggtgctgtcaacaactgcatccgg
241  M  A  E  E  D  L  A  P  G  K  S  S  V  A  V  N  N  C  I  R
781 cagctttcctactgcaaaaacgacatccgggacacagtcggcatctggggagagggcaad
261  Q  L  S  Y  C  K  N  D  I  R  D  T  V  G  I  W  G  E  G  K
841 gacatgtacctgatcctggaaaatgacactctcagcctggtggaccccatggaccgctct
281  D  M  Y  L  I  L  E  N  D  T  L  S  L  V  D  P  M  D  R  S
901 gtgttacactcccagcccatcgtgagcatccgagtggtggggtgtgggcccagacaacggc
301  V  L  H  S  Q  P  I  V  S  I  R  V  W  G  V  G  R  D  N  G
961 cgagactttgcttatgtggcaagagacaaagacacgaga
321  R  D  F  A  Y  V  A  R  D  K  D  T  R

```

The WW domain is highlighted in dark pink and the first PTB domain in purple. Numbers on the sequence are arbitrary and are only consigned for comparative purposes. By the time of the submission of this thesis work the isolation and characterization of the Fe65 Like 1 protein from rat has not been reported. Nevertheless since the genome of *rattus norvegicus* is known, there is a predicted Fe65 like 1 protein (gi: 62660482) that is annotated as a potential gene product of chromosome 14 region 10,490,390 to 10,752,085 (gi: 62660484). Searching performed on this mRNA for the sequence that was isolated in the Y2H screening identified four potential exons and four introns on the predicted mRNA sequence. On the above sequence the four exons are delimited with black arrows. The position of the exons relative to the predicted mRNA is highlighted in pink in the following sequence.

---

## II.VI. Predicted nucleotide and amino acid sequence of rat Fe65 Like 1

### (APBB2)

```
1 atggcacaagtgagctcacatcccagagaaggttgattctgcctcgggaagaggctgtgt
1 M A Q V S S H F R E G C I L P R K R L C
61 gactttttctcgggtgtctgcacagcaccgactctggcagcactgtagcttcttgggaagca
21 D F F S V S A Q H R L W Q H C S F L E A
121 gaaatcttccacaggatactagacgaggaagagaaaaatgctggcccaacattcaggccc
41 E I F H R I L D E E E K N A G P T F R P
181 ccaaaggatgactgtaaggcattgctagatcatgacttgtcacacagcaatggatgacac
61 P K D D C K A L L D H D L S H S N G D H
241 acagctctggtgcccttggaacacatcagcaagaatctagccatactctacgagaatctt
81 T A L V P L E N I S K N L A I L Y E N L
301 aggcattctgatgcacacggatgggacctgagcagcagcggacagcttagcagaagcagaa
101 R H L M H T D G P C E R A D S L A E A E
361 gtggttttgtttcaaagaaatggctctgaaggacaggaagaagagaggaagttcttcagt
121 V V L F Q R N G S E G Q E E E R K F F S
421 acagctatggacaaagctacaacccgaggccactcacgacagcctcagcagccctggctt
141 T A M D K A T T R G H S R Q P Q Q P W L
481 ggtaggagagagaaagctgcatcctccctcgaggccttaacacaccagatgcctgcgata
161 G R R E K A A S S L E A L T H Q M P A I
541 aagcagtgggcagcaagggaaacctttggcagtggtgagacatgattctctcatggagcaa
181 K Q W Q Q G N L W R V V R H D S L M E Q
601 cttgccatcagcgggtgctgacgattcacctgaagactccagccgccccttcactaagatc
201 L A I S G A D D S P E D S S R P F T K I
661 tacaggaagggctgttcccccaggcttcagtgctctgttcagagaatttcaaattgtt
221 Y R K G L F P K G F S V S V Q R I S N V
721 gttgattgtgtggcttttgagtcagctcataaaataaacggggaaccgtgcacttgctg
241 V D C V A F E S A H K I N G E T V H L L
781 tggcttcagctccttaggagatctgagagatctgattcaggtgtcggcaccttggcagtg
261 W L Q L L R R S E R S D S G V G T L A V
841 tttatggcaagcagcgggaaccacagacattctggagggtaaagatctccacccccaggag
281 F M A S S G T T D I L E G K D L H P Q E
901 tcctcaggctgtgagattttgccctcccaccccaggagaactaagagcttcctcaattac
301 S S G C E I L P S H P R R T K S F L N Y
961 tatgcagaccctggaacacctggcttagagaactaggacagaacctggggccatgccaaggg
321 Y A D L E T S A R E L G Q N L G P C Q G
1021 gttggagaggagaaagccagccaggcccaggcccaggcccagtagtcatcattgggaatgg
341 V G E E K A Q P G P G Q A P V V I G N G
1081 gacttgggtgccacagaaaccaaacaccccagtcagcccagaggatggccaagtagcc
361 D L V P Q K P N K P Q S S P E D G Q V A
```



---

## Predicted nucleotide and amino acid sequence of rat Fe65 Like 1 (APBB2)

(cont)

1141 acagtatcatccagcccagagaccaagaagaccaccctaaaacaggagccaaaaccgac  
381 T V S S S P E T K K D H P K T G A K T D

1200 tgtgcactccatcggatccagaacctggcaccaagtgatgaggaatccagctggacaacg  
400 C A L H R I Q N L A P S D E E S S W T T

1261 ctgtcccaagacagcgcctccccagctccccagatgaaacaggatgctgtgagtattgg  
421 L S Q D S A S P S S P D E T G C C E Y W

1321 agctttgccacatcttccaccatcgtcattgtcatctccttttaccacaggataagccc  
441 S F A T S S T I V I V I S F Y Q Q D K P

1381 ccctttgaagtacttttccaagtcaatctcagcagcaatttagaatacaaacccagcagat  
461 P F E V L F Q V N L S S N L E Y K P A D

1441 atctggagtgatcactcatttcagacagatccggatttgccgcctggctggaaaagagtc  
481 I W S D H S F Q T D P D L P P G W K R V

1500 agtgacattgctgggacctattactggcacatcccaacagggacgactcagtgggaacgg  
500 S D I A G T Y Y W H I P T G T T Q W E R

1561 cccgtctctatcccagcggatctccacggttctaggaagggtcacttagctctgtaacg  
521 P V S I P A D L H G S R K G S L S S V T

1621 ccattctcccaccccagagaacgagaacagccatggagtgattttgctgttctgaatggg  
541 P S P T P E N E K Q P W S D F A V L N G

1681 ggaagattaatagtgacatttggaggatttgcattgcagccacagttaaccagacccc  
561 G K I N S D I W K D L H A A T V N P D P

1741 agtttaaaagagtttgaaggagcaacactgcgctatgcatccttgaacctcagaaacgcc  
581 S L K E F E G A T L R Y A S L K L R N A

1800 cctcatgccgatgacgatgattcttgtagtatcaacagtgaccacagaagccaagggtgcc  
600 P H A D D D D S C S I N S D P E A K G A

1861 acactcctatttaaaaggctcctctgagcccagggcccttcagctcggctgtgagaacag  
621 T L L F K R S S E P E A L Q L G C E E Q

1921 ggctcagctctccctctgcccggctcagacacttgtgtggaatcatgtcacagcgg  
641 G L S S P S A A G S D T C V E I M S Q R

1981 gcttctctacttcccattctctataacctggcaccaggagcgggctttcagccgtcgtgt  
661 A S L L P I S I P G T R S E G F Q P S C

2041 gcagcagctggctcactgggcattctgctcattcaacgacaagtgtgcacacatgggtgctg  
681 A A A G H W A S A H S T T S V H T W V L

2100 accaggctcaggaggaagcctggtaataatcttccccagcaccgacaatgatccgagt  
700 T Q A Q E E S L V I I F P S T D N D P S

2161 gacaagaactgccaaagacgagggactgtggtcaactctggcccaatgctgccaacagca  
721 D K N C Q R R G T V V N S G P M L P T A

2221 gtcaaacatgcttctgctgacaaaacaggctctagtgctttggaatgggtccacagccat  
741 V K H A S A D K T G S S A L E W S T A H



---

**Predicted nucleotide and amino acid sequence of rat Fe65 Like 1 (APBB2) (cont)**

2281 gaggtaccagatgaagtgactgctttggccacttacttagacctgtgccaaaggctcctac  
761 E V P D E V T A L A T Y L D L C Q G S Y

2341 tgcagctgtgaggaaggaggaggagctctgacattcatcgccaacaccttggcttgggct  
781 C S C E E G G G A L T F I A N T L A W A

2400 ggcattcaagcatcaccagcagcagatgcagtcagccacccttttgtgaagactttccgct  
800 G I Q A S P A A D A V S H P F V R L S A

2461 tttcacggtgccggtttcctgtccggtcatatccagatcatgacgctgcacaccccacga  
821 F H G A G F L S G H I Q I M T L H T P R

2521 gagttgaagtgctgctgcttgcctcactgtatttctaggacttgttccctgatgttcagccc  
841 E L K C C C L L T V F L G L V P D V Q P

2581 actcaacagcttagcaacagttacggagagctaggccttccaatgtgttttgcctgtgcgt  
861 T Q Q L S N S Y G E L G L P M C F A V R

2641 tctctgggctgggttagagatggcagaggaggaccttgcccccggaagagcagtggttgc  
881 S L G W V E M A E E D L A P G K S S V A

2700 gtcaacaactgcatccggcagctttcctactgcaaaaacgacatccgggacacagtcggc  
900 V N N C I R Q L S Y C K N D I R D T V G

2761 atctggggagagggcaaaagacatgtacctgatcctggaaaatgacactctcagcctggtg  
921 I W G E G K D M Y L I L E N D T L S L V

2821 gaccccatggaccgctctgtgtttacactcccagcccatcgtgagcctccgagtggtgggt  
941 D P M D R S V L H S Q P I V S I R V W G

2881 gtgggcccagagacaacggccgaatcatagaacatgacggaaagcacagcccgcctccagag  
961 V G R D N G R I I E H D G K H S P P P E

2941 gtgctcgccagctcgctcaccagctctagtttccgcccgcctcatcggggaattccatttca  
981 V L A S S L T S L V S A A I I G N S I S

3000 aagacaagcggagattaccgaaggcattatataccagagagaggctgagagtcagacactt  
1000 K T S G D Y R R H Y I Q R E A A S Q T L

3061 caagaagtagacttaggctccttgaagacagtcacacagcatggcacagcagacagtagtt  
1021 Q E V D L G S L K T V N S M A Q Q T V V

3121 acttcagtgaggagagcccacctaggagaaggagagcagaaagcagctgccgaaagcatg  
1041 T S V G R A H L G E G E Q K A A A E S M

3181 gctgtcaactggggccagggttggcctgattctgtcatgtcagagcacgcagttattcctg  
1061 A V N W G Q V G L I L S C Q S T Q L F L

3241 cacatgctgctttccagggtcagtggttcacatacactgagaagggagtaggcttgcag  
1081 H M L L S R V S G F T Y T E K G V G L Q

3300 ctgactaaatttagcctgctccactctcagaatggctcatcttgtatgaagcccagctcc  
1100 L T K F S L L H S Q N G S S C M K P S S

3361 gggccattggatttttggttgttgatgtttcaaatccagcaaacgtaccgagtgatggag  
1121 G P I G F W L L M F Q I Q Q T Y R V M E

---

**Predicted nucleotide and amino acid sequence of rat Fe65 Like 1 (APBB2) (cont)**

3421 cagctgccattcccctgggtaccagctgcagctctaataagaatatccaggggcatgaag  
1141 Q L P F P W V P A A A L I E Y P G A M K

3481 cagaacctgaggctggctcctctgggggaataattaccggggagagcagcaaaaggacaag  
1161 Q N L R L V L W G N N Y R G E Q Q K D K

3541 aagaaaggatttgggaagcacaggggttcaggactttgcttatgtggcaagagacaaagac  
1181 K K G F G S T G V Q D F A Y V A R D K D

3600 acgagaattctgaaatgccatgtgtttcgatgtgacacaccagcaaaagccattgccaca  
1200 T R I L K C H V F R C D T P A K A I A T

3661 agtctccacgaaatctgttccaagattatggctgaacggaagaatgccaaagccctggcc  
1221 S L H E I C S K I M A E R K N A K A L A

3721 tgcagctccttacaggagaggaccaatatgagctctcgatgtccctttgcaagtagatttt  
1241 C S S L Q E R T N M S L D V P L Q V D F

3781 ccaacaccaaaagacggagctggtgcagaagttccacgtgcagtacctgggcatgttacct  
1261 P T P K T E L V Q K F H V Q Y L G M L P

3841 gtagaccgacctgtcggcatggacacctgaacagtgccatagagaatcttatgacgtca  
1281 V D R P V G M D T L N S A I E N L M T S

3900 tccagcaaggaggactggccttcgggtgaacatgaacgtggccgatgccactgtgacagtc  
1300 S S K E D W P S V N M N V A D A T V T V

3961 atcaatgaaaagaatgaagaggagatcttgggtggaatgtcgggtgcgctttctgtccttc  
1321 I N E K N E E E I L V E C R V R F L S F

4021 atgggcgctcgggaaggacgtccatacgtttgccttcatcatggacactgggaaccagcgc  
1341 M G V G K D V H T F A F I M D T G N Q R

4081 tttgagtgccacgtgttctggtgtgagcctaatagcagccaatgtgtcgggaagctgtccag  
1361 F E C H V F W C E P N A A N V S E A V Q

4141 gctgcctgcatgaatgaagaggagatcttgggtggaatgtcgggtgcgctttctgtccttc  
1381 A A C M N E E E I L V E C R V R F L S F

4200 atgggcgctcgggaaggacgtccatacgtttgccttcatcatggacactgggaaccagcgc  
1400 M G V G K D V H T F A F I M D T G N Q R

4261 tttgagtgccacgtgttctggtgtgagcctaatagcagccaatgtgtcgggaagctgtccag  
1421 F E C H V F W C E P N A A N V S E A V Q

4321 gctgcctgcatgctgcgatatacagaagtgttggtagccaggccaccttcacagaagtc  
1441 A A C M L R Y Q K C L V A R P P S Q K V

4381 cgccccccacccccgccagccgattcagtgacccggagagtcacaaccaatgtgaagcga  
1461 R P P P P P A D S V T R R V T T N V K R

4441 ggggtcttatctctcattgacactttgaaacagaagcggcctgtcacagagacaccctag  
1481 G V L S L I D T L K Q K R P V T E T P \*

Predicted Fe65 like 1 protein (gi: 62660482) annotated as a potential gene product of chromosome 14 region 10,490,390 to 10,752,085 (gi: 62660484). The position of the exons relative to the predicted mRNA is highlighted in pink.

---

## ACKNOWLEDGMENTS

In first place I would like to say *muchas gracias* to PD Dr. Florentina Soto for her great work as supervisor of this work and for being a true friend, enjoying with me happy moments and supporting me on difficult ones.

I am grateful to Prof. Dr. Walter Stühmer for his interest and generous support during the whole project, and I am indebted to Prof. Dr. Hans-Joachim Fritz and Prof. Dr. Herbert Jäckle for taking the role of *Referent* and *Korrefent* of this thesis work, respectively.

In addition, I would like to thank PD Dr. Sigrid Hoyer-Fender and Prof. Dr. Ivo Feußner for kindly accepting the examiner role at my *Rigorosum* examination.

Many people were involved at many points of my thesis. In particular I would like to thank Kerstin Dümke for helping me with “everything” in the lab, teaching me from lab techniques to German lessons. A special acknowledge to Anja Bremm and Dr. Maria Rubio who made key experiments that I present on this thesis work. At last, but not least, I’m indebt to Dr. Daniel Kerschensteiner for essential discussions that allowed the final outcome of the project, and for infinite patience on teaching me electrophysiology. Support on this technique is also gratefully acknowledged from Prof. Dr. Walter Stühmer, Dr. Luis Pardo and Dr. Rafael Garcia.

Many warm thanks to my colleagues at the Department of molecular biology of neuronal signals for creating a comfortable work environment. From the latin crowd, as Amaya, Eva, Jose, Camino, Fernanda, Nayuf, Araceli, Victor, and David, to the german ones, as Arnt, Sara, Barbara, Annett, and Klaus, not forgetting the international ones, as Milena, Miso, Katja, Anjana, and Siji,... I will miss you all!

Special thanks to *süße* Ute Rust for being such a good friend and for dealing with all my bureaucratic issues.

Spending more than three years out of my country has only been possible thanks to the invaluable support from my whole family and friends in Argentina... *esto es por ustedes!*

Finally, I want to acknowledge the person who “simply” makes everything possible in my life, and because of whom I know the infinite meanings of love... *Carlos te amo.*

---

## LEBENS LAUF

Name: Marianela Masin  
Geburtsdatum: 18. Januar 1978  
Geburtsort: Reconquista, Argentinien  
Nationalität: argentinisch  
Adresse: Hainbuchenring 1  
37077 Göttingen

Bildungsweg

1984 - 1990 Grundschole „Escuela ciudad de Reconquista N° 6044“  
1991 - 1996 Gymnasium „General San José de San Martín“,  
Reconquista, Argentinien, mit einem technischem  
Abschluss für Architektur  
1997 - 2002 Studium der Biotechnologie an der „Universidad  
Nacional del Litoral“, Santa Fe, Argentinien, mit einem  
Diplomabschluss in Biotechnologie  
seit 2003 Anfertigung der Doktorarbeit im Max-Planck-Institut  
für Experimentelle Medizin, Göttingen, mit dem Thema  
„Identification and Characterization of the molecular  
complex formed by the P2X<sub>2</sub> receptor subunit and the  
adapter protein Fe65 in rat brain“ bei PD Dr. Florentina  
Soto

---

## VERÖFFENTLICHUNGEN

- *Original Artikel:*

Marianela Masin, Daniel Kerschensteiner, Kerstin Dumke, Maria E. Rubio and Florentina Soto.

Fe65 interacts with P2X<sub>2</sub> subunits at excitatory synapses and modulates receptor function.

**J Biol Chem.** 281(7): 4100-4108 (2006).

- *Vortrag:*

**Eingeladener Sprecher für das Treffen: “First joint Italian-German purine club meeting”, September 2005, Chieti, Italy**

Molecular complex formed by the P2X<sub>2</sub> receptor and Fe65 at excitatory synapses.

- *Poster Präsentationen:*

**Neuroscience 2004, Oktober 2004, San Diego, California, USA**

Marianela Masin, Anja Bremm, Daniel Kerschensteiner, Kerstin Dümke, Maria E. Rubio and Florentina Soto.

Identification of proteins interacting with P2X<sub>2</sub> receptors in rat brain.

**8<sup>th</sup> International symposium on adenosine and adenine nucleotides, Mai 2006, Ferrara, Italy**

Annette Nicke, Marianela Masin, Benjamin Marquez-Klaka, Jürgen Rettinger, Florentina Soto.

Identification and characterization of a functional P2X<sub>7</sub> splice variant with an alternative transmembrane domain.